Simultaneous absorptiometric determination of copper, nickel, iron and cobalt in refinery process streams: potential on-line application.

by

Evelyn Archery

Thesis presented in fulfillment of the requirement for the degree of **Master of Science** at the **University of Stellenbosch**.

Supervisor: Professor K.R Koch December 2005

I, Evelyn Archery the undersigned hereby declare that the work contained in the thesis is my own original work and that I have not previously in its entirety or in part submitted it at any university for a degree.

Signature:…….. Date:

Acknowledgements

I must offer my gratitude to Jesus Christ, God Almighty for giving me the strength, courage and grace and wisdom to complete this project.

Special thanks to my parents in Durban who offered many prayers and support during this two year period. I am blessed to have Sarahni, Reshmi, Tessy, Gladys and Elrika who stood by side steadfastly. I am thankful to the Rustenburg Assembly of God for their constant prayers.

I am deeply grateful to Dr David Robinson as a great mentor and Prof Klaus Koch as an encouraging supervisor. Thanks to Peter Chennells and the Rustenburg Base Metal Refinery Laboratory Management for their support. Thanks to RBMR for sponsoring the project and providing me the necessary resources. Thanks to Theo van Schalkwyk for his useful suggestions. Thanks to Arjan Westra, Sibusiso Mtongana for their great advice and suggestions. I would like to thank the PGM group for their support during my visits to the department.

Abstract

A method for the simultaneous spectrophotometric determination $Cu(aq)^{2+}$, $Ni(aq)^{2+}$, $Co(aq)^{2+}$, and $Fe(aq)^{2+,\ 3+}$ in refinery process streams based on multiwavelength analysis is proposed.

The individual concentrations of the metallic ions present in quaternary mixtures was achieved by using molar absorptivities of each element at the wavelength of interest[1] solving a simultaneous equation.

A calibration model was setup simulating the refinery. The concentration of the elements predicted here were then used to predict the elements in an unknown sample. Simultaneous multicomponent determination of Cu^{2+}, Ni^{2+}, and Co^{2+} in process streams is possible. A good comparison of the laboratory analysis to the new method is proved.

Abstrak

’n Metode gebaseer op multi-golflengte analise, word voorgestel vir die gelyktydige spektrofotometriese bepaling van $Cu(aq)^{2+}$, $Ni(aq)^{2+}$,$Co\ (aq)^{2+}$ and $Fe(aq)^{2+}$ in die strome van ‘n rafineerdery proses

Die individuele konsentrasies van die metaal ione teenwoordig in die vier-delige mengsel, word bepaal deur die gebruik van die molere absorpsie van elke element by die golflengte van belang, vir die gelyktydige oplossing van die vergelyking.

’n Kalibrasie model van die Rafineerdery is opgestel. Die konsentrasies van die elemente voorspel is gebruik om die elemente in ‘n onbekende monster te voorspel. Gelyktydige multi-komponent bepaling van die proses strome is moontlik. ‘n Goeie ooreenkoms tussen die Laboratorium analise en die nuwe metode is bewys.

Contents

Table of Contents

List of Figures

List of Tables

Chapter 1

Introduction

1.1 Problem in the refinery

The determination of copper, nickel, iron and cobalt at the Rustenburg Base Metal Refinery (RBMR) is currently achieved using various laboratory based analytical techniques.[1, 2, 3, 4] This analysis is carried out primarily for process control. The current analytical techniques are time-consuming, inefficient, and costly. However, the plant requires fast, preferably on-line analytical methods which provide real-time data that save time and money.

The current process of analysis involves the movement of a sample from a sampling point in the refinery to the laboratory on an hourly or four hourly period. The sample then undergoes the necessary treatment, the copper, nickel, iron and cobalt concentration is determined and reported to the plant. This process is time-consuming and does not constitute effective process control, in view of the delay between the analysis value reported and the state of the process solution in the plant.

This problem suggested an investigation into the development of an improved method for the analysis of copper, nickel, iron and cobalt, in approximately real time, which would be suitable for potential on-line application.[5,6]

UV– visible spectrophotometry, being the simplest analytical tool relative to titrimetry, Atomic Absorption Spectroscopy and Inductively Coupled Plasma, was investigated as a possible alternative to the current methodology, in view of the relatively high copper, nickel and cobalt concentrations in the RBMR process streams, i.e. 30-100g/L nickel, 30-80g/L copper and 30-70g/L cobalt.[7] The current methodology involves titrimetric analysis for copper and nickel analysis and atomic absorption analysis for iron and cobalt analysis. This is discussed in detail later in the chapter.

1.2 Anglo Platinum Overview

The Anglo Platinum Group is the world's largest producer of platinum group metals (PGM's). Its expanding operations currently comprise six mines, three smelters, Rustenburg Base Metal Refinery (RBMR) and a Precious Metal Refinery (PMR), situated in the Limpopo, Mpumulanga and North Western provinces of South Africa. The Anglo Platinum Group exploits the world's richest reserve of PGM's.[8,9] (see Fig 1.1)

Anglo Platinum mines both Merensky and UG2 reefs over the bushveld indigenous complex (see Fig 1.2) covering an area which spans some three hundred kilometers. The Merensky and UG2 reefs have distinct differences in their geological composition.

The ore from different mine shafts is treated at eight concentrators, which produce a combination of metallics (gravimetrically concentrated) and flotation concentrate. The metallics are sent directly to PMR and the concentrate proceeds to either one of the smelters. The smelter product proceeds to the Anglo Platinum Converter Plant (ACP). The matte from ACP is transported by tractors to RBMR. This matte typically contains 29 % copper, 44% nickel, 1% cobalt, 3% iron and 23 % sulphur. (see Fig 1.1)

The Rustenburg Base Metal Refinery comprises a platinum enrichment, i.e. matte converter plant (MC plant) and a Base Metal refinery (BMR). The enriched platinum group metals (PGM) concentrate is refined to pure metals at PMR in a separate process.

The MC plant was commissioned in 1975 and the BMR in 1981. The BMR is a medium sized base metals refinery and has a capacity of 21 000 tons per annum (tpa) nickel, 12 000 tpa copper, 1100 tpa cobalt sulphate crystal and 55 000 tpa sodium sulphate. The plant was designed to produce high quality products efficiently. The overall process is shown schematically in Fig 1.3.

Anglo Platinum Process

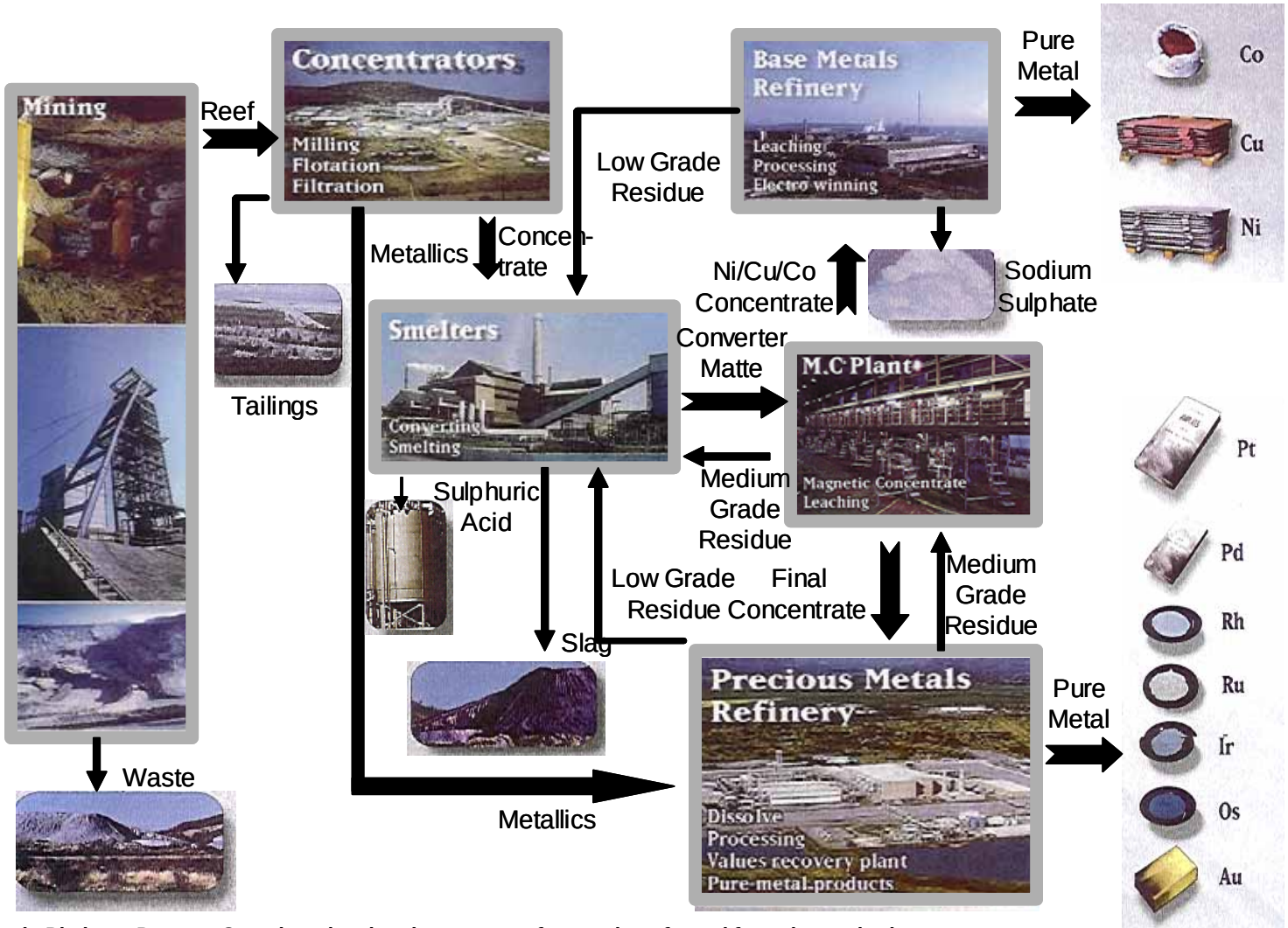

Fig 1.1 Anglo Platinum Process Overview showing the process of extraction of metal from the ore body.

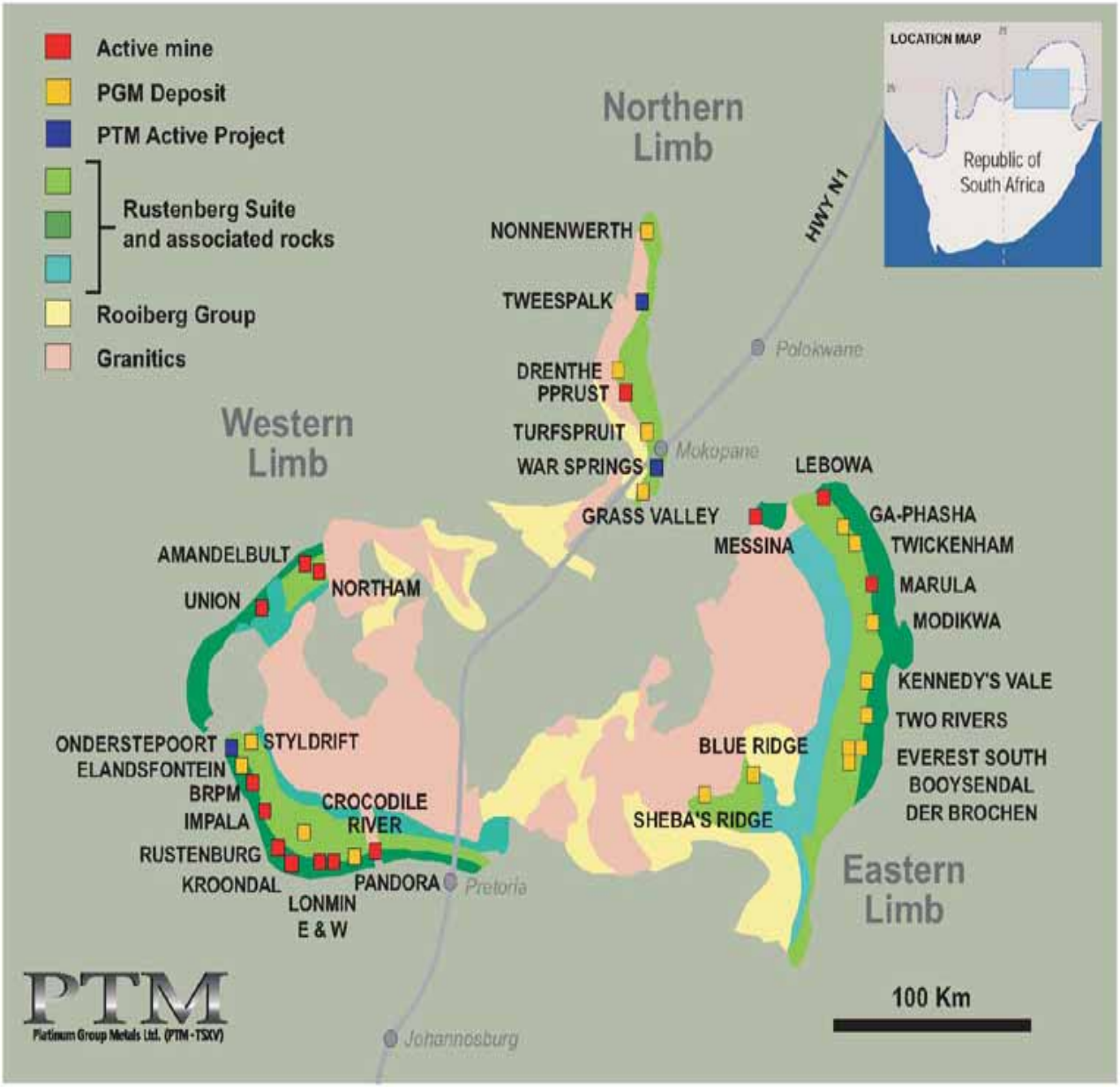

Fig 1.2 Map of Bushveld Complex showing the platinum rich expanse of area that is mined in South Africa.[10]

1.3 Rustenburg Base Metal Refinery Process

This process will be discussed strictly from the literature documented in the Hydrometallurgy Journal, researched by Hofirek Z who has worked on this site.[8,9]

The Rustenburg Base Metals Refinery treats the Ni-Cu coverter matte produced at the smelter for the selective recovery of electrowon nickel metal, electrowon copper metal, cobalt sulphate crystals and a PGM concentrate.

Initially, the converter matte is separated magnetically into a PGM-containing metallic fraction and a non-magnetic sulphide fraction. The metallic fraction is enriched in a small hydrometallurgical plant to provide feed for the Precious Metals Refinery while the sulphide fraction undergoes a three-stage leach process in the Base Metals Refinery.

The leach filtrate (PVLL) from the PGM enrichment at MC plant, is a Ni-Co-Cu sulphate solution which together with Nickel Copper Matte (NCM) from the magnetic separation process, forms the feedstock for the BMR.

The refinery is composed of 5 major sections, comprising the following processes:

- PGM enrichment
- Nickel circuit
- Copper circuit
- Cobalt sulphate plant
- Sodium sulphate plant

The nickel circuit, copper circuit and cobalt sulphate plant will be discussed in detail in this chapter, as this is of concern for this project. The refinery process streams are highly concentrated in nickel, copper and cobalt (30-100g/L nickel, 30-80g/L copper and 30-70g/L cobalt) and lead to the final product of metallic nickel, copper cathodes and cobalt sulphate crystals.

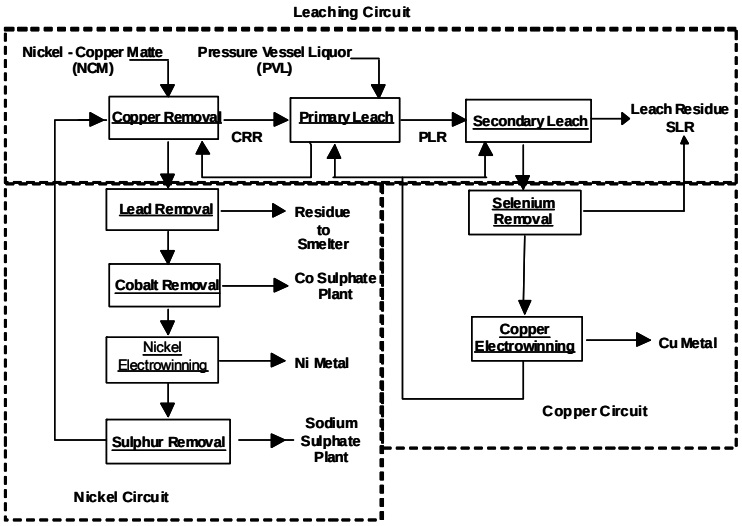

Nomenclature

CRR-copper removal residue

PLR- primary leach residue

SLR- secondary leach residue

Fig 1.3 RBMR Process flow diagram describing the overall refining of base metals from nickel-copper matte.

1.3.1 The Nickel Circuit

The feed material to the process viz. nickel copper matte (NCM) and pressure vessel leach liquor (PVLL) are both inputs to the nickel circuit. Both these input streams are contaminated to varying degrees with elements from the ore body. These streams are subjected to further purification to remove lead and cobalt prior to production of nickel metal in the electrowinning cells. Also, any sulphur (which is in sulphide form) oxidised in the leaching stages, is removed at the end of the nickel circuit in the "sulphur removal" stage. (see Fig 1.3)

1.3.1.1 Copper Removal

The primary input to the base metal refinery, NCM, initially enters the copper removal stage where it is contacted with Primary Leach Solution (PLS) in a series of continuous stirred reactors. The reactors are all aerated at 180-200 Nm^3/hr and maintained at a temperature of 80^0C. The major objective is to process the PLS by removing dissolved copper and iron. About 10-15(w/w)% of nickel in the matte is dissolved in the PLS stream.

During the copper removal stage, copper can be precipitated from solution by one of two processes:

a) by metathesis with heazelwoodite (Ni_3S_2) at solution pH below 2.5

or $2Ni_3S_2 + 2Cu^{2+} + 2H^+ + ½\ O_2 \longrightarrow Cu_2S + 3NiS + 3Ni^{2+} + H_2O$ (1)

b) by hydrolysis at a pH above 4.5 to yield antlerite.

$3Cu^{2+} + SO_4^{2-} + 4H_2O \longrightarrow Cu_3(OH)_4SO_4$ (antlerite) $+ 4H^+$ (2)

The dissolved iron is precipitated from solution by one of the following sequences:

At pH above 2.5, the ferrous (Fe^{2+}) iron is oxidised.

$2Fe^{2+} + 2H^+ + ½\ O_2 \longrightarrow 2Fe^{3+} + H_2O$ (3)

At pH above 3.5, the ferric ion becomes unstable and undergoes hydrolysis $Fe(OH)_3$.

$Fe^{3+} + 3H_2O \longrightarrow Fe(OH)_3 + 3H^+$ (4)

or

$Fe^{3+} + SO_4^{2-} + H_2O \longrightarrow Fe(OH)SO_4 + H^+$ (5)

Excess acid is consumed by the decomposition of heazlewoodite according to the following reaction (6):

$Ni_3S_2 + 2H^+ + ½\ O_2 \longrightarrow 2NiS + Ni^{2+} + H_2O$ (6)

The acid consuming reactions outlined in (1), (3) and (6) result in an increase in pH which leads to the initiation of the hydrolysis reactions. It is desirable to hold the terminal pH in the last copper removal reactor in the range 5.3 – 6.0.

The copper removal stage results in two products viz. copper removal residue (CRR), which is 32 % djureleite ($Cu_{1.96}{}^*S$) and 12-15% antlerite which is pumped to the primary leach stage and the copper removal solution (CRS) which is fed to the nickel purification section in the nickel circuit for purification. (see Fig 1.3)

1.3.1.2 Primary Leaching

The main objective of the primary leach of the NCM is to ensure maximum nickel dissolution (>75 %) with minimal dissolution of copper and iron. The CRR, copper spent solution and PVLL from MC plant and spillage solutions are mixed in the feed tank to the secondary leach stage.

The CRR contains: 30- 35(w/w) % nickel, 26-30(w/w)% copper, 0.5(w/w)% cobalt, 2(w/w)% iron, 25(w/w)% sulphur and 7.5(w/w) % other impurities.

The major nickel phases in NCM are Ni_3S_2 (20-25%) and Ni_7S_6 (NiS)(30-35%). Major constituents in copper mineralogical phases are $Cu_{1.96}{}^{*}S$ (30-32%) and $Cu_3(OH)SO_4$ (12-15%). The chemistry of the primary leach process is extremely complex and this will be discussed qualititatively.

Four leaching periods can be distinguished in this primary leach process:

I. Slurry mixing at ambient temperature and pH of about 2.5
II. Preheating of slurry in the absence of air
III. Oxidising leach with air injection and agitation
IV. Non-oxidising leach with agitation but no aeration.

Slurry mixing

During slurry mixing at ambient temperature, rapid dissolution of anterlite occurs. This process consumes a large amount of acid.(H_2SO_4)

$$Cu_3(OH)_4SO_4 + 4H^+ \longrightarrow 3Cu^{2+} + SO_4^{2-} + 4H_2O \quad (7)$$

Feed preparation and preheating

Excess acid is further consumed by the decomposition of heazlewoodite (Ni_3S_2)(6).

* Standard nomenclature for different mineralogical phases.

Thereafter some of the cupric ions in solution are precipitated by the metathesis reaction(1) with heazlewoodite. Reaction(1) continues throughout the heat-up period and the dissolved copper in solution is precipitated among other trace elements. Stoichiometric quantities of

nickel are leached into solution (50%), i.e. considering reaction (1), the quantity of Ni_3S_2 brought with the solution is equal to the quantity which will remain in solid form as NiS.

Oxidising leach

Two phases with differing chemistry can be identified during the oxidative leach period(III) viz: an acidic phase, and acid- free phase. In the acidic phase, acid promotes the following reactions in their presence of oxygen.

$$Cu_2 + 2H^+ + ½\ O_2 \longrightarrow CuS\ (\textit{covellite}) + Cu^{2+} + H_2O \quad (8)$$

$$4NiS + 2H^+ + ½\ O_2 \longrightarrow Ni_3S_4\ (\textit{polydmite}) + Ni^{2+} + H_2O \quad (9)$$

To a limited extent, part of the millerite (NiS, intermediate phase in NCM) is also solubilized by direct oxidation:

$$NiS + 2O_2 \longrightarrow Ni^{2+} + SO_4^{2-} \quad (10)$$

The consumption of acid in reactions (8) and (9) results in the solution acidity decrease to zero. In the acid free phase, no overall concentration changes of metal occur, but the copper is shifted from the sulphide phase to the sulphate by dynamic equilibrium between reactions (8) and (2).

Non-oxidising leach

During the non-oxidising leach period, a large proportion of the soluble copper product from reaction (8) needs to be re-precipitated as Cu_9S_5 to prevent overloading the precipitation capacity of the copper removal stage. The overall reaction of the non-oxidising leach stage can be represented by the following:

$$4Ni_3S_4 + 9Cu^{2+} + 8\ H_2O \longrightarrow Cu_9S_5 + 9NiS + 3Ni^{2+} + 2SO_4^{2-} + 16H^+ \quad (11)$$

The free acid generated in this reaction dissolves again antlerite by reaction (7). Experimentally, the amount of millerite in residues is found not to increase according to the stoichiometry of reaction (11) and this suggests a further secondary reaction:

$$NiS + Cu^{2+} \longrightarrow CuS + Ni^{2+} \quad (12)$$

This reaction mechanism is supported by increases in the covellite (CuS) residue content.

The principle factors affecting the chemistry and kinetics of dissolution of the primary leach are initial acid concentration, aeration rate and temperature.

Leaches with insufficient acid may result in a large presence of basic nickel sulphates in the non-oxidising stage of the leach(IV) due to the Ni^{2+} ion precipitating at pH 3 according to

$$3Ni^{2+} + SO_4^{2-} + 4H_2O \longrightarrow Ni_3(OH)_4SO_4 + 4H^+ \qquad (13)$$

In order to satisfy the chemical constraints of the copper removal stage, high concentrations of soluble copper must be precipitated during the non-oxidising leach.

Soluble copper entering the non-oxidising stage is precipitated following the dissolution of polydymite(Ni_3S_4)(11) or millerite(NiS)(12). For this reason, the nickel dissolution during the oxidation period should be limited(9,10). This can be done by lowering the pressure or temperature in the autoclave, but this action impacts unfavourably on the kinetics of dissolution of the non-oxidising leach.(see Fig 1.4)

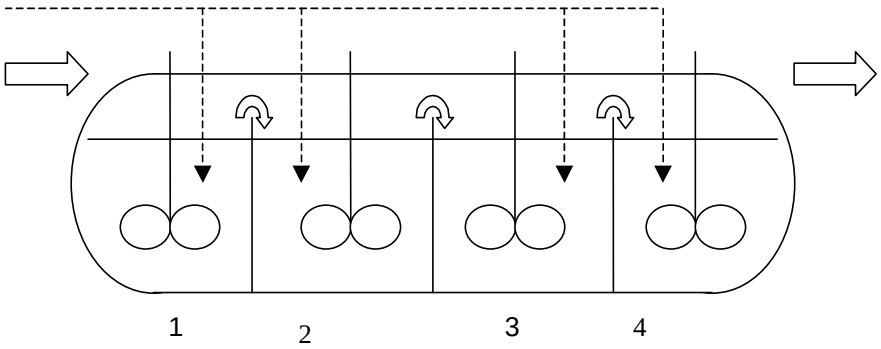

Fig 1.4 Schematic representation of an autoclave with the 4 different compartments.

The addition of oxygen is essential for both these reactions, and the air inputs of 900-1200 nm^3/h to compartments one and two can therefore be used as a control measure.

Temperature during the non-oxidizing leach also plays an important role on the kinetics of copper precipitation and acid regeneration (reactions 2,11,12). Above 140°C copper is precipitated very rapidly and residence times in the autoclave would easily ensure copper free solutions.

However, the generated acid is consumed by the dissolution of iron which adversely affect the copper removal stage. A facility therefore exists to control leach temperatures in the third and fourth compartment by injection of a small volume of copper removal solution (CRS)(1-4 m^3/hr) into the third compartment. Chemically, this has little effect, but acts as a "quenching" medium for non-oxidising leach. This means that CRS quenches the heat of the reaction, i.e. acts as a coolant.

Increasing the input rate of CRS, reduces the temperature which limits the precipitation of copper and the generation of acid, thereby the dissolution of iron is lowered. A discharge temperature of 135°C is considered optimal.

Solid-liquid separation of primary leach solution (PLS) and primary leach residue (PLR) is performed in thickeners. The underflow PLR is filtered and washed on belt filter and consists of 48-55(w/w)% copper, 7-12(w/w)% nickel, 2-5(w/w)% iron, 22-25(w/w)% sulphur, 0.1-0.3(w/w)% cobalt and 9-20(w/w)% other constituents. The overflow PLS proceeds to the copper removal section. The PLS returns to the copper removal tank whilst primary leach residue proceeds to secondary leaching.

1.3.1.3 Lead Removal

The position that nickel holds in the electrochemical series, makes it necessary to provide a feed solution to electrowinning that is free of the more electronegative elements, such as lead and cobalt. [10] Besides copper and iron, specific removal steps must also be employed to remove lead and cobalt. Other impurities such as zinc and manganese are also rejected to some extent during these processing stages.

Lead, in the nickel circuit, is derived from the oxidation of lead sulphide (PbS) present in the Ni-Cu Matte mentioned earlier, in the copper removal reactors, and from the slow dissolution of the lead anodes (anodes are made of lead-strontium) in the tankhouse (area where copper and nickel electrowinning takes place). [8,9]

The lead is precipitated from solution by direct injection of barium hydroxide. In the pipe reactor rapid and uniform distribution of the $Ba(OH)_2$ reagent leads to almost instantaneous precipitation according to the following reactions:

$Ba(OH)_2 \longrightarrow Ba^{2+} + 2\,(OH)^-$

$Ba^{2+} + SO_4^{2-} \longrightarrow BaSO_4$ (precipitate)

$Ba^{2+} + Pb^{2+} + 2SO_4^{2-} \longrightarrow BaSO_4.\,PbSO_4$ (precipitate) (14)

Filtration of the fine precipitate, $BaSO_4.\,PbSO_4$ is improved by ageing the slurry in the press feed tank. This cake containing lead and other trace metals from the ore is sent back to Waterval smelter where it is disposed in the smelter slag as waste product. (see Fig 1.1).

1.3.1.4 Cobalt Removal

Cobalt sulphate is the most valuable of the base metal products produced by the refinery. For this reason, it is desirable to recover as much cobalt as possible in the form of $CoSO_4.7H_2O$, in which it is marketed and sold.

In order to separate dissolved cobalt from the lead-removal discharge stream, an "Outokumpu" process is used.[11] This process is accomplished by taking advantage of the differences in stability of the oxidised hydroxides of cobalt and nickel in the pH range of 5.6-5.7.

Nickel(III)hydroxide($Ni(OH)_3$), which is not a commercially available product, is internally manufactured in the tankhouse and is used in the oxidation of cobalt. The reagent is produced electrolytically utilising a fraction of nickel feed for its extraction and a small quantity of sodium hydroxide via the following reactions:

a) Nickel sulphate is first converted to Ni(II) hydroxide by reaction with sodium hydroxide.

$NiSO_4 + 2NaOH \longrightarrow Ni(OH)_2 + Na_2SO_4$ (15)

b) Electrolytic production of Ni(III) hydroxide is simplistically represented by the following reactions:

Water reaction:

$H_2O \longrightarrow H^+ + OH^-$

Anode reaction :

$OH^- + Ni(OH)_2 \longrightarrow Ni(OH)_3 + e^-$

Cathode reaction:

$H^+ + e^- \longrightarrow \frac{1}{2} H_2$

Overall:

$Ni(OH)_2 + H_2O \longrightarrow Ni(OH)_3 + \frac{1}{2} H_2$ (16)

The sodium hydroxide for reaction (15) is added in excess and is used to raise the pH in the cobalt precipitation section to the desired range of between 5.6 and 5.7(pH at which nickel is precipitated). Provision is also made for fine control of the pH by a separate caustic line.

The nickel(III) hydroxide slurry is added to the first of the three reactors in series in quantities corresponding to a Ni^{3+}: Co^{2+} ratio of 3:1. The following reaction takes place, ideally at 80^0C:

$Ni(OH)_3 + CoSO_4 \longrightarrow Co(OH)_3 + NiSO_4$ (17)

The use of nickel(III) hydroxide has several advantages in that it is an efficient scavenger for low levels of Cu^{2+}, Fe^{2+}, Pb^{2+} and Zn^{2+} in solution. The cobalt removal stage is utilized as the last purification step before electrowinning of nickel.

Within this processes, it is possible to produce a cobalt free nickel liquor(< 5mg Co/dm^3), the precipitated solids are heavily contaminated with nickel due partly to some of the excess sodium hydroxide reacting with nickel sulphate, to form insoluble $Ni(OH)_2$ (15).

It is thus necessary for the precipitated solids to be further refined before pure cobalt can be recovered.

After filtration, the primary cake which contains the elements that precipitated during the cobalt removal stage, is re-pulped and passed to the cobalt treatment reactors where the spent nickel solution is added under pH control. Acid contained within the spent solution re-dissolves the nickel.

$2H^+ + Ni(OH)_2 \longrightarrow Ni^{2+} + 2H_2O$ (18)

The cobalt rich residue is filtered out from the nickel bearing solution and after re-washing with demineralised water it is sent to the cobalt sulphate plant where cobalt sulphate is produced. The cobalt treatment filtrate which contains a low concentration of nickel, is recycled to the copper removal stage, where the nickel can be returned to the process.

1.3.1.5 Nickel Electrowinning

Nickel metal is electrowon from purified nickel feed solution using lead anodes and nickel cathodes. Ni^{2+}(aq) is reduced to Ni(s) when electricity is supplied to the electrowinning cells.(see Fig 1.5).

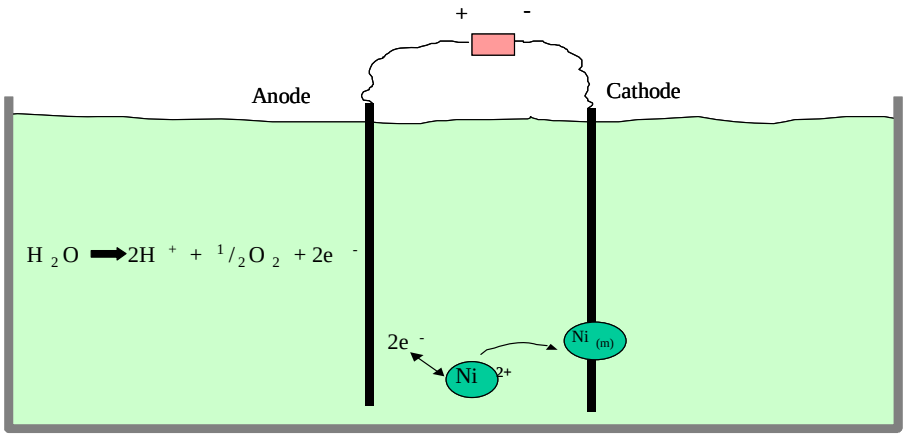

Fig 1.5 Schematic presentation of electrowinning of nickel.

This process can be depicted as follows:

Reaction:

$Ni^{2+} + 2e^-$ ⟶ Ni(s)

At the anode, the picture above shows that electrons is supplied to the Ni^{2+} ion by decomposition of water(H_2O) into hydrogen ions(H^+) and oxygen gas(1/2 O_2).

The anodic reaction are as follows:

H_2O ⟶ $2H^+ + ½\ O_2(g) + 2e^-$ (20)

Oxygen as formed in this reaction, is in a gaseous form. As such, gas bubbles will be generated at the place where water decomposes. These gas bubbles will rise to the surface of the solution and the oxygen released into the atmosphere.

The reaction at the cathode is:

$$Ni^{2+} + 2e^{-} \longrightarrow Ni \quad (19)$$

The standard reduction potential table containing common reactions is used to calculate the voltage required to enable the electroplating of nickel.[12]

The voltage is calculated using the formula:

$$E_{Cell} = E_{Anode} - E_{Cathode}$$

Where E_{Cell} = voltage required, i.e. cell voltage

E_{Anode} = The standard potential of the anodic reaction

$E_{Cathode}$ = The standard potential of the cathodic reaction

However, this voltage is negative and the reaction will not take place spontaneously. Therefore a voltage higher than the calculated value will have to be applied for this reaction to take place in the electrowinning cell.

$$H_2O \longrightarrow 2H^{+} + \tfrac{1}{2} O_2(g) + 2e^{-} \quad (20)$$

Combining (19) and (20), an overall cell reaction is obtained

$$Ni^{2+} + H_2O \longrightarrow Ni + 2H^{+} + \tfrac{1}{2} O_2 \quad (21)$$

At high cell voltage with an almost neutral catholyte there are many elements which would be reduced at the cathodic surface and co-deposited with nickel. This indicates the necessity of extensive nickel feed purification. The nickel cathode produced is sold in various forms.

1.3.1.6 Sulphur Removal

The last stage of the nickel circuit (Fig 1.3) produces sodium sulphate. The sulphur removal step also enables water introduced into the process to be removed. The nickel spent solution is split into two streams. One stream is treated with sodium hydroxide to achieve neutralisation of excess sulphuric acid from a pH of 2.5 to a pH of 5.8. (see eq 22)

The solution is then passed into a second precipitation reactor where the pH is raised to 8.8. to achieve $Ni(OH)_2$ precipitation. The pH control is critical in order to produce a filterable slurry of $Ni(OH)_2$, and Na_2SO_4.

Neutralisation

$$H_2SO_4 + 2NaOH \longrightarrow Na_2SO_4 + H_2O \qquad (22)$$

Precipitation

$$NiSO_4 + 2NaOH \longrightarrow Ni(OH)_2 + Na_2SO_4 \qquad (24)$$

Temperature control in this stage is important and is maintained at 75°C for efficient precipitation. The precipitated nickel(II)hydroxide is filtered on rotary vacuum drum filters. The sodium sulphate filtrate is re-filtered through filter presses to remove fine particles of $Ni(OH)_2$ after further pH adjustment. The filtrate is pumped to the sodium sulphate recovery plant.

The nickel(II) hydroxide filter cakes are re-pulped under controlled pH conditions at 3.2. This re-pulped stream then joins the remainder of the spent nickel stream in the nickel dissolution section. The nickel is re-dissolved according to (18) and (18a):

$$2H+ + Ni(OH)_2 \longrightarrow Ni^{2+} + 2H_2O \qquad (18)$$

$$NiCO_3 + 2H^+ \longrightarrow Ni^{2+} + CO_2(g) + H_2O \qquad (18a)$$

The nickel(II) hydroxide and acid solution is pumped back to copper removal to re-circulate the nickel and remove impurities (mainly lead and copper).

1.3.2 The Copper Circuit

The copper circuit can be divided into three stages

- Secondary leaching
- Selenium removal
- Copper electrowinning

Formatted: Indent: Left: 17.85 pt, Hanging: 17.85 pt, Bulleted + Level: 1 + Aligned at: 18 pt + Tab after: 36 pt + Indent at: 36 pt

1.3.2.1 Secondary leaching

The primary objective of the secondary leach is to complete the extraction of nickel (>99%) and copper (>97%) from NCM. The leach also provides a means of removal of iron which is precipitated in the secondary leach residue (SLR). The iron that entered the BMR at the beginning of the process is thus removed in SLR, and thus the aim of removing iron (contaminant) in the process is achieved.

The primary leach residue, spent copper solution residue and plant spillages are mixed to form the feed to the secondary leach stage. The slurry is injected via air pumps without preheating into the first compartment of the Three Sherrit Gordon autoclaves, divided into 4 compartments by vertical weirs, in which secondary leaching takes place.

The air entering the leach is approximately 30% oxygen enriched which translates into the various compartments. One of the autoclaves has been modified to allow dual functionality so that it may be used as a primary or secondary leaching vessel.

In secondary leaching, each compartment is agitated and aerated at controlled rates. Optimum pressures and temperatures are maintained in the autoclaves.

Table 1.1 Typical elemental composition of PLR

Element	(w/w)%
Copper	48-55
Cobalt	0.1-0.3
Iron	2-5
Nickel	7-12
Other	9-20
Sulphur	22-26

The major nickel phases are polydmite Ni_3S_4 (8-10%) and millerite NiS (4-5%). Major copper mineralogical phases are digenite, Cu_9S_5 (30-35%), covellite CuS (40-45%) and antlerite $Cu_3(OH)_4SO_4$ (0-5%).

Two leaching periods can be distinguished:

a) Slurry mixing at ambient temperature

b) Oxidising leach in the presence of air.

During the slurry mixing phase, all metals in the form of re-precipitated hydroxides or basic sulphates rapidly dissolve the copper according to reaction(7) and the iron and nickel species according to reactions (26) and (27) respectively.

$$Cu_3(OH)_4SO_4 + 4H^+ \longrightarrow 3Cu^{2+} + SO_4^{2-} + 4H_2O \quad (7)$$

$$Fe_2O_3.xH_2O + 6H^+ \longrightarrow 2Fe^{3+} + (x+3)H_2O \quad (26)$$

$$Ni_3(OH)_4SO_4 + 4H^+ \longrightarrow 3Ni^{2+} + SO_4^{2-} + 4H_2O \quad (27)$$

These reactions consume significant quantities of sulphuric acid. During the oxidation phase, the major reaction is acid decomposition of digenite:

$$Cu_9S_5 + 8H^+ + 2O_2 \longrightarrow 5CuS + 4Cu^{2+} + 4H_2O \quad (28)$$

Covellite is then directly oxidized (29) or decomposed to elemental sulphur (30). Direct oxidation is favoured in the latter stages of the leach where there is no acid consumption, whereas decomposition is favoured in the early stages when high acid concentrations are present.

$$CuS + 2O_2 \longrightarrow Cu^{2+} + SO_4^{2-} \quad (29)$$

$$CuS + 2H^+ + \tfrac{1}{2} O_2 \longrightarrow Cu^{2+} + S^0(s) + H_2O \quad (30)$$

Millerite (NiS) is either directly oxidised by reaction (10), converted to polydymite by (9) or acid leached as follows:

$$NiS + 2H^- + \tfrac{1}{2} O_2 \longrightarrow Ni^{2+} + S^0(s) + H_2O \quad (31)$$

Polydymite reacts as follows:

$$Ni_3S_4 + 6O_2 \longrightarrow 3Ni^{2+} + 3SO_4^{2-} + S^0(s) \quad (32)$$

$$Ni_3S_4 + 7.5\ O_2 + H_2O \longrightarrow 3Ni^{2+} + 4\ SO_4^{2-} + 2H^+ \quad (33)$$

The high temperature oxidising environment results in ferric ion hydrolysis at conditions of moderate acid concentration. Depending on leach conditions, iron precipitates as natrojarosite(34) or hematite(35).

$$3Fe^{3+} + Na^+ + 2SO_4^{2-} + 6\ H_2O \longrightarrow Na[Fe_3(OH)_6(SO_4)_2] + 6H^+ \quad (34)$$

$$2Fe^{3+} + 3\ H_2O \longrightarrow Fe_2O_3 + 6H^+ \quad (35)$$

Both reactions release a considerable amount of acid which is generally consumed in digenite decomposition as described in reaction (28). The effect of operating conditions on the chemistry of the secondary leach is very important. The chemistry of the main mineralogical phase, i.e. copper sulphides defines the leach parameters. The acid decomposition of digenite(28) is rapid. The rate determining step being the oxidation of covellite.[(29) and (30)]. Temperature and oxygen partial pressure significantly increase the rate of oxidation; and the maxima of these parameters is limited by corrosion considerations and design specifications of the autoclaves. The parameters, temperature and oxygen pressure cannot be infinitely high, as this can damage the lining of the autoclaves. However, these parameters must be high to improve the rate of the reaction.

Elemental sulphur can be formed by partial oxidation of covellite or millerite (30, 31) or the dissolution of polydymite (32). The sulphur can melt and agglomerate as “sulphur balls” which gives rise to blocked discharged screens. High acidity, low temperature and low oxygen partial pressure conditions favour the formation of elemental sulphur. For this reason care must be taken to avoid high initial acid excess and correct aeration rates and temperatures should be maintained.

The precipitation of iron in the secondary leach is important, since soluble iron reduces the current efficiency in the copper electrowinning process. Iron, during precipitation collects

impurities such as selenium, arsenic, antimony and tellurium. Hematite has a lower solubility and better collection properties than jarosite. However, it has inferior filtration and settling properties.

In order to achieve the conditions required for minimum elemental sulphur formation (low acidity, increased temperature, high oxygen partial pressure), low residual soluble iron levels can be expected. At low acidity and high temperature, the formation of hematite is favoured and not jarosite (high acidity and low temperature (130°C)).

Secondary leach Residue Treatment

The secondary leach residue is filtered, re-pulped and transferred to the MC plant where it is filtered, dried and shipped to a toll refinery where it is toll-refined to remove traces of copper, nickel and PGM's. The filtrate is returned from the MC plant to the secondary leach spillage tank.

1.3.2.2 *Selenium Removal*

After the discharge slurry from the secondary leach is filtered, the copper rich filtrate requires a specific removal stage for only one impurity, selenium. As a result of high reversible oxidation/reduction potential, 0.34V, selenium is dissolved under the harsh conditions of the first stages of the secondary leach and is not completely co-precipitated with iron.

More severe conditions are necessary to remove this (Se) contaminant and these are provided by a pressure process with sodium sulphite as the reagent at a temperature of 80°C.

Sodium sulphite is injected into the stream in the reduction pipe reactor and causes the following sequence of events to occur.

Reduction of cupric to cuprous.

$$2Cu^{2+} + SO_3^{2-} + H_2O \longrightarrow 2Cu^{+} + SO_4^{2-} + 2H^{+} \quad (36)$$

Reduction of Se^{4+} and / Se^{6+} to Se^{2-}

$$SeO_3^{2-} + 8Cu^{+} + 6H^{+} \longrightarrow Cu_2Se + 6Cu^{2+} + 3\,H_2O \quad (37)$$

$SeO_4^{2-} + 10Cu^{+} + 8H^{+} \longrightarrow Cu_2Se + 8Cu^{2+} + 4H_2O$ (38)

Further reduction of cupric to cuprous.

$Cu_2Se + x\ Cu^{2+} \longrightarrow Cu_{2-x}\ Se + 2xCu^{+}$ (39)

Cuprous ion may react by disproportionation to form metallic copper.

$2Cu^{+} \longrightarrow Cu^{0} + Cu^{2+}$ (40)

This is obviously undesirable and the metallic copper along with any cuprous is re-oxidised in the oxidation pipe reactor.

$Cu + ½\ O_2 + 2H^{+} \longrightarrow Cu^{2+} + H_2O$ (41)

$2Cu^{+} + ½\ O_2 + 2H^{+} \longrightarrow 2Cu^{2-} + H_2O$ (42)

The discharge stream from the selenium removal is now filtered on a filter press to remove the selenium rich cake. The selenium-rich cake is pumped back to secondary leach filtration and the selenium leaves the circuit with the SLR.

1.3.2.3 Copper Electrowinning

The copper feed solution is cooled in plate heat exchangers prior to electrowinning. This prevents excessive acid mist in the tankhouse. Lead anodes and copper cathodes are used.

The cathode reaction is given by

$2Cu^{+} \longrightarrow Cu^{0} + Cu^{2+}$ (40)

Similar to the nickel electrowinning, current is passed via the decomposition of water :

$H_2O \longrightarrow ½\ O_2 + 2H^{+} + 2e^{-}$ (20)

Combining equations (20) and (40), an overall cell reaction is obtained

$Cu^{2+} + H_2O \longrightarrow Cu + 2H^{+} + ½\ O_2$

There are no other elements preferentially plated considering the position of copper in the electrochemical series. However, high iron in the copper feed will result in a loss of current efficiency due to the side reaction of iron reduction and can lead to " burning straps" at the liquor line.

$2Fe^{3+} + Cu \longrightarrow Cu^{2+} + 2Fe^{2+}$ (42)

This can dissolve the copper straps which hold the cathodes suspended in the copper solution and cause cathodes to fall into the cell and cause short circuits. The spent copper solution is recycled to both the primary and secondary leach where it supplies sulphuric acid for base metal dissolution.

1.3.3 Cobalt sulphate Production

Cobalt final "wash cake" obtained from the Co removal stage, is first dissolved in the cobalt dissolution reactors with sulphuric acid and formaldehyde as a reductant.

$$4Co(OH)_3 + HCHO + 4H_2SO_4 \longrightarrow 4CoSO_4 + CO_2 + 11H_2O \quad (43)$$

Because of the necessity for very pure Solvent Extraction feed (SX), provision is also made to remove co-dissolved iron and copper impurities. Dissolved iron is oxidized and then precipitated as follows:

$$2FeSO_4 + H_2SO_4 + ½\ O_2 \longrightarrow Fe_2(SO_4)_3 + H_2O \quad (44)$$

$$Fe_2(SO_4)_3 + 6NaOH \longrightarrow 3Na_2SO_4 + 2Fe(OH)_3 \quad (45)$$

Copper is precipitated by barium sulphide (BaS) addition

$$CuSO_4 + BaS \longrightarrow CuS + BaSO_4 \quad (46)$$

All the iron and copper solids are then filtered out, leaving a pure cobalt and nickel containing SX feed solution. The cobalt is then separated from Ni^{2+} species by solvent extraction using the following reagents dissolved in Kerosol 200.(Table 1.2)

Table 1.2 The composition of organic in cobalt extraction.

Di-2-ethyl-hexyl-phosphoric-acid (D2EHPA)	Extractant	15%
Kerosol 200	Carrier	75-78%
Tri-butyl phosphate	Phase modifier	5%

2.6-*di*-tert-butyl-*p*-cresol	Anti oxidant	1%

Several solvent extraction cells are used. The organic phase is introduced into cell no 2. and flows counter current to the SX feed introduced in cell 8. Cell 1 is the settler and is used to remove organic traces from the raffinate. The following reaction occurs where R represents the organic chain of the extractant and Me^{2+} is the metal being extracted e.g. Co^{2+}:

$$2R\text{-}Na + Me^{2+} \longrightarrow R_2Me + 2Na^{+} \quad (47)$$

The cobalt depleted nickel solution (raffinate) is returned to the nickel circuit (reports to nickel precipitation section). The nickel loaded into the organic is then removed by displacement with a pure inorganic cobalt sulphate solution. This takes place counter current in cells 9-14.

$$R_2\text{-}Ni + CoSO_4 \longrightarrow R_2Co + NiSO_4 \quad (48)$$

The cobalt in the relatively pure loaded organic phase is now stripped into the aqueous phase by counter current contact with 10% sulphuric acid. This takes place in cells 15,16 and 17.

$$R_2\text{-}Co + H_2SO_4 \longrightarrow CoSO_4 + 2RH \quad (49)$$

The aqueous cobalt stream is then concentrated via evaporation under vacuum in a double effect crystalliser to produce a stable heptahydrate crystal which is bagged and sold. The stripped organic phase is then contacted with an acid solution which serves to remove trace base metals e.g. Mn^{2+} and impurities in cell 18 using reaction (49). Stripped organic is then regenerated in cell 19 by using sodium hydroxide:

$$RH + NaOH \longrightarrow R\text{-}Na + H_2O \quad (50)$$

1.4 Chemical process control and determination of metal content in Rustenburg Base Metal Refinery.

The chemical process control in the refinery is critical to the efficient management of the production of copper, nickel and cobalt sulphate. It is necessary that determination of metal content in the entire process is optimised using the best methods of analysis.

Currently, the major problem is the time delay between analysis and process control function, i.e. time lag and therefore ineffective process control. This problem gave rise to the study below.

1.5 Process control analysis

The BMR process requires extensive chemical process control. The traditional method is slow, costly, and susceptible to many errors. As a result of this it is imperative that the analytical chemist design a more efficient method of analysis for the process that is faster, cost effective and accurate. The current methods of analysis which are used are all batch mode, laboratory based determinations.

- Copper Analysis : Short Iodide Method
- Nickel Analysis : EDTA Method
- Cobalt Analysis : Atomic Absorption Analysis
- Fe Analysis : Atomic Absorption Analysis

The Short Iodide method involves taking an aliquot of sample, adding several reagents and titrating with sodium thiosulphate to determine the copper concentration. The EDTA method for nickel determination involves taking an aliquot of sample and adding several reagents and titrating with EDTA to determine the nickel concentration.[13] These methods are time-consuming, inefficient, requires skilled personnel and is subject to titrimetric endpoint errors.

The Atomic Absorption method involves large dilution of the sample (as high as x150 fold) and then measurement on the Atomic Absorption Spectrometer. The error associated with the large dilution does not facilitate the best measurement for cobalt and iron.

The role of the analytical chemist in the refinery is to develop a method in comparison to the above that's more efficient. Strategically, to develop the simplest, fastest, cheapest analytical tool off-line that would be versatile for on-line analysis.

UV-visible spectrophotometry will be investigated as an alternative tool to the current methods of analysis. Generally, this simple tool has the advantages of high sensitivity,

moderate to high selectivity, good accuracy and fast analysis. This is discussed in detail in Chapter 2.

1.6 On-line analysis

1.6.1 Principles of on-line analysis

The possibility of using on-line analysis for analysis of these metals was a secondary objective of this study.

Traditionally, in off-line analysis, samples from the process environment are obtained manually, transported to a centralized analytical laboratory and analysed by technical staff; the staff evaluate the data obtained and report the results to those involved in the operating system; corrective action is taken if required by adjusting conditions of the operating system accordingly. The time lag between analysis and effective process control is however, a major problem, resulting in relatively ineffective process control.

On the other hand in the on-line, modern process analytical chemistry approach, analysis is performed at or inside an operating system (plant site) with an analytical system (process analytical system or process analyzer), where corrective action is immediately taken.[14] These two approaches i.e. traditional process analytical chemistry method and modern process analytical chemistry are shown schematically in Figs 1.6 and 1.7.

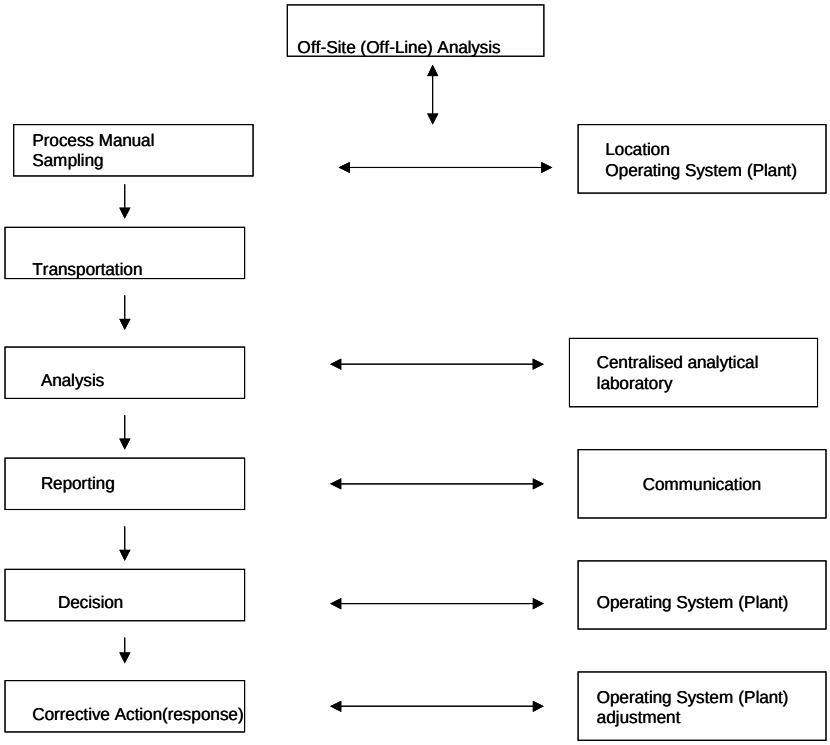

Fig 1.6 Traditional approach to process control

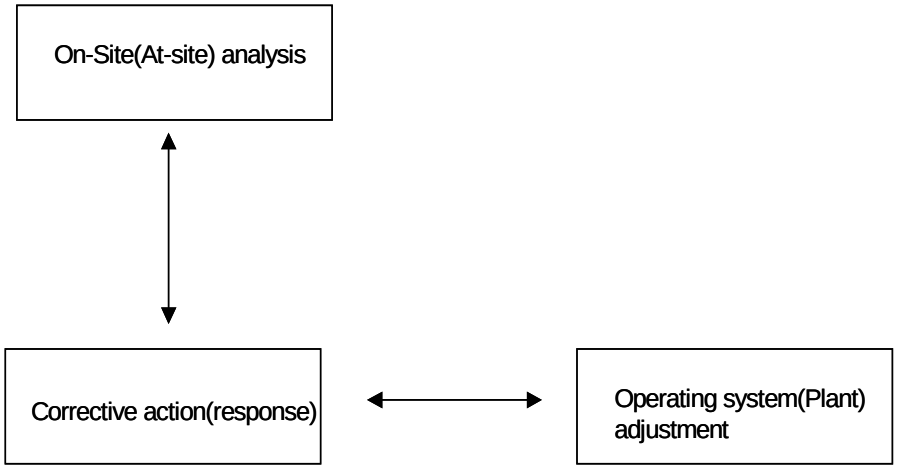

Fig 1.7 Process analytical chemistry approach to process control

There is not always a direct communication in the traditional approach to process control, and a typical operation from sampling to corrective action may take several hours. This feature is known as time–delayed monitoring. Processes in chemical manufacturing plants are usually designed to accommodate this time delay, at a cost of longer cycle times and reduced plant utilization compared to when using a process analytical approach, i.e. on-line analysis.

Direct ‘real time’ communication is a very important part of analytical process approach in which corrective action can immediately be implemented once results are available. The term *real-time* monitoring has been coined for this type of approach.

On site (at-site) analysis is divided into three categories. In *at-line* analysis, the sample is still manually sampled, but the measurement is carried out on a dedicated analyzer located at the sampling site. Sample preparation is simplified and the measurement technique modified to permit the use of robust reliable instrumentation to cope with the production environment.

The term *close-time monitoring* (near real-time monitoring) is used to describe this type of operation. In *on-line* analysis, the sample is automatically sampled and fed into a dedicated analyzing system where analysis is automatically performed with an automatic feedback to the operating system (e.g. process stream for industrial chemical processes) for adjustment and corrective action. In *in-line* analysis, the analyzing probe is situated inside the operating system (or process stream). Transduction is performed inside the operating system, with a feedback to the processor outside the operating system, with facilities for automatic adjustment and corrective action. Real-time monitoring or a good approximation to real time is attained with *on-line* and *in-line* analysis.

1.6.2 Planning, design and sample manipulation

In the planning and design of instrumentation for dynamic real-time or semi-real-time analysis systems, the following points should be considered very carefully:

- Selection of the process variable (characterizing the quality of the process)
- Quantitative relation between the measured parameter and analyte to be determined
- Places of sampling (or analysing points)
- Frequency of the measurements and correlation time of the process required; for continuous measurements, the time constant of the measurement system
- Duration time of the measurements; measurement time could be short.
- Tolerance limits (upper and lower) of the measured variable
- Selection of sensing or analysing instrument(s)
- Cost and maintenance of instruments
- Calibration frequency of the instruments used
- Total cost of measurements and regulations involved

- Reliability, ease of operation and simplicity.

For effective data handling and real-time determinations, the system should be fully computerised, which includes control of pumps, valves, data acquisition, data processing and data transfer to a central bank with automatic feedback.

The equipment which penetrates the operating system's (e.g. plant's process envelope in industrial chemical processes) envelope is called the sampling probe. The sampling probe must ensure that the sample taken is representative of the entire operating system (process stream in chemical processes). Once a sample has been extracted from the operating system, it must be transferred to the analyser. A preconditioning system, situated close to the sampling point, may be used to treat the sample in such a way as to eliminate problems, e.g. by solid particles, droplets or condensate, which may lead to blockage or fouling of the sample-transport line and to regulate the pressure and temperature of the sample provided to the system.

The sample-transport line must transport the sample from the preconditioning system point to the analyser in an acceptable time and without the composition of the sample being affected appreciably. Speed and representativeness are the key issues. The sample-conditioning modules are designed to ensure that the sample is acceptable to the analyser and that it is truly representative. The analyser accepts the conditioned sample, senses or processes the analyte into a product that is measured, and produces an appropriate output signal.

A modern process analyzer system normally contains seven parts:

- the sampling point
- the preconditioning system
- the sample-transport line
- the sample-conditioning system
- the analyser (analytical measurement or sensor unit) itself
- the analyser control unit or the programmer and
- the associated output equipment

1.6.3 Measurements and quantification of analyte

Measurements in process analysers are based on physiochemical properties of the analyte used to determine usually quantitative chemical information classified as follows:

a) Methods based on measurement of process streams with intensive physical properties (density, light absorption, refraction, etc.).
b) Methods based on the measurement of intensive properties after using chemical reaction(s) for increasing selectivity and sensitivity (spectrophotometry using colour-forming or chromogenic reagents, etc).
c) Measurement of extensive physical properties using chemical reaction(s) (for example gravimetry, titrimetry, coulometry, etc).
d) Two dimensional analytical methods. One coordinate is related to the *quality* (nature) and other to the *quantity* of the components (for e.g. polarography, chromatography, spectroscopy, etc).

The procedures of class (a) are preferred on the grounds of simplicity in process control, but they are not applicable if high selectivity or sensitivity is required.

1.6.4 Detection System

The detection system in a process analyser can be destructive or non-destructive sensor. In a destructive mode the sample is destroyed, for example in inductively coupled plasma (ICP) spectroscopy where the sample is eventually fed into a plasma. With non-destructive detection, the composition of the original sample is maintained, for example when using a pH probe as detector; although a change at micro level occurs at the electrode surface-solution interface, the bulk of the process stream remains unchanged.

The scope of the Process Analytical Chemistry approach has been broadened with the introduction of a new generation of devices, accompanied by new terminology, in process analysers. The terms non-invasive and non-intrusive are widely used. With non-invasive technique, the sensing probe does not physically come into contact with the process stream and all non-invasive measurements rely on the transmission of information through the wall of the vessel. Non-invasive techniques are primarily focused on the measurement of physical parameters. At present, there are a small number of chemical measurements that can be made this way. A transducer, in this context, is a device for converting a chemical or physical parameter into an electrical signal. Non-invasive therefore means that, in all cases the transducer does not come into contact directly with the process medium. A familiar

example of this is a thermowell, which is simply a piece of tubing welded into the wall of the vessel and closed at the innermost end. To measure the process temperature, a thermocouple or platinum resistance thermometer is inserted into the tube. To be able to make a representative measurement of the process fluid temperature, this tube needs to extend some distance into the fluid. It is therefore intrusive. An obvious disadvantage of an intrusive technique is that the probe may disturb the process fluid or may be eroded by the passage of entrained abrasive material.

A pH probe is an example of an invasive intrusive analyzer. For this to function, the pH-sensitive element needs to be in intimate contact with the process fluid, preferably where there is some kind of flow. This suffers the disadvantage of an intrusive monitor.

1.7 Potential impact to the plant

Chemical analysis has always played an essential role in the process control of metallurgical processes. As a result of this efficient, quality, quantity, cost effective, accurate chemical analysis means efficient process control. Therefore, the use of on-line provides a potentially beneficial option.

On-line analysis has several advantages. On-line analysis is fast, accurate, cost effective, non-labour intensive and practical in comparison to manual analysis by laboratory personnel which is slow, subject to human error and labour-intensive.

An increase in productivity with on-line analysis, as a consequence that information is delivered real-time and is not delayed by manual processing and generation of results. As a result, development of an analytical technique that is versatile for on-line analysis is an important consideration meeting the demand of the plant real-time.

UV-visible spectrophotometry is an analytical tool that readily lends itself to automation because of its cost effectiveness, efficiency and overall simplicity. Therefore, it has found itself favourable for the study.

1.8 Specific objective of study

The main objectives of the study:

1. To investigate UV-visible spectrophotometry as a method of determination for analysis of copper, nickel, cobalt and iron in mixtures simulating refinery process streams.
2. To investigate simultaneous determination of copper, nickel, cobalt and iron in refinery plant samples within a 10% relative accuracy specification.
3. To investigate application of UV-visible spectrophotometry to on-line analysis.

References

1. A.I. Vogel, *A textbook of quantitative inorganic analysis*, 3rd edn., 377.
2. A. I. Vogel, *A textbook of quantitative inorganic analysis*, 3rd edn., 435.
3. C.B. Belcher, *Talanta*, 1963, **10**, 75.
4. T.A Rafter, and F. T. Seelye, *Nature*, 1950, **165**, 317.
5. S.D. Frans and J.M Harris *Analytical Chemistry*, 1985, **57**, 2660-2684.
6. A.M Garcia Rodriguez, A. Garcia de Torres, J.M Cano Pavon- and C.Bosch Ojeda.*Talanta*. 1998, **47**, 463-470.
7. Skoog, West,and Holler, *Fundamentals of Analytical Chemistry*, 1996, 7th edn., 569.
8. Z. Hofirek PJ. Nofal. Hydrometallurgy, 1995, 39, 91-116.
9. Z. Hofirek and D.G.E. Kerfoot, Hydrometallurgy, 1992, 29, 357-381.
10. www.platinumgroupmetals.net/i/maps/, April 2004.
11. B. Nyman A.Aatonen, S.E Hultholm, K. Karpale. Hydrometallurgy. 1992, 29, 461-478
12. J.D Lee, Concise Inorganic Chemistry, 1996,167.
13. A I.Vogel, A textbook of quantitative inorganic analysis.1961, 3rd edn., 435.
14. J F. Van Staden, Pure Applied Chemistry, 1999, 71, 2303-2308.

Formatted: Indent: Left: 0 pt, First line: 0 pt, Numbered + Level: 1 + Numbering Style: 1, 2, 3, … + Start at: 1 + Alignment: Left + Aligned at: 0 pt + Tab after: 18 pt + Indent at: 18 pt, Tabs: 27 pt, List tab + Not at 18 pt

Chapter 2

Basic review of absorptiometric analysis

UV-visible spectroscopy is widely used for the qualitative and quantitative determination of myriad inorganic and organic species.[1] There are various applications for this technique such as analysis of drugs in the pharmaceutical industry, determination of calcium in municipal water, determination of mercury in soil and determination of vanadium in steel for example.[2]

2.1 Principles of UV-visible spectroscopy

UV and visible radiation comprises only a small part (i.e. 100-400nm for UV and 400-800nm for visible region) of the electromagnetic spectrum, which includes other forms of radiation known as radio, infrared, cosmic and X-rays as shown in Fig 2.1 below.

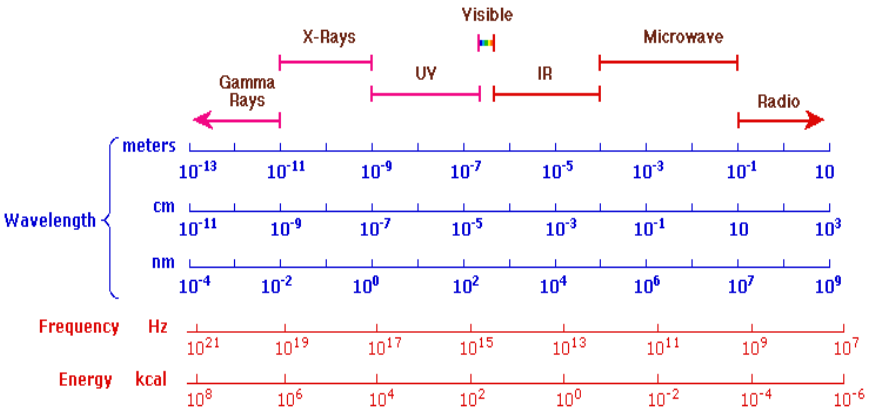

Fig 2.1 The electromagnetic spectrum showing different forms of radiation of which UV-visible is one.[3]

The energy of a photon of electromagnetic radiation is defined by:

$$E=h\upsilon$$

Where *E* is the energy (J), *h* is Planck's constant ($6.62 * 10^{-34}$Js), and υ is the frequency of the radiation(s^{-1}). Electromagnetic radiation can be considered a combination of alternating electric and magnetic fields that travel through space with a wave motion. Because radiation acts as a wave, its properties can be defined either in terms of wavelength or frequency, which is related to the speed of light by the following equation:

$$\upsilon = c/\lambda$$

where υ is frequency in s^{-1}, c is the speed of light ($3*10^8 ms^{-1}$), and λ is wavelength(m). In UV-visible spectroscopy, wavelength is expressed generally in nanometers(nm).

2.1.1 Molecular absorption

Molecules on absorption of a photon of energy undergo three types of quantised transitions when excited by ultraviolet, visible and infrared radiation. These are electronic,vibrational and rotational transitions. [4]

Electronic transitions involve promoting an electron residing in a low-energy orbital, generally the highest occupied molecular orbital (HOMO) to a higher-energy orbital, i.e. lowest unoccupied molecular orbital (LUMO). Generally, UV-visible radiation is sufficient only for "valence electron transitions"and not core electrons which are excited by X-ray radiation.

Vibrational transitions occur when a molecule has a multitude of quantised vibrational states with vibrations of the bonds that hold the molecule together.

Fig 2.2 shows diagrammatically the processes that occur when a polyatomic species absorbs ultraviolet radiation. The energies E_1 and E_2, two of the several electronic states of a molecule are shown relative to the energy of its ground state E_0. Each horizontal line represents a vibrational level and each vibrational level is associated with each of the electronic states of a molecule

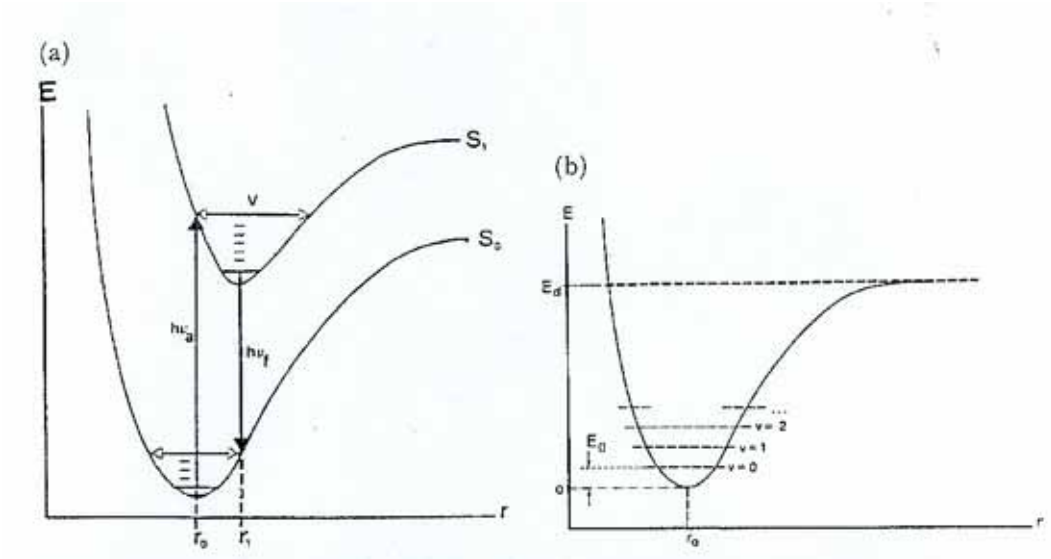

Fig 2.2 (a) In a potential energy diagram optical transitions are vertical and vibrational motions are horizontal (b)The zero point energy E_0 is the energy of the v=0 level.[5]

Molecular absorption in the UV and visible region consists of absorption *bands* made up of closely spaced lines. In solution, the absorbing species is surrounded by solvent, and the band nature of molecular absorption often becomes broad because the individual electronic transitions between each level have superimposed on them a vibrational mode, which result in many closely spaced electronic transitions which are resolved, so that the bands are broad.

Additionally, the life-times of

1. the electronic excited states is very short 10^{-10}- 10^{-15} seconds, which means by Heisenberg's uncertainty principle, the energy of each state is less certain, which translates into broader absorption bands.
2. The solvent-solute (absorbing species) interactions also lead to broader absorption bands due to the fact that molecular collisions, slightly alter the energy gaps leading to broader bands.

2.1.2 Beer Lambert Law

When light passes through a sample, the amount of light absorbed is the difference between the incident radiation (I_0) and the transmitted radiation(I). The amount of light absorbed is expressed as either transmittance or absorbance. Transmittance (T) is usually given in terms of a fraction of 1, or as a percentage, and is defined as follows:

$$T=I/I_0 \text{ or } \%\ T= (I/I_0)*100(\%)$$

Absorbance is defined as follows:

$$A= -\log_{10} T$$

Light absorption is a function of the concentration of the absorbing molecules. The functional relationship between the quantity measured in absorption analysis, absorbance (A) and the quantity sought, concentration,(c) is known as the *Beer Lambert Law* which can be written as

$$A = \log (I/I_0)= alc$$

where *a* is the proportionality constant called the absorptivity and *l* is the path length of the radiation through the absorbing medium. Since absorbance is a unitless quantity; the absorptivity will thus require units that likewise render the right side of the equation dimensionless.

When the concentration is expressed in moles per liter and *l* is in centimetres, the proportionality constant is called the molar absorptivity and is given the symbol ε. Thus,

$$A = \varepsilon cl$$

where ε has the units $Lcm^{-1}mol^{-1}$.

The molar absorptivity expresses the transition probability of an electron between the allowed quantum states at a given wavelength. A high value of ε, means a high probability of absorption of photons of light, and means that the aborbance is high at that λ at a given concentration of absorbing molecules.

The molar absorptivity is characteristic of a given substance under a precisely defined set of conditions, such as wavelength, solvent and temperature. The molar absorptivity depends on the nature of the absorbing species and on the wavelength of the incident radiation. The molar absorptivity of a chemical species at a given wavelength is a measure of how strongly the species absorbs light at that wavelength.[6]

Beer's law also applies to solutions containing more than one absorbing substance. This law can therefore be used to analyse mixtures. According to Beer's law, a linear relationship exists between absorbance and path length at a fixed concentration. However, deviations from the Beer's law do exist and as a result is only linear for relatively dilute solutions. Some of these deviations are fundamental and represent *real* limitations to the law, whilst others occur as a consequence of the manner in which absorbance measurements are made, i.e. *instrumental* deviations or as result of chemical changes associated with the concentration changes, i.e. *chemical* deviations.

a) Real Limitations to Beer's Laws

Beer's law is successful in describing the absorption concentration behaviour of media containing relatively low analyte concentrations only and in this sense is a *limiting* law. At high concentrations (>0.01M), the average distances between the species responsible for absorption is diminished to the point where each affects the charge distribution of its neighbours. Such interactions in turn can slightly alter the energy levels and the transition probabilities of the electrons at a given wavelength of radiation. Because the extent of interactions depends upon concentration of the solute-solvent, the extent of this phenomenon results in deviations from the linearity of Beer's law.

A similar effect is encountered in media containing low concentrations of absorbing molecules but high concentrations of other species, particularly electrolytes. The close proximity of ions to the absorbing molecules alters the molar absorptivity of the latter by electrostatic interactions, which leads to deviations from Beer's law. This effect can be minimised by dilution.

While the effect of molecular interactions is not significant at concentrations below 0.01M, some exceptions are encountered for large organic ions and molecules. For example, the molar absorptivity at 436nm for the cation of methylene blue is reported to increase by 88% as the dye concentration is increased from 10^{-5} to 10^{-2}M; even below 10^{-6}M, strict adherence to Beer's law is not observed.

Deviations from Beer's law also arise because molar absorptivity is slightly dependant on the refractive index of the solution. Thus, if concentration changes cause significant alterations in the refractive index of a solution, departures from Beer's law are observed. In general, this effect is small and rarely significant at concentrations less than 0.01M.

b) Chemical Deviations from Beer's Law

Deviations from Beers' Law also occur when the analyte undergoes association, dissociation, or reaction with the solvent to give products with absorbing characteristics that differ from those of the analyte. The extent of such departures can be predicted from the molar absorptivities of the absorbing species and the equilibrium constants for the reactions involved.

c) Instrumental deviations from Beer's Law

Polychromatic radiation

Beer's law only applies ideally when absorbance is measured with monochromatic radiation. Monochromatic sources, such as lasers, are not practical for routine analytical instruments. Instead, a polychromatic continuous source is employed in conjunction with a grating or a filter that isolates a more or less symmetric band of wavelengths around the desired one, the following derivation illustrates how much a non-monochromatic light source may lead to deviations from Beer's law.

Consider a beam made up of just two wavelengths λ^1 and λ^2, and assume that Beer's law applies strictly to each. With this assumption, for radiation λ^1

$$A^1 = \log I_0{}^1/I^1 = \varepsilon^1 lc$$

$$I^1{}_0/I^1 = 10^{\varepsilon 1lc} \text{ and } I^1 = I_0{}^1 10^{-\varepsilon 1lc}$$

Similarly, for λ^2

$$I_0{}^2/I^2 = 10^{\varepsilon 2lc} \text{ and } I^2 = I_0{}^2 10^{-\varepsilon 2lc}$$

When an absorbance measurement is made with radiation composed of both wavelengths, the power of the beam emerging from the solution is given by $I^1 + I^2$ and that of the beam emerging from the solvent by $I_0{}^1 + I_0{}^2$. Therefore, the measured absorbance A_m is

$$A_m = \log (I_0{}^1 + I_0{}^2)/(I^1 + I^2)$$

which can be rewritten as

$$A_m = \log (I_0{}^1 + I_0{}^2)/(I_0{}^1 10^{-\varepsilon 1lc} + I^2 10^{-\varepsilon 2lc})$$

$$= \log (I_0{}^1 + I_0{}^2) - \log (I_0{}^1 10^{-\varepsilon 1lc} + I^2 10^{-\varepsilon 2lc})$$

when $\varepsilon^1 = \varepsilon^2$, this equation simplifies to

$$A_m = \varepsilon^1 lc$$

and Beer's law is strictly followed. However, the relationship between A_m and the concentration is not linear when molar absorptivities differ. Moreover, departures from linearity become greater as the difference between ε^1 and ε^2 increases. When this treatment is expanded to include additional wavelengths, the effect remains the same.

Generally, the better the monochromator of the instrument, the less it suffers from non-linearity due to polychromatic radiation. This effect, is however, not very significant given that in general, the bandwidth in UV-visible spectrometry are broad, and that the slit-width of the instrument is very small comparable to the resolution achievable from a real instrument for the practical application.

Instrumental deviations in the presence of stray radiation

The radiation employed for absorbance measurements is usually contaminated with small amounts of stray radiation due to instrumental imperfections. Stray radiation is the result of scattering phenomena off the surfaces of prisms, lenses, filters and windows. When measurements are made in the presence of stray radiation, the observed absorbance is given by

$$A^1 = \log (I_0/I_s)/ (I + I_s)$$

where I_s is the power of stray radiation.

For e.g. stray radiation in the monochromator, the exit beam of a monochromator is usually contaminated with small amounts of radiation having wavelengths far removed from that of the instrument setting. The effects of stray radiation in monochromators are minimised by introducing baffles at appropriate spots in the monochromator and by coating the interior surfaces with flat black paint. In addition, the monochromator is sealed with windows over slits to prevent entrance of dust and fumes.

In spite of "theoretical" limitations, chemical deviations and instrumental deviations to Beer's law, there are other sources of error that can contribute to the errors overall encountered in absorbance measurements.

Regardless of the above mentioned limitations to Beer's law, in practice it can be shown that with the appropriate precautions and calibration procedures, UV-visible spectroscopy can be used for quantitative analyses and conditions can be found which in practice lead to essentially linear Beer's law.

Analysis of mixtures

The concentration of each of the elements present in a mixture can be determined by absorbance measurements at two different wavelengths, given Beer's law behaviour by each constituent and provided that ε values are known for the pure species at a given wavelength.

Absorbance is proportional to the number of molecules that absorb radiation at the specified wavelength. This principle is true if more than one absorbing species is present. All multicomponent quantitative methods are based on the principle that absorbance at any wavelength of a mixture is equal to the sum of the absorbance of each component in the mixture at that wavelength.

This means the total absorbance at a specified wavelength and specified path length *l* of a mixture of solutes x, y, and z is given by

$$A_{total} = A_X + A_y + A_z$$

Where A_X, A_y, A_z are the absorbancies that each of the designated solutes would have at the same concentration in the absence of the other two solutes. This in turn depends on the molar absorptivity and the concentration of, each component. Thus for two components *x* and *y*, the equations are:

$$A^{\lambda 1}{}_{(x+y)} = A^{\lambda 1}{}_{x} + A^{\lambda 1}{}_{y} = \varepsilon^{\lambda 1}{}_{x} l c_x + \varepsilon^{\lambda 1}{}_{y} l c_y$$

$$A^{\lambda 2}{}_{(x+y)} = A^{\lambda 2}{}_{x} + A^{\lambda 2}{}_{y} = \varepsilon^{\lambda 2} l c_x + \varepsilon^{\lambda 2} l c_y$$

Where $A^{\lambda 1}$ is the absorbance at wavelength ^{1}, $A^{\lambda 2}$ is absorbance at wavelength ^{2}, $\varepsilon^{\lambda 1}$ is molar absorptivity at wavelength ^{1}, $\varepsilon^{\lambda 2}$ is molar absorptivity at wavelength ^{2}, c is concentration.

2.1.3 Error in absorbance measurements

a) Cells

UV-visible spectroscopy is used to measure absorbancies of solutions. A sample container known as the cell or cuvette contains the solution. It is important that these cells are transparent at all wavelengths since any absorbance from the cell itself reduces the effective linear dynamic range for the sample.

Cells are made of different material such as glass, quartz, plastic and fused silica. Cells made of plastic are not resistant to all solvents and absorb strongly below 300nm, making them unsuitable for measurements in this region. Glass cells are more expensive than plastic cells but more durable. Glass absorbs strongly below 320nm and thus is unsuitable for measurements in this area. Quartz or fused silica cells is required for the ultraviolet region <350nm and may be used in the visible region and to about 3000nm in the infrared.

The design of the cell is critical to minimizing the errors in absorbance measurements. Because measured absorbance depends on path length, the precision of the path length is important in absolute measurements. Cell path tolerances for cells of good quality are ±0.01mm for path lengths from 0.5 to 100nm. For maximum quantitative accuracy, the same cell should be used for both standard and sample measurements.

Non flat or non parallel optical surfaces can deviate the optical beam and cause apparent absorbance errors. Cells that have flat and parallel optical surfaces minimise their

influence as optical components. Scratched cells and dirty cells can cause significant absorbance.

b) Reaction conditions

The solvent used as well as the concentration, pH and temperature of the sample can affect the position and intensity of absorption bands of molecules. These parameters should be controlled to ensure maximum precision when comparing spectra measured under different conditions.

The polarity of a solvent can modify the electronic environment of the absorbing chromophore. The magnitude of the shift can be correlated with solvent polarity. Thus, the absorption maximum of acetone can vary from 259 to 279nm depending on the solvent used. For comparative analysis, a single solvent should be used for all measurements.

Concentration affects only the intensity of the bands. However, at high concentrations, molecular interactions occur e.g. dimerisation may cause changes in the shape and position of the band. These changes in turn affect the linearity of the concentration versus absorbance relationship and may lead to inaccurate quantitative results.

The effects of pH on absorbance spectra can be very large and result primarily from the shifting of equilibrium between two different forms, e.g. pH indicators change colour at different pH values. If the spectrum under study is found to be affected by pH, a buffer should be used to control this parameter.

Temperature can also affect absorbance measurements.[7] Temperature may affect equilibria, which can be either *chemical* or *physical*. An example of physical equilibrium, is the denaturation of nucleic acids as the temperature is increased, which changes absorpivity. In the case of organic solvents, changes in the refractive index with temperature can be significant. If temperature is found to have a significant effect on the measurements, the sample temperature should be controlled using a thermostatted holder.

c) Weak and strong absorbances

Low sensitivity is a common problem and is not related to the low concentration of analyte, but an inherent limitation of the method and the molar absorptivity of the metal complex species. Sensitivity of the measurement is defined as the response per unit analyte concentration, which here is dependant on the value of ε for the various metal complexes. At low absorbances, noise in the measurement results in a loss of precision such that any single measurement may be inaccurate. Reducing the noise level directly improves the precision of the results.

On the other hand, when samples absorb too strongly, the linear dynamic range of the instrument is exceeded and the relationship between absorbance and concentration becomes nonlinear. In this case, the sample is diluted to an absorbance level within the linear dynamic range that obeys Beer's law.

d) Interferences from substances

Ideally, the absorbance that is measured should only be due to the target analyte, however, absorbances that interfere with measurements occur for chemical and physical reasons. The presence of any other species that absorbs in the same region as the target species will result in an error in the absorbance measurement.

e) Scattering

Particles that are suspended in solution can cause scattering in analyses. The scattering of radiation results in apparent background absorbance that interferes with absorbance measurement. This happens because light instead of passing through the solution to the detector, is scattered at an angle.

Two types of scattering can occur, viz. Rayleigh and Tyndell scattering. Rayleigh scattering occurs when particles are small relative to the wavelength of light and is inversely proportional to the fourth power of the wavelength. Tyndell scattering occurs when the particles are large relative to the wavelength of light and is inversely proportional to the square of the wavelength. Filtering samples prior to measurement minimizes scattering.

f) Uncalibrated instrument

An uncalibrated instrument can give errors in absorbance measurements. If the instrument has been moved from one location to another in the laboratory, and in the circumstances where there are many operators to the instrument, it is necessary that the calibration on the instrument be checked. There are instrument validation tests that are setup in a spectrophotometer that can be run to calibrate the instrument. The instrument can be calibrated using the potassium dichromate and potassium permanganate method.[8]

Calibration of UV-visible spectrometer

Standard solutions of potassium dichromate and potassium permanganate are made up in 0.7M orthophosphoric and 1M sulphuric acid mixture. The spectra of these solutions are recorded and the molar absorptivities determined of the dichromate and permanganate species. Mixtures containing a fixed concentration of potassium permanganate and potassium dichromate are prepared in different combinations and the spectra recorded. The absorptivities are calculated and the results compared to literature.[6] A good correlation is an indication that the calibration on the instrument is in order and the spectrometer can be used with confidence.

2.1.4 Instrumentation

The spectrometer is the instrument used to measure the absorbance or transmittance of a sample as a function of wavelength. The key components of a spectrometer are: (1) a stable source of radiant energy, (2) a wavelength selector that permits the isolation of a restricted wavelength region, (3) one or more sample containers, (4) a radiation detector which converts radiant energy to a measurable signal and (5) a signal processor and readout. The assembly of these components can be seen in the figure below.

Fig 2.3 Schematic representation of key components of a spectrometer

Two light sources are commonly used in UV-visible spectrophotometers. The deuterium lamp yields a good intensity continuum in the UV region from 160-375nm. At longer wavelengths (>360nm), the lamp generates emission lines which are superimposed on the continuum. Modern deuterium lamps have low noise, however, noise from the lamp is

often the limiting factor in overall instrument noise performance. Over time, the intensity of light from a deuterium arc lamp decreases steadily. Such a lamp has a half-life (the time required for the intensity to fall to half its value) of approximately 1000 hours.

The tungsten-halogen or xenon lamps yield good intensity in the wavelength region 320-2500nm. This type of lamp has very low noise and low drift and typically has a useful life of 10000 hours.

The spectrometer is equipped with a wavelength selector, a device that restricts the radiation being measured to a narrow band that is absorbed or emitted by the analyte. Such a device, enhances the selectivity and sensitivity of the instrument. In addition, for absorptiometric measurements, narrow bandwidths increase the likelihood of adherence to Beer's law.

A wavelength selector such as a monochromator is used in the uv-visible spectrophotometer. A monochromator is made up of (1) an entrance slit, (2) a collimating lens or mirror to produce a parallel beam, (3) a prism or grating to disperse the radiation into its component wavelengths, and (4) a focusing element that projects a series of rectangular images of the entrance of the slit upon a planar surface called the *focal plane*. Monochromators have entrance and exit windows to protect components from dust and corrosive laboratory fumes.

The detector converts the light signal into an electrical signal. Ideally, it should give a linear response over a wide range with low noise and high sensitivity. Spectrophotometers usually contain either a photomultiplier tube detector or a photodiode detector.

Polychromatic light from the source is focused on the entrance slit of the monochromator, which selectively transmits a narrow band of light. This light then passes through the sample area, where the sample is seated in a cuvette to the detector. The detector converts this light signal into an electrical signal.

The absorbance of a sample is determined by measuring the intensity of light reaching the detector without the sample (the blank) and comparing it with the intensity of light reaching the detector after passing through the sample.

2.1.5 Summary of overall characteristics of UV-visible spectroscopy

UV-visible spectroscopy is one of the most useful tools for quantitative and qualitative analysis. The most important characteristics of this spectrophotometric method are

1. *Wide applicability*. Enormous numbers of inorganic, organic and biochemical species absorb ultraviolet or visible radiation and are thus amenable to direct quantitative determination. Many nonabsorbing species can also be determined after chemical conversion to absorbing derivatives.
2. *High sensitivity.* Detection limits range from 10^{-4} to 10^{-5}M. This range can be extended to 10^{-6} or even 10^{-7}M with certain procedural modifications.
3. *Moderate to high selectivity.* Generally, a wavelength can be identified at which the analyte alone absorbs, thus making preliminary separations unnecessary. Furthermore, where overlapping absorption bands do occur, corrections based upon additional measurements at other wavelengths eliminate the need for separation steps.
4. *Good accuracy.* The relative errors in concentration encountered with a typical spectrophotometric procedure employing uv-visible radiation lie in the range of 1 to 5%. Such errors can be decreased to a few tenths of a percent with special precautions.
5. *Ease and convenience.* Spectrophotometric measurements are easily and rapidly performed with modern instruments. In addition, the methods readily lend themselves to automation.[9]

The application of uv-visible spectroscopy to the analysis of transition metal ions, i.e. of cobalt, copper, iron and nickel will be discussed specifically, since these are transition metals that are of interest in the Rustenburg Base Metal Refinery. It is necessary to first understand the chemistry of the species concerned and then proceed with the application. (see Chapter 1)

2.1.6 Determination of analytical errors

All experiments are in analytical chemistry are subject to various errors. As a result, it is essential that these errors are estimated and their significance assessed.[10] There are two principal statistical techniques that can be used to evaluate errors occurring in analytical experiments. The first tool involves analysis of replicate measurements and the second

tool deals with calibration analysis. These tools are critical for overall error analysis on an experiment. Each experiment has a contribution from *random* and *systematic* errors.

Random errors are revealed when replicate measurements of a single quantity are made; they cause the individual readings to fall on either side of the mean. Such errors are said to affect the *precision* of the results – large random errors lead to poor precision and *vice versa*. Systematic errors, on the other hand, cause all the results in a series to deviate from the true value of a measured quantity. Such errors affect the *accuracy* – closeness to truth. *Bias* is used to describe the systematic error.

The use of replicate results on independently, as an indication of systematic errors is of little value and additional experimental precautions must be taken. Standard reference materials or a quality control standard for which the true value of the measured quantity is known in advance, may be used.

Systematic errors may arise from equipment, whereas random errors are of human origin. Instruments inevitably generate random errors, and some causes of human systematic errors (e.g.colour blindness, number bias) are easily identified. Nonetheless, considerable bias can arise from the erroneous assumption that analytical instruments are perfectly accurate, and frequent calibration and checking of instruments are an important protection against systematic errors.

The standard deviation can be used as a measure of the random error of the replicate measurement.

The results of instrumental analyses are evaluated using calibration methods. A typical calibration experiment is performed by making up a series of standard solutions containing known amounts of analyte and taking each solution separately through an instrumental analysis procedure with a well defined protocol. For each solution, the instrument generates a signal, and these signals are plotted on the y-axis of a calibration graph, with standard concentrations on the x-axis. A straight line or curve is drawn through the calibration points and may then be used for the determination of a test sample. The unknown is taken through exactly the same protocol as the standards, the instrument signal is recorded and the test concentration estimated from the calibration graph by interpolation.

This approach to the determination of concentration poses several problems. It is uncertain what type of line, straight or curved should be drawn through the calibration points, given that the instrument signals obtained from the standards will be subject to random errors. The limit of detection of the analysis must be taken into consideration

Linear calibration

Correlation coefficient

Analytical procedures are designed to give a calibration graph over the concentration range of interest, and analysts who use such methods routinely may assume linearity with only occasional checks. In the development of new methods, it is necessary that the assumption of linearity must be carefully investigated.

A graph is plotted of the instrument response on the y-axis against the known concentrations of the standards on the x-axis. One of the calibration points should be a '*blank*', i.e. a sample containing all the reagents, solvents, etc., present in other standards but no analyte. It is poor practice to subtract the blank signal from those of the other standards before plotting the graph. The blank point is subject to errors as are all the other points and should be treated in the same way.

Linearity is tested using the correlation coefficient, *r*. Generally r falls between -1 and +1. in the hypothetical situation when $r = -1$, all the points on the graph would lie on a perfect straight line of negative slope; if $r = +1$, all the points would lie exactly on a line of positive slope; and $r = 0$ indicates no linear correlation between x and y. This linearity can also be tested by the 'Least Squares' Line.[11]

2.2 Transition metal ions in aqueous solution

Transition elements are those metals that have partially filled *d* or *f* shells in any one of their commonly occurring oxidation states.[12] The elements of concern in this work are copper, nickel, cobalt and iron.

These elements exhibit variable oxidation states, and their co-ordination ions and compounds are often coloured in one if not all oxidation states. Because of their partially filled shells, they form at least some paramagnetic compounds, due to unpaired electron density in their atomic or molecular orbitals.

Transition metal ions in aqueous solutions, generally exist as complex ions in which water molecules, acting as Lewis bases, "coordinate" to the small cation (which acts as a Lewis acid). The water molecules in these structures are known as ligands forming a dative

covalent bond to the metal via the oxygen atom lone pairs. The distinguishing characteristic of such bonds is that the shared electron pairs that constitute the bond come only from one bonded species, usually from the ligand which acts as a Lewis base, in contrast to normal covalent bond, in which the atom donates one electron to the shared pair which constitutes the chemical bond.[13]

Uncoordinated metal cations M^{n+}, thus usually exist in the gas phase only and in solution invariably form hydrated cations depending on conditions. Aqueous $Cu^{2+}(aq)$ ions are generally co-ordinated with 4 H_2O molecules resulting in the aqua species $Cu(H_2O)_4^{2+}$, aqueous species of Ni^{2+} are co-ordinated to 6 H_2O molecules generally forming an octahedral $Ni(H_2O)_6^{2+}$ complex ion in aqueous solutions at slightly acidic pH values. Co^{2+} is generally also co-ordinated to 6 H_2O molecules, viz. $Co(H_2O)_6^{2+}$ and Fe^{2+} is similarly coordinated to 6 H_2O molecules as the octahedral $Fe(H_2O)_6^{2+}$. In these oxidation states, the different complex metal ions display different colours as shown in the table below.

Table 2.1 The transition metal ions complexes and their colours in water.

Ion	Colour
Cu^{2+}	Blue
Ni^{2+}	Green
Co^{2+}	Red
Fe^{2+}	Green
Fe^{3+}	Orange, yellow or brown

The colour of the transition metal ion in aqueous solution is associated with an incomplete *d* level (between 1 and 9*d* electrons) and the nature of the ligands surrounding the ion.[14]

The colour and magnetism of transition metal complexes is explained by the crystal field theory which highlights the effects of ligands approach on *d*-orbital energies of the metal ion. This is reviewed fully in the literature[15]

A complex metal ion has a particular colour for one of two reasons:

- It reflects (transmits) light of that colour. Thus, if a substance absorbs all wavelengths except green, the reflected light enters the eye and is interpreted as green.

- It absorbs light of the complementary colour. Thus, if a substance absorbs only red, the complement of green, the remaining mixture of reflected wavelengths enters the eye and is interpreted as green also.
-

2.2.*1 Splitting of d orbitals in an octahedral field of ligands*

The crystal field model explains that the properties of complexes as a result from the splitting of *d*-orbital energies, which arises from electrostatic interactions between metal ion and ligands. [16] The model assumes that a complex ion forms as result of *electrostatic attractions between the metal cation and the negative charge of the ligands*. This negative charge is either partial in a polar neutral ligand like NH_3 or full in an anionic ligand like Cl^- anion. The ligands approach the metal ion along the x, y and z axes, which minimises the overall energy of the system.

The Fig 2.4 below shows six ligands moving toward a metal ion to form an octahedral complex. As the ligands approach, their electron pairs repel electrons in the five *d* orbitals of the metal. In the isolated metal ion, the *d* orbitals are affected as the complex forms. As the ligands approach, their electron pairs repel electrons in the five *d* orbitals of the metal. In the isolated metal ion, the *d* orbitals have equal energies despite their different orientations. In the electrostatic field of ligands, however, the *d* electrons are *repelled unequally because they have different orientations*. Since the ligands move along the *x,y* and *z* axes, they approach *directly toward* the lobes of the $d_{x^2-y^2}$ and d_{z^2} orbitals but *between* the lobes of the $d_{xy,}$ d_{xz}, and d_{yz} orbitals. As a result, electrons in the $d_{x^2-y^2}$ and d_{z^2} orbitals experience *stronger* repulsions than those in the $d_{xy,}d_{xz}$, and d_{yz} orbitals.

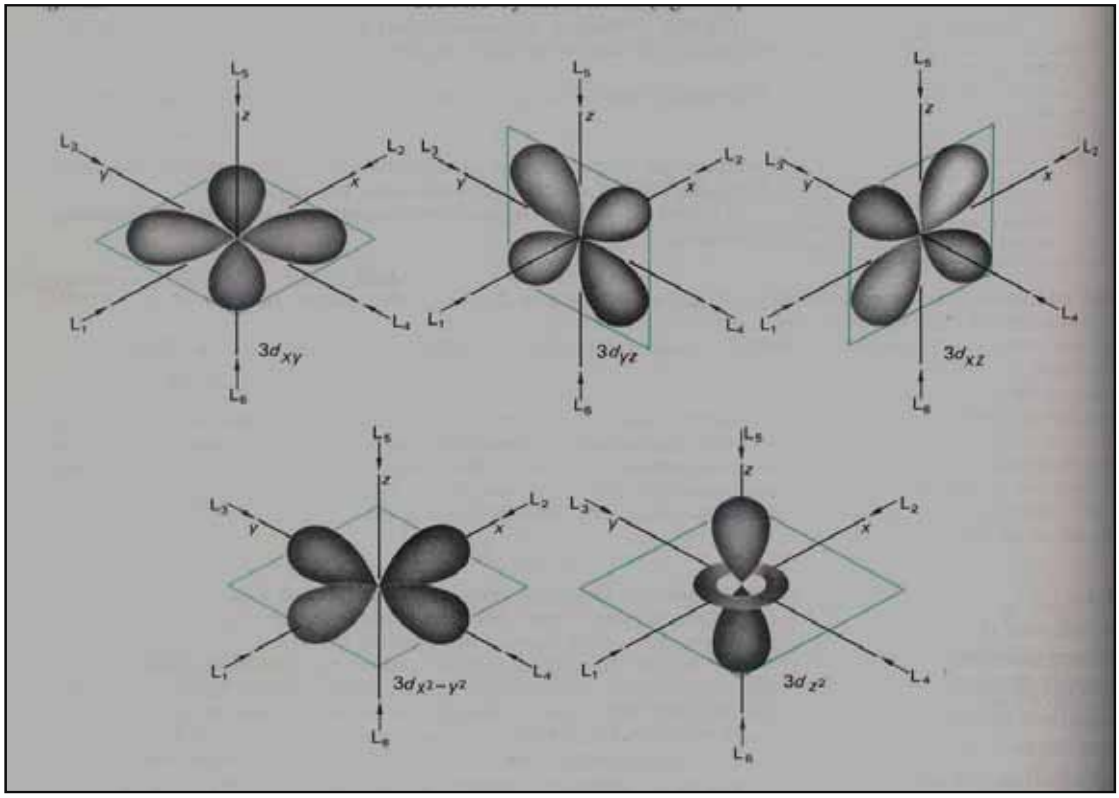

Fig 2.4 The five** d **orbitals in an octahedral field of ligands. The direction of the ligand influences the strength of repulsion of electrons in the various metal** d **orbitals. [17]

An energy diagram of the orbitals shows that all five *d* orbitals are higher in energy than in the free metal ion because of repulsions from the approaching ligands, but the orbital energies with two *d* orbitals higher than the other three.(see Fig 2.4 above)

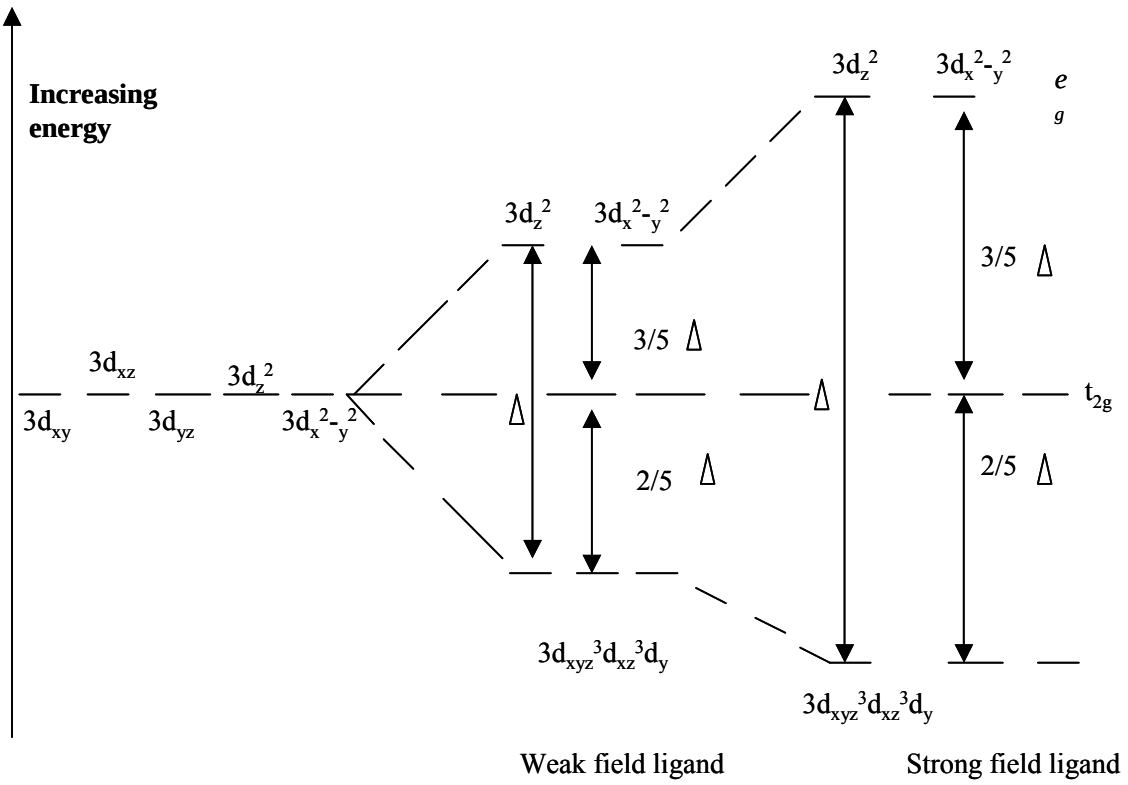

Fig 2.5 The splitting of the 3d levels in an octahedral environment of ligands.

The 3*d* levels are split into an upper group of two (doubly degenerate, labelled e_g) and a lower group of three (trebly degenerate, labeled t_{2g}) orbitals; the splitting of the levels is energy difference, represented by the symbol Δ. If we assume the zero of energy as the state of affairs that would obtain if each of the five 3*d* orbitals had interacted equally with the six ligands, then each of the upper two orbitals is raised by 3/5 Δ (or 6/5 Δ collectively) while each of the lower three orbitals is lowered by 2/5 Δ (or 6/5 Δ collectively) so that no net energy gain or loss occurs. As the diagram shows the degree of splitting depends upon the strength of the crystal field generated by the individual ligand

Complex transition metal ions are coloured because radiation in the visible spectrum is of the appropiate frequency to promote an electronic transition between the t_{2g} and e_g orbitals. The relationship between the energy difference and the frequency of light absorbed is given by

$$\Delta = h\nu$$

where *h* is Planck's constant and *v* is the frequency of light absorbed. Hydrated Cu^{2+} ions are blue since light towards the red end of the visible spectrum is absorbed in bringing about the electronic transition.

These electronic transitions are corresponding to the Δ, generally referred to as *d-d* transitions. These transitions are weak for all first row transition metal ions in the periodic table.(ε < 1000) However, it is also possible to have much more intense electronic absorptions, which arise out of different type of metal to ligand charge transfer (MLCT) type absorptions, which can be much more intense (ε > 1000) for example:

$$Fe^{2+} + SCN^- \longrightarrow [Fe(SCN)_6]^{4-}$$

(deep blood red complex)

The deep blood red complex $[Fe(SCN)_6]^{4-}$, has a very high ε. In acidic aqueous solutions free from strongly complexing ligands, the $Cu(H_2O)_6^{2+}$ colours are due to *d-d* transitions with ε < 1000.

2.2.2 Explaining the colours of transition metal complexes

The remarkably diverse colours of coordination compounds are determined by the energy difference (Δ) between the t_{2g} and e_g orbitals sets in their complex ions. When the ion absorbs light in the visible range, electrons are excited from the lower energy t_{2g} level to the higher e_g level. The difference between two electronic energy levels in the ion is equal to the energy of the absorbed photon:

$$\Delta E_{electron} = E_{photon} = h\upsilon$$

Since only certain wavelengths of incoming white light are absorbed, the substance has colour. Absorption spectra show the wavelengths absorbed by a given metal ion with different ligands and by different metal ions with the same ligand. Thus, the energy of absorbed light can be related to Δ values, and two other important points emerge:

1. For a given ligand, the colour depends on the oxidation state of the metal ion e.g. A solution of $[V(H_2O)_6]^{2+}$ ion is violet, and a solution of $[V(H_2O)_6]^{3+}$ is yellow.
2. For a given metal ion, the colour depends on the co-ordinated ligands, e.g. $[Cr(NH_3)_6]^{3+}$ ion is yellow while $[Cr(NH_3)_5Cl]^{2+}$ ion is purple.

2.3 Absorption spectra of $[Cu(H_2O)_6]^{2+}$ species in aqueous solution.

Copper has one *s* electron outside a completed *d* shell. Copper has variable oxidation states i.e. +1, +2 and +3. The relative stabilities of Cu^{1+} and Cu^{2+} in aqueous solution depend very strongly on the nature of the anions or other ligands present and vary considerably with solvent or the nature of neighbouring atoms in a crystal.

In aqueous solution only low equilibrium concentrations of Cu^{1+} (<10^{-2} M) can exist and the only simple compounds that are stable are the highly insoluble ones such as CuCl or CuCN. This instability of Cu^{2+} toward water is due partly to the greater lattice and solvation energies and higher formation constants for complexes of the Cu^{2+} ion, so that the ionic Cu^{1+} derivatives are unstable.[18]

On the other hand, Cu^{2+} is the most stable oxidation state and oxidation to +3 is more difficult. Cu^{2+} has the d^9 electronic configuration and has an unpaired electron. Its compounds are coloured due to *d-d* electronic transitions and the compounds of Cu^{2+} are generally paramagnetic. The hydrated ion $[Cu(H_2O)_6]^{2+}$ is formed when the hydroxide or carbonate is dissolved in acid, or when copper sulphate is dissolved in water. This ion has the characteristic blue colour associated with copper salts, and has a distorted octahedral shape. There are two long bonds trans to each other and four short bonds. This is called tetragonal distortion and is a consequence of the d^9 configuration.

The blue colour is due to the presence of an absorption band in the 600-900nm region of the spectrum.(see Fig 2.6 below)

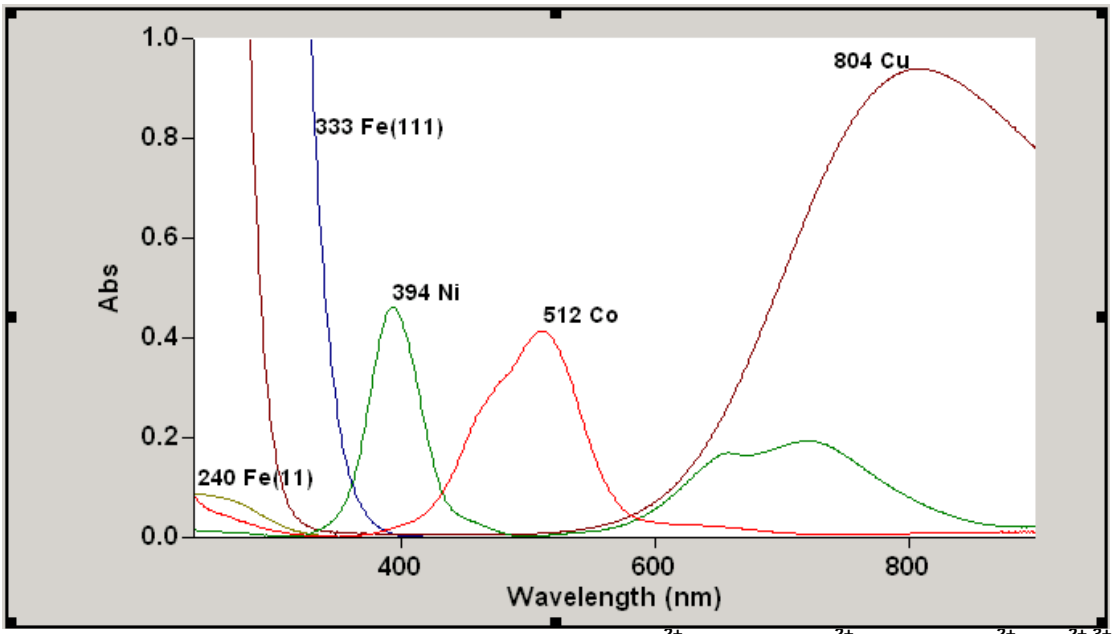

Fig 2.6 Absorption spectrum of characteristic $[Cu(H_2O)_6]^{2+}$, $[Co(H_2O)_6]^{2+}$, $[Ni(H_2O)_6]^{2+}$, $Fe^{2+,3+}$(aq) in 0.7M orthophosphoric and 1M sulphuric acid mixture.

2.4 Absorption spectra of $[Co(H_2O)_6]^{2+}$ species in aqueous solution

Co^{1+} exists in many complexes with π bonded ligands e.g $[Co(CO)_4]^-$ reacts with organic isonitriles R-NC, giving $[Co(CNR)_5]^+$ which has a trigonal bypyramid structure.

Cobalt has variable oxidation states ranging from +1, +2 to +3. Co^{2+} has a d^7 electronic configuration. These species forms an extensive group of simple and hydrated salts. The hydrated salts are red or pink and contain the $[Co(H_2O)_6]^{2+}$ ion or other octahedrally coordinated ions. The hydrated ion is stable in water.

Co^{2+} complexes may be tetrahedral or octahedral. Since there is only a small difference between the two forms they sometime exist in equilibrium. Co^{2+} forms more tetrahedral complexes than any other transition metal ion.

Co^{2+} ions are fairly stable and difficult to oxidise. However, Co^{3+} ions are less stable and are reduced by water. Co^{3+} is extremely inert, particularly low spin Co^{3+}. In contrast, many Co^{2+} complexes are readily oxidised to Co^{3+} complexes and these complexes are very stable. In water, $[Co(H_2O)_6]^{2+}$ is stable, however, if a ligand with a stronger field ligand than water co-ordinates to Co^{2+}, the Co^{2+} complex solutions interaction with O_2 is oxidised to Co^{3+} complexes.[17] In my experiments Co^{2+}(aq) species is the predominant species in the sulphuric/phosphoric acid mixture. From Fig 2.6, we observe that Co^{2+} (aq) has a maximum absorption at 512nm.

2.5 Absorption spectra of $[Ni(H_2O)_6]^{2+}$ species in aqueous solution

Nickel has many oxidation states which are (+1), (+2), (3)and (4) but its chemistry is predominantly that of the +2 oxidation state. Ni^{2+} has a d^8 electronic configuration, exist in aqueous solution of its salts as a hexaqua nickel ion, $[Ni(H_2O)_6]^{2+}$. Aqueous solutions of nickel salts such as, $NiSO_4$, $NiCl_2$ has a pale green colour. The wavelengths involved here cover the near UV, through to the visible to the near IR portions of the spectrum. Ni^{2+} also forms many complexes, which are mainly square planar or octahedral. The Ni^{2+} ion is observed to absorb strongly at 394nm according to Fig 2.6.

2.6 Absorption spectra of $[Fe^{2+}(H_2O)_6]^{2+}$ and $[Fe^{3+}(H_2O)_6]^{3+}$ species in aqueous solution

The main oxidation states for iron are +2 and +3. Fe^{2+} is the most stable in aqueous solution. Fe^{3+} is slightly oxidizing. Fe^{2+} has a d^6 electronic configuration whereas Fe^{3+} has a d^5 electronic configuration.

Aqueous solutions of Fe^{2+} in the absence of complexing anions contain the pale blue-green ion $[Fe(H_2O)_6]^{2+}$, which is oxidized in acid solution. Oxidation is easier in basic solution but neutral and acid solutions of Fe^{2+} oxidise less rapidly with increasing acidity. This is because Fe^{3+} is actually present in the form of hydroxo complexes, except in extremely acid solutions, and there may also be kinetic reasons.

Phosphorous ligands give a variety of complexes such as *cis* and *trans* -FeX_2 (diphos) where X can be a halogen, hydrogen or methyl group. Fe^{2+} absorbs in the UV region < 300nm and Fe^{3+}<390nm. (refer to Fig 2.6).

The analysis of transition metals by uv-visible spectroscopy in synthetic solutions and in refinery plant streams will be practically investigated.

References

1. Skoog, West and Holler, *Fundamentals of analytical chemistry*, 6th edn., 561.
2. J.A. Howell and L.G. Hargis, *Analytical Chemistry*, 1978, **50**, 243.
3. T. Owen, *Fundamentals of UV-Visible spectroscopy*, 1998, **10**.
4. Skoog, West and Holler, *Fundamentals of analytical chemistry*, 6th edn., 514.
5. P. Suppan, *Chemistry and Light*, 1994, 39.
6. D. A. Skoog and D. M.West, *Fundamentals of analytical chemistry*, 4th edn., 493.
7. J.A. Howell and L.G. Hargis, ,*Analytical Chemistry*, 1978,**50**,5, 245.
8. A. I. Vogel, *A textbook of quantitative inorganic analysis*, 3rd edn., 817.
9. Skoog, West and Holler, *Fundamentals of analytical chemistry*, 6th edn., 570-571.
10. J C. Miller and J N. Miller, *Analyst*, 1988, **113**, 1351-1355.
11. J. C. Miller and J N. Miller, *Analyst*, 1988, **113**,1351-1355.
12. F.A Cotton and G. Wilkinson, *Advanced Inorganic Chemistry*, 5th edn., 625.
13. J.D Lee, *Concise Inorganic Chemistry*, 1996, 5th edn., 784.
14. G.F. Liptrot, *Modern Inorganic Chemistry*, 1972,395.
15. Silberberg, Chemistry,*The molecular nature of matter and change*, 2nd edn.,1026-1034.
16. F. A Cotton,G. Wilkinson and P. L. Gaus, *Basic Inorganic Chemistry*,3rd edn.,504. F.A. Cotton and G. Wilkinson, *Advanced Inorganic Chemistry*, 5th edn., 757.
17. F.A. Cotton and G. Wilkinson, *Advanced Inorganic Chemistry*, 5th edn., 735.

Chapter 3

Experimental

In this chapter , the experimental techniques used and the experiments performed in order to investigate the simultaneous absorptiometric analysis of Cu^{2+}(aq),Ni^{2+}(aq), Co^{2+}(aq) and $Fe^{2+,3+}$(aq), in synthetic mixtures and refinery streams, will be described.

3.1 Validation of the Varian Carey 100 spectrophotometer

The Varian Carey 100 spectrophotometer has many operators and is used on a daily basis. It is necessary to check the calibration on the instrument regularly to ensure that the response measured from the instrument is credible.

The instrument has standard validation tests, i.e. photometric noise test, wavelength accuracy test, wavelength reproducibility test and baseline flatness test, set up within the instrument. These tests can be run on a monthly basis to monitor the instrument. In addition, the calibration of the instrument can be checked using the potassium dichromate and potassium permanganate method reported in the literature.[1]

Calibration of the instrument

$K_2Cr_2O_7$ and $KMnO_4$ were weighed out to prepare respectively, 0.0005M , 0.001M and 0.002M, standard solutions of each and made up to mark using the diluent, i.e. 0.7M H_3PO_4 and 1M H_2SO_4 mixture.(as the diluent)

Spectra of these standard solutions were measured at $\lambda_{240\text{-}600nm}$, taking note specifically of the absorbances at 440nm and 545nm. (see Table 3.1).

Table 3.1 Absorbances measured for the standard solutions of $K_2Cr_2O_7$ and $KMnO_4$ respectively.

	Absorbance			Absorbance	
$K_2Cr_2O_7$ M	**440nm**	**545nm**	**$KMNO_4$ M**	**440nm**	**545nm**
0.0005	0.177	0.005	**0.0005**	0.049	0.207
0.001	0.369	0.003	**0.001**	0.120	0.754
0.002	0.727	0.011	**0.002**	0.280	2.785

The absorbance data was then used to calculate the molar absorptivity of the dichromate and permanganate ions in solution using Beer's law. (see Table 3.2)

Table 3.2 Absorptivities determined for the $Cr_2O_7^{2-}$ and MnO_4^- ions in 0.7M H_3PO_4 and 1M H_2SO_4 mixture.

Stock Solution	Absorptivity	
	440nm	545nm
$K_2Cr_2O_7$	366.3	6.050
$KMNO_4$	126.45	610.1

Mixtures of 0.001M $K_2Cr_2O_7$ and 0.0005M $KMnO_4$ were then prepared in varying ratios, with addition of 1mL concentrated H_2SO_4 to each mixture. The spectra of these mixtures were recorded and the absorbance measured at 440nm. (see Table 3.3 and Fig 3.1).

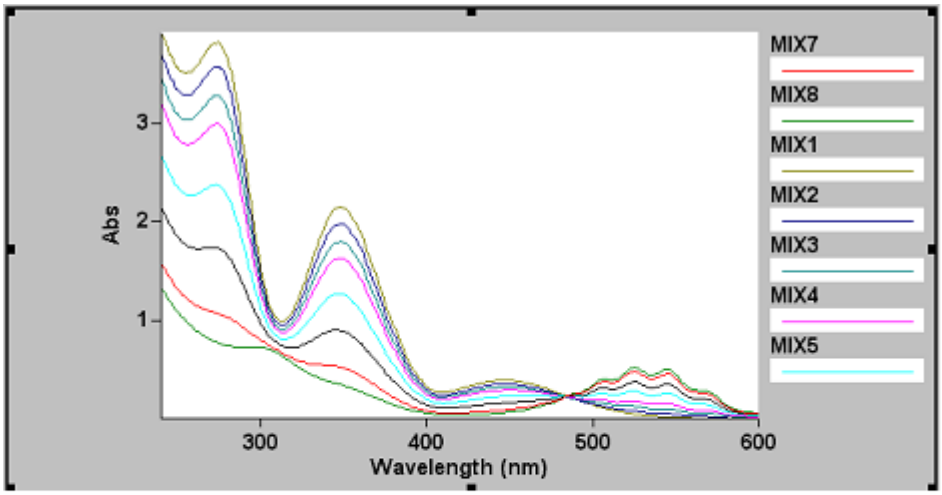

Fig 3.1 Absorption spectra of the various ratios of 0.001M $K_2Cr_2O_7$ and 0.0005M $KMNO_4$ in 0.7M H_3PO_4+ 1M H_2SO_4 mixture.

Table 3.3 Comparison of absorbance obtained in mixture of 0.001M $K_2Cr_2O_7$M and 0.0005M $KMNO_4$ in the diluent against literature. [2]

Mixture No.	0.001 M $K_2Cr_2O_7$ (mL)	0.0005M $KMNO_4$ (ml)	Absorbance exp.	Absorbance calculated [7]	Absorbance theoretical[7]
1	50	0	0.390		0.371
2	45	5	0.336	0.340	0.338
3	40	10	0.313	0.308	0.307
4	35	15	0.284	0.277	0.277
5	25	25	0.218	0.214	0.211
6	15	35	0.150	0.151	0.147
7	5	45	0.077	0.088	0.086
8	0	50	0.049		0.057

The calculated absorbance values are obtained from Beer's law, using the known concentration of the mixture and the calculated absorptivity at 440nm. The experimental

absorbances obtained, the calculated absorbances and the theoretical absorbances from literature compare well. (see Table 3.3)

3.2 Calibration of glassware

The glassware used, such as volumetric flasks and pipettes are designed to contain accurate volumes of liquids. In the refinery laboratory, this glassware is used by many people for several different applications. Therefore, it is necessary that the calibration of the glassware is checked regularly to detect any changes. A-Grade volumetric flasks were used for all the experiments.[3]

Materials

Demineralised Water

Apparatus

- Analytical balance
- Pipette filler
- Thermometer
- Pipettes
- Volumetric flasks

Method

Pre-calibration procedure[3]

Prior to checking the calibration on glassware, the glassware must be inspected. The glassware should be clean, dry and free of cracks or other defects.

The calibration was done in a room maintained at constant temperature of 17^0C. The demineralised water and the glassware was placed in the room an hour before calibration. This would allow for the glassware and demineralised water to reach the room temperature. The balances were also calibrated before use.

Calibration procedure

Volumetric flasks

The volumetric flask was placed on an appropriate balance and the balance tared. The flask was then filled with demineralised water to the mark. The mass of the flask, recorded and the temperature of the water used in the calibration was recorded.

Pipettes

An empty volumetric flask was placed on the balance and tared. The temperature of the demineralised water used was recorded. The pipette was filled with water to the mark. It was then emptied into the volumetric flask and allowed to drain for a further 15 seconds. The weight of the volumetric flask was recorded.

The mass and temperature of the water, and a factor from literature are needed to calculate the tolerances on the glassware.[4](see Table 3.4 below).

Table 3.4 Temperature correction of glass volumetric apparatus[4]

Temperature (^{0}C)	Weight (g)	Vol. Of 1g H_2O	Temperature(^{0}C)	Weight (g)	Vol. Of 1g H_2O
15	998.00	1.0020	**24**	996.33	1.0037
16	997.86	1.0021	**25**	996.09	1.0039
17	997.71	1.0023	**26**	995.85	1.0042
18	997.54	1.0025	**27**	995.49	1.0045
19	997.37	1.0026	**28**	995.32	1.0047
20	997.18	1.0028	**29**	995.05	1.005
21	996.98	1.0030	**30**	994.76	1.0053
22	996.78	1.0032	**31**	994.47	1.0056
23	996.56	1.0034	**32**	994.17	1.0059

A calibration value must be calculated and compared to the tolerances in literature. The formula to calculate the calibration value is as follows:

Calibration value = a x b

where

a = mass of water (g)

b= factor obtained from Table 3.4.

This value is compared to the tolerances given in Table 3.5. These values must be within tolerances given for the glassware being tested to be considered as calibrated.

Table 3.5 Tolerances for nominal capacity

Volume (mL)	1-99	100-99	100-999	1000-2000	2000
Tolerance	0.05	0.10	0.15	0.15	0.25

The results obtained for the pipettes and volumetric glassware were within the 0.05 tolerance limits. Therefore, I could confidently proceed with using the glassware.

3.3 Preparation of stock solutions

Stock solutions of the sulphate salts of copper, nickel, cobalt, ferrous and ferric ions were prepared in a 0.7M H_3PO_4/1M H_2SO_4 mixture.

The sulphuric/orthophosphoric mixture was chosen as a diluent because the refinery streams are in sulphuric acid medium and orthophosphoric acid masks iron that may cause interference in the analysis.[5] Also, the quantity of iron that is masked by the phosphate ion is not known in solution, and it was still necessary later in the experiments to investigate the interference that may be caused by the unmasked iron. This mixture is a neutral buffer and the above mentioned ions dissolve easily in it.

Materials	**Supplier**
• Demineralised H_2O	
• H_2SO_4	Associated Chemical Enterprises
• Orthophosphoric acid	Saarchem, 85%
• $CuSO_4.5H_2O$	Saarchem, 99-100.5%
• $NiSO_4.6H_2O$	Promark, 98%
• $Fe_2(SO_4)_3$	Associated Chemical Enterprises
• $FeSO_4$	Alfar Aesar, 99.999%
• $CoSO_4.7H_2O$	Alfar Aesar, 99.999%

Apparatus	
• Analytical balance	Mettler
• Spectrophotometer	Varian Carey 100
• 1cm matched quartz cuvettes	
• A-Grade volumetric flasks	
• Calibrated pipettes	
• Beakers	
• Measuring cylinders	

Five litres of 0.7M H_3PO_4 and 1M H_2SO_4 mixture was prepared in a volumetric flask and made up to mark using demineralised water. This mixture was prepared regularly.

Preparation of 0.7M H_3PO_4 and 1M H_2SO_4 mixture as a matrix for absorption measurements.

A five litre beaker was filled with demineralised water to half its volume. The beaker was then placed in a water bath with ice cubes. 270 mL of H_2SO_4 was transferred using a measuring cylinder into the beaker very slowly, in a fume hood. The solution was then left to cool. After being cooled to room temperature, i.e. 25^0C, 240mL of H_3PO_4 was added to the solution. The mixture was then transferred to a five litre volumetric flask and made up to the mark with demineralised water. This mixture was used as diluent for further experiments.

Preparation of stock solutions of copper sulphate, nickel sulphate, cobalt sulphate, ferrous sulphate and ferric sulphate in the 0.7M H_3PO_4 and 1M H_2SO_4 mixture.

Accurate masses of analytical grade $CuSO_4.5H_2O$, $NiSO_4.6H_2O$, $Fe_2(SO_4)_3$, $FeSO_4$ and $CoSO_4.7H_2O$ were weighed into separate beakers to prepare the desired 50g/L stock solution of each metal. The diluent was added to each beaker and the mixture left on a hotplate for thirty minutes to allow complete dissolution. The solution was then transferred into the appropriate volumetric flask using the diluent and made up to mark.

Similarly, 5g/L of ferrous sulphate and ferric sulphate were prepared individually. However, these salts dissolve readily in the diluent and do not require heating.

The stock solution were standardised by the following literature methods:

- 50g/L copper sulphate solution — Short Iodide Method [6]
- 50g/L nickel sulphate solution — EDTA Method [7]
- 5g/L ferrous sulphate — $K_2Cr_2O_7$ titration[8]
- 5g/L ferric sulphate — Reduction & $K_2Cr_2O_7$ titration[8]
- 50g/L cobalt sulphate — Primary standard

Standardisation of copper sulphate solution

Materials

- copper sulphate stock solution
- 20 % sodium carbonate
- 60 % potassium Iodide

- 0.1 N sodium thiosulphate
- 2g/L starch solution
- 20 % acetic Acid
- sodium fluoride

Method

A 2 mL aliquot of copper sulphate stock solution was pipetted into a 250 mL beaker. 5mL of 20% sodium carbonate was added, while mixing, until a thick precipitate forms. 5mL of acetic acid was then added, while mixing, until the solution is clear. Then 2 grams of sodium fluoride was added and swirled to mix. To this mixture, was then added 5mL of 60 % potassium iodide to solution and mixed well. This mixture was then titrated with 0.1N sodium thiosulphate to a light yellow colour. A few milliliters of starch solution was then added to obtain just a blue colour. This was then titrated a bit further until the blue colour just disappeared and the reading on the burette recorded.

Calculation

$$Cu_{conc} = (\text{titration (mL)} * 6.3547) / \text{aliquot (mL)}$$

where Cu_{conc} = copper concentration (g/L)
titration (mL) = volume (mL) 0.1 N thiosulphate

Standardisation of nickel sulphate stock solution

Materials

- nickel sulphate stock solution
- demineralised water
- 50% hydrochloric acid
- dimethylglyoxime reagent
- ammonia solution

Method

A 3mL aliquot of the nickel stock solution was pipetted into a 500mL volumetric flask and made up to mark using demineralised water. 100mL of this diluted solution was transferred into the 400mL beaker. Demineralised water was added up to 200mL and 5mL 1:1 hydrochloric acid was added as well. The beaker was covered with a watch glass and glass rod inserted. This mixture was heated to 70-80 ^{o}C on a steam bath. Then 1:1 ammonia was

added dropwise directly to the solution and the solution was stirred constantly until precipitation occurred. This mixture was allowed to stand on a steam bath for 20-30 minutes, and the solution was tested for complete precipitation when the red precipitate had settled out. The precipitate was allowed to stand for an hour, cooling at the same time. The cold solution was filtered using a Gooch crucible, previously heated to 120^{o} C, and weighed after cooling in a dessicator. The precipitate, i.e. Ni $(C_4H_7O_2N_2)_2$ was washed with cold water until free from chloride, and dryed in an oven at 120^{o}C for an hour. It was allowed to cool in a dessicator and then weighed. The drying was repeated until a constant weight was achieved.

Calculation

Ni (g) = 0.2032 x mass of Ni $(C_4H_7O_2N_2)_2$

Standardisation of ferrous sulphate stock solution

Materials

- ferrous sulphate stock solution
- 0.1 N potassium dichromate
- sodium diphenylamine sulphonate(I) (indicator)

Method

20 mL of ferrous sulphate stock solution was pipetted into 250mL beaker. 8 drops of indicators (I) was added to the solution and the solution was titrated with 0.1 N potassium dichromate to a grayish-blue tint near the end point. At the end-point, the solution has a violet-blue colouration. This titration was carried out in replicate. The titrated value was recorded.

Calculation

1mL 0.1 N potassium dichromate = 0.05585g Fe.

Standardisation of ferric sulphate

Materials

- ferric sulphate stock solution
- demineralised water

- 2*N* sulphuric acid
- stannous chloride solution
- hydrochloric acid
- 5 % mercuric chloride
- sodium diphenylamine
- 2.5 % sulphuric acid
- phosphoric acid

Method

25 mL aliquot of ferric sulphate stock solution was pipetted into a 250mL beaker. Stannous chloride was added dropwise from a burette with stirring, until the yellow colour of the solution nearly disappeared. Reduction is completed by diluting the concentrated solution of stannous chloride with two volumes of dilute hydrochloric acid and adding the dilute solution dropwise, with agitation after each addition, until the liquid has a faint green odour, free from any tinge of yellow. 5% mercuric chloride was added, dropwise to form a white precipitate. Then 200mL of 2.5 % sulphuric acid was added, and 5mL of phosphoric acid and 0.3-0.4 mL of sodium diphenylamine sulphonate indicator. This solution was then titrated rapidly with 0.1 N potassium dichromate to the first permanent violet-blue colouration. This titration was carried out in triplicate. The titration value was recorded and the iron value calculated similarly to the standardisation of ferrous stock solution.

Standardisation of the cobalt sulphate stock solution

Method

Cobalt sulphate was prepared as a primary standard. This compound had a certificate of analysis and the concentration prepared was checked with atomic absorption analysis. The stock solution was diluted and the solution measured.

These stock solutions were kept in a cupboard in a temperature controlled room at 25^0C. The concentration of these stocks was regularly monitored.

3.4 Sample measuring procedure

The cuvettes were rinsed three times with the solution that is being measured. A blank, i.e. the diluent, was first measured and all samples were measured against the blank. A quality control sample of known concentration was measured at regular intervals during the recording of spectra for several samples. If this sample was not within 10% accuracy, the sample run would stop, the instrument would be recalibrated and sample measurement continued. Also, cuvettes were cleaned with 10% HNO_3 acid after use.

All required solutions, i.e. synthetic mixtures for further experiments were prepared from the stock solutions.

3.5 Preparation of refinery samples

Refinery samples are collected from their respective sampling point by a sampler on an hourly basis. The 250 mL sample is filtered and cooled to room temperature, i.e. 25^0C. A 2mL aliquot of the sample was taken and pipetted into a 25mL volumetric flask and the spectra recorded.

3.6 Calculation of concentration in solution

The absorbance data was extracted at specific wavelengths was used to simultaneously calculate the concentration of the three species, using simple spreadsheet calculations. This fundamentally exercised Beer's law for multicomponent analysis discussed earlier in chapter 2. This involved using Solver in Excel and solving three simultaneous equations, determining the concentration of Cu^{2+}(aq), Co^{2+}(aq) and Ni^{2+}(aq) in solution. (see Appendix, Calculation)

References

1. A. I. Vogel, *A textbook of quantitative inorganic analysis*, 1961, **3**, 819**.**
2. A. I. Vogel, *A textbook of quantitative inorganic analysis*, 1961, **3**, 818.
3. Calibration of glassware, WI/Lab/Q1.4, Rustenburg Base Metal Refiners (Pty) Ltd.
4. D. R. Lide, *Handbook of chemistry and physics*, **71**, 15-17, 1990-1991.
5. O. E. Lanford and S. J. Kiehl, *A study of the reaction of ferric ion with orthophosphate in acid solution with thiocyanate as an indicator for ferric ions.*
6. V.S Dillon, *Assay Practice on the Witwatersrand*, 1958, 276.
7. A. I. Vogel, *A textbook of quantitative inorganic analysis*, 1961, **3**, 479,.
8. A. I. Vogel, *A textbook of quantitative inorganic analysis*, 1961, **3**, 309.

Chapter 4

Results and Discussion

In the BMR process streams, Cu^{2+}(aq), Co^{2+} (aq), Ni^{2+}(aq) species are present in the concentration range of 20-100g/L as cited in literature.[1] Fe^{2+}(aq) is also present in the range of <1g/L, while Fe^{3+}(aq) is not present in significant concentrations in the BMR as this species affects the electrowinning of copper and nickel cathodes. Five process streams from the BMR were identified as critical streams for method development for spectrophotometric potentially online analysis of Cu^{2+}(aq), Co^{2+} (aq), Ni^{2+}(aq) species.

The following streams were chosen:

- "nickel feed " 80g/L nickel
- "nickel product" 80-90g/L nickel
- "copper feed" 70-90g/L copper, 30-40g/L nickel
- "copper spent" 30-50g/L copper
- "cobalt sample" 50-60g/L cobalt

4.1 Analysis of refinery streams

A 2mL aliquot of these samples was pipetted into 25mL volumetric flasks and made up to mark using the diluent (0.7M H_3PO_4 and1M H_2SO_4). The absorption spectrum of each of the streams was recorded to determine the characteristic absorption spectra of the potential species present for each stream.

The "nickel feed" and "nickel product" spectrum with λ_{max} = 394nm and absorption at 804nm was observed as shown in Fig 4.1. This spectrum is similar to the spectrum for the $[Ni(H_2O)_6]^{2+}$ species reported in literature.[2] Therefore, it can be deduced that $[Ni(H_2O)_6]^{2+}$ is the predominant species in the "nickel feed" and "nickel product" streams.

In Fig 4.2, the spectrum of "copper feed" and "copper spent" λ_{max} = 804nm and significant absorption λ = 394nm was observed. Similarly, as reported in literature, this spectrum indicates the presence of $[Cu(H_2O)_6]^{2+}$ and $Ni(H_2O)_6^{2+}$ respectively. In Fig 4.3, the spectrum of "cobalt sample", λ_{max} = 512nm was observed which is characteristic of the $[Co(H_2O)_6]^{2+}$ species in aqueous solution.

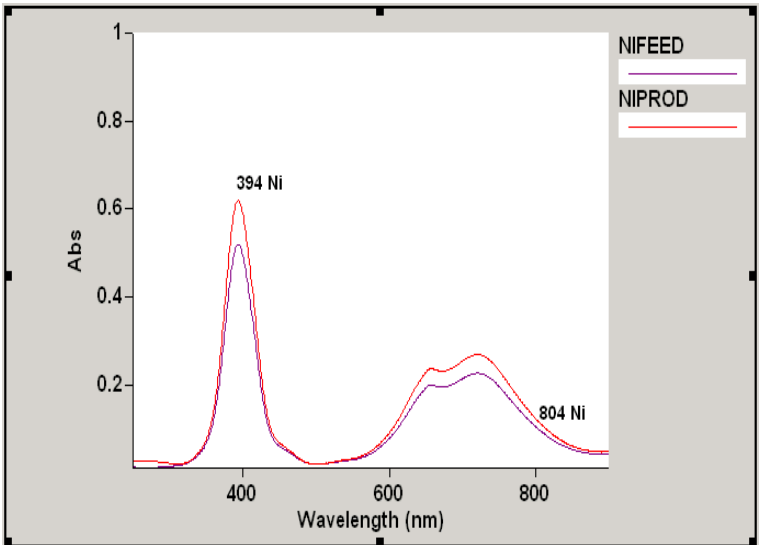

Fig 4.1 Absorption spectrum of "nickel feed" and "nickel product" in 0.7M H_3PO_4 and 1M H_2SO_4 mixture, λ_{max} = 394nm.

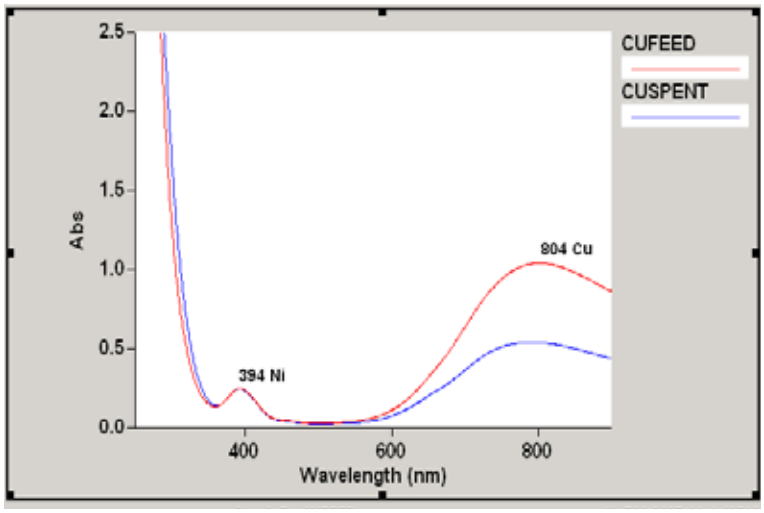

Fig 4.2 Absorption spectrum of "copper feed" and "copper spent" in 0.7M H_3PO_4 and 1M H_2SO_4 mixture, λ_{max1} = 804nm and λ_{max2}= 394nm .

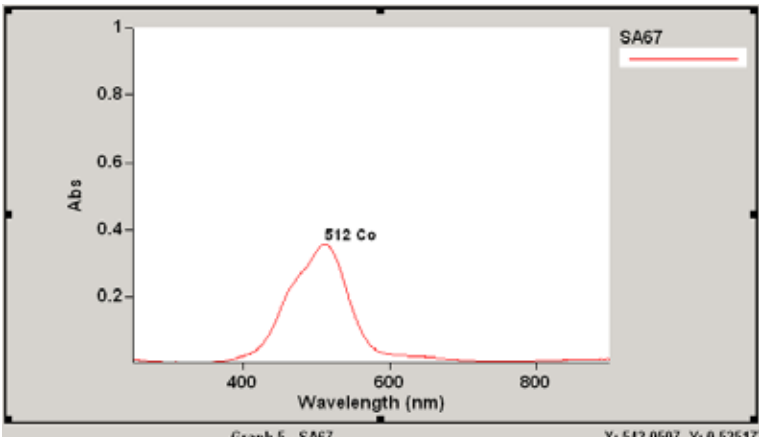

Fig 4.3 Absorption spectrum of "cobalt sample" in 0.7M H_3PO_4 and 1M H_2SO_4 mixture, λ_{max}= 512nm.

In view of the fact that the spectra of the BMR process streams are similar to $[Ni(H_2O)_6]^{2+}$, $[Cu(H_2O)_6]^{2+}$ and $[Co(H_2O)_6]^{2+}$ species, stimulated an investigation into the synthetic

system of $[Ni(H_2O)_6]^{2+}$, $[Cu(H_2O)_6]^{2+}$ and $[Co(H_2O)_6]^{2+}$ species in the diluent. Therefore characterization and understanding the behaviour of these species in the presence of each other is necessary, before this technique can be used for quantitative analysis of the five BMR streams mentioned earlier.

4.2 Absorptiometric analysis of synthetic solutions of $[Ni(H_2O)_6]^{2+}$, $[Cu(H_2O)_6]^{2+}$,$[Co(H_2O)_6]^{2+}$,$[Fe(H_2O)_6]^{2+}$and $[Fe(H_2O)_6]^{3+}$species .

Standard solutions of accurately known mass of copper sulphate, cobalt sulphate and nickel sulphate were used to prepare a concentration close to approximately 5g/L copper, cobalt and nickel solutions in the diluent respectively. Similarly, an accurately known amount of ferrous and ferric sulphate was used to prepare a concentration close to 1g/L ferrous and ferric solution in the diluent. The spectrum was recorded for each of the solutions. The absorption maxima for each of the species were identified, i.e. $\lambda_{max}Ni(aq)^{2+}$ = 394nm, $\lambda_{max}Cu(aq)^{2+}$ = 804nm, $\lambda_{max}Co(aq)^{2+}$ = 512nm. However, $Fe(aq)^{2+}$, λ_{max} = 240nm and $Fe(aq)^{3+}$, λ_{max} = 305nm. (see Fig 4.4)

An absorbance of <0.1 is measured for 1g/L $Fe^{2+}(aq)$ throughout the 204-800nm wavelength range. This low absorbance is an indication of low sensitivity and hence determination of this species using uv-visible spectroscopy is not an appropriate tool for analysis. On the other hand, $Fe^{3+}(aq)$ gives absorbance of ~4 at ~1g/L. The measurement of absorbances >2.5 is not good practice, since stray light and instrumental noise is likely to significantly affect such measurements.[3] Therefore, the use of uv-visible spectroscopy in this study for $Fe^{3+}(aq)$ and $Fe^{2+}(aq)$ determination is not suitable at the 1g/L concentration range of interest.

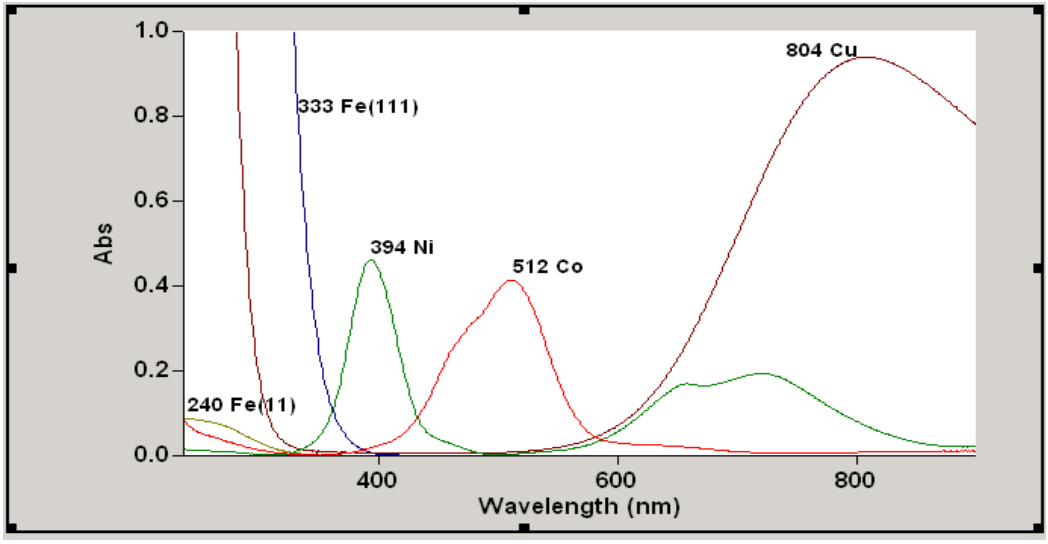

Fig 4.4 Absorption spectra of 5g/L $Cu^{2+}(aq)$, $Ni^{2+}(aq)$, $Co^{2+}(aq)$ and $Fe^{2+,3+}(aq)$ species in 0.7M H_3PO_4 and 1M H_2SO_4 mixture.

From Fig 4.4, it is clear that the absorption spectrum of synthetic solutions of $[Ni(H_2O)_6]^{2+}$ shows a potential spectral overlap in the region, near. λ = 804nm where $[Cu(H_2O)_6]^{2+}$ absorbs and absorbs to a small degree where $[Co(H_2O)_6]^{2+}$ absorbs, at λ = 512nm. Similarly $[Cu(H_2O)_6]^{2+}$ and $[Co(H_2O)_6]^{2+}$ absorbs to some extent in the regions, λ = 394nm and λ = 512nm where ($[Ni(H_2O)_6]^{2+}$ and $[Co(H_2O)_6]^{2+}$), and λ = 804nm, λ = 394nm ($[Cu(H_2O)_6]^{2+}$ and $[Ni(H_2O)_6]^{2+}$) absorbs respectively. In a mixture of these species, it would be necessary to include all the contributory absorbances for each of the species to determine their concentrations, according to Beer's law, depending where the analytical measurement is taken.

From Fig 4.4, it is also seen that $Fe(aq)^{2+}$ absorbs in the region $\lambda \leq$ 300nm separate from $[Cu(H_2O)_6]^{2+}$, $[Ni(H_2O)_6]^{2+}$ and $[Co(H_2O)_6]^{2+}$ species. Therefore in a mixture of these species, it will not be necessary to correct for $Fe(aq)^{2+}$ absorbances in the equation to determine the concentration of each of the species. However, the potential interference of $Fe(aq)^{2+}$ on the analysis was investigated and will be discussed later in the chapter, to substantiate the absence of $Fe(aq)^{2+}$ in the calculation.

Therefore for potential process analysis, it will be necessary to measure $[Ni(H_2O)_6]^{2+}$ at λ =394nm and $[Cu(H_2O)_6]^{2+}$ at λ =804nm and correct for the contribution of $[Ni(H_2O)_6]^{2+}$ absorbance at λ =804nm in the $[Cu(H_2O)_6]^{2+}$ determination. $[Co(H_2O)_6]^{2+}$ can be determined at λ =512nm. Conclusively, the absorbance contribution of each of the species at the relevant wavelengths will be used to calculate the concentration of a specific species, by multicomponent analysis.

4.3 Calibration for the absorptiometric determination of synthetic solutions of copper, nickel and cobalt in the diluent.

Determination of molar absorptivity for $[Cu(H_2O)_6]^{2+}$,$[Co(H_2O)_6]^{2+}$ and $[Ni(H_2O)_6]^{2+}$ species

According to Beer's law, the molar absorptivity can be used to determine the concentration of a species in solution. Standard solutions for the $[Cu(H_2O)_6]^{2+}$, $[Co(H_2O)_6]^{2+}$ and $[Ni(H_2O)_6]^{2+}$ species, were prepared in the concentration range, 2-10g/L. (see Appendix, Table 1) All these standards were made up to the mark using the diluent. The spectra of these standard solutions were recorded and the measured absorbance used to calculate

the experimental molar absorptivity of the species in solution at the absorption maxima. (see Table 4.1)

Table 4.1 ***Experimentally determined ε to be used for calculations of copper, nickel and cobalt concentrations in synthetic solutions and BMR streams in 0.7M H_3PO_4 and 1M H_2SO_4 mixture.***

Species(aq)	394nm	512nm	804nm
Ni^{2+}	0.092 ± 0.002	0.002 ± 0.002	0.016 ± 0.002
Cu^{2+}	0.005 ± 0.007	0.005 ± 0.007	0.191 ± 0.008
Co^{2+}	0.004 ± 0.001	0.084 ± 0.002	0.002 ± 0.001

In addition, the absorptivities were determined on either side of the absorption maxima. (see Appendix, Table 2) This would facilitate determination of the species at the wavelength of least interference and greatest sensitivity. (see Table 4.2)

Table 4.2 ***Determined absorptivities of copper, nickel and cobalt at three λ regions, i.e. 389-398nm, 508-517nm and 800-809nm. (n=2)***

	Average Absorptivity			Std Deviation		
Species	389-398nm	508-517nm	800-809nm	389-398nm	508-517nm	800-809nm
Ni^{2+}(aq)	0.0913	0.0024	0.0164	0.0010	0.0001	0.0008
Co^{2+}(aq)	0.0042	0.0846	0.0017	0.0005	0.0005	0.0001
Cu^{2+}(aq)	0.0047	0.0048	0.1909	0.0000	0.0001	0.0002

Fluctuations in temperature, instrument noise may cause the absorption maximum to shift to some extent, resulting in experimental error. Determinations at several wavelengths, permit a more accurate and selective analysis. However, the results obtained revealed no significant difference between the absorptivity at the maximum absorbance compared to the absorptivity on either side of the maximum. Therefore for method development, λ_{394}, λ_{512}, and λ_{804} will be used to measure $[Ni(H_2O)_6]^{2+}$, $[Cu((H_2O)_6]^{2+}$ and $[Co((H_2O)_6]^{2+}$ respectively.

Determination of linearity

A calibration curve, i.e. absorbance vs. concentration was plotted for the standard solutions for each of the species. Linear curves were obtained for copper, nickel and cobalt and this confirmed the Beer Lambert Law for the concentration range of interest, i.e. 2-10g/L as shown in Fig 4.5, 4.6 and 4.7.[4]

Since, the refinery streams consist of each of the species in the concentration range of 20-100g/L, using a 2-10g/L range for method development is justified by a x 10 dilution

fold of the process sample streams, as Beer's law is obeyed for the concentration range so obtained.

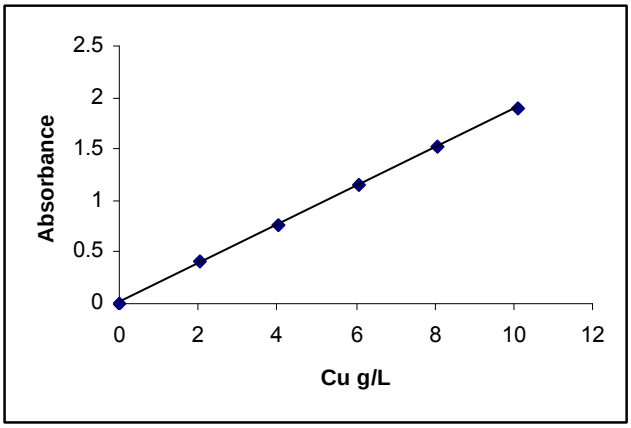

Fig 4.5 Graph depicting the linear relationship between absorbance and concentration of copper. y= 0.1877 x (±0.0013) + 0.0103(±0.0079), λ_{max} = 804nm, R^2 = 0.999.

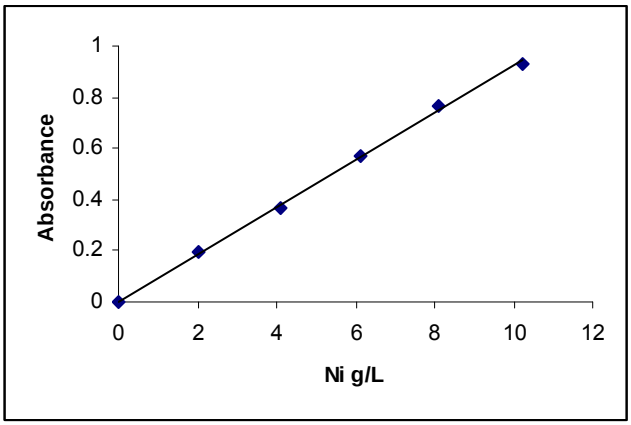

Fig 4.6 Graph depicting the linear relationship between absorbance and concentration of nickel. y= 0.0921x(±0.0013) + 0.0015(±0.0079), λ_{max} = 394nm, R^2 = 0.999.

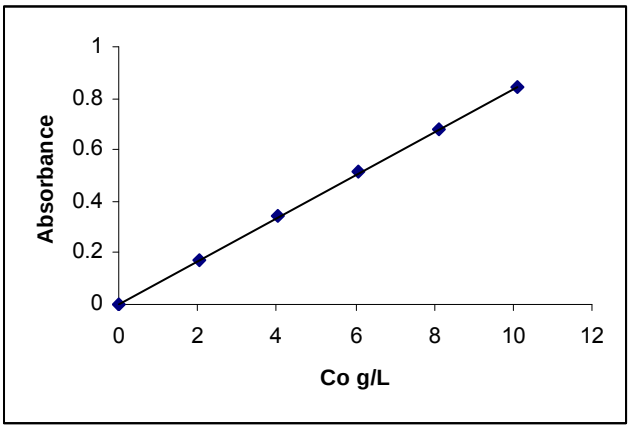

Fig 4.7 Graph depicting the linear relationship between absorbance and concentration of cobalt. y= 0.0834x (±0.0005) + 0.0024(±0.0030) , λ_{max} = 512nm, R^2 = 0.999.

4.4 Analysis of binary mixtures

Two-component solutions containing any of the two elements were carried out to determine the potential mutual interferences that may exist when two elements are in the same solution. Binary mixtures containing known accurately amounts of analyte were made up in diluent, where the concentration of one analyte was kept constant in all the mixtures and the concentration of the other analyte varied. All measurements were performed in duplicate.

In the case of determining potential spectral interferences on copper, a ~5g/L copper mixture with 0, 1, 3, 5g/L nickel was made up in the diluent respectively. The spectra were recorded and the concentration of copper determined by multicomponent analysis using spreadsheet calculations, specifically Solver in Excel.[5](see Chapter 2, 38-39 and Appendix for Calculations). The Solver optimization tool in Excel, with tangential estimate, forward derivative and Newton search was used. The known concentration of the copper was compared to the determined copper concentration as the nickel concentration increased in solution, and the differences between the known values and the determined values (as a percentage) were critically analysed, to see if these would be adequate for plant assay. This percentage difference is known as relative error, Δ.

$$\text{Relative error} = \Delta$$

$$\Delta\ \% = ([\text{known conc.}] - [\text{determined conc.}])/([\text{known conc.}] * 100$$

The relative error, Δ will be used throughout the discussion as the benchmark for depicting the relationship between the plant criterion of acceptability and the experimental results obtained. This analysis was based on the 10% criterion of acceptability for the new method, by the refinery for process control. The potential spectral interferences for the binary mixture containing cobalt and nickel was treated in the same manner.

The results of this study for the binary mixture of cobalt and copper is shown in Fig 4.8 below. The differences in copper concentration observed as the cobalt concentration increases is within 5% error as shown by the error bar. The interference of cobalt on copper is < 2% (see appendix, Table 3). Therefore the small interference of cobalt on copper concentration is within statistical control of the online method. These errors observed may be attributed to random errors or systematic errors. (Chapter 2, 2.1.6)

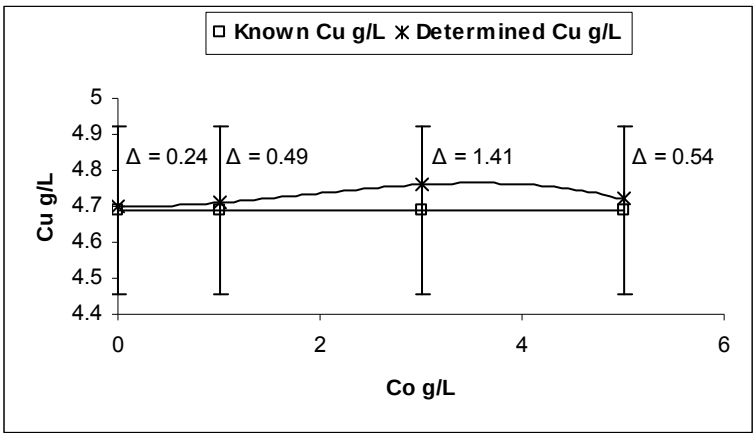

Fig 4.8 Graph depicting the effect of increasing cobalt concentration, 0-5g/L on measured copper, showing relative error, Δ within 5% error.

Similarly, the potential interference of nickel on copper is not significant, the error being ~ 2%. (see Fig 4.9) Therefore the interference of cobalt and nickel and copper is negligible for the purposes of this study as the plant specification is ±10%. (see appendix, Table 4)

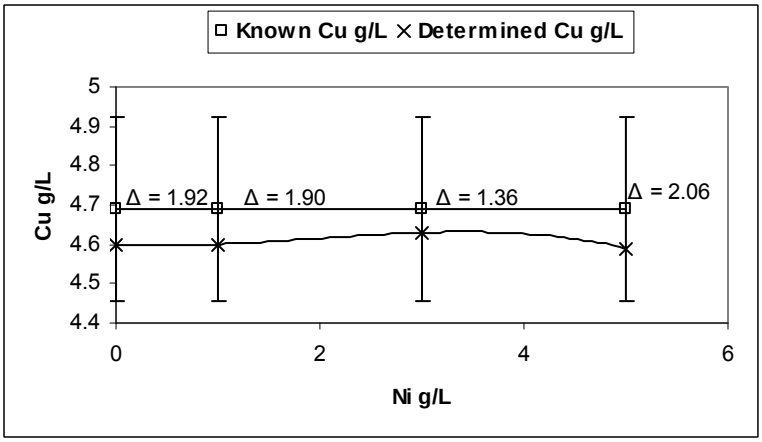

Fig 4.9 Graph depicting the effect of increasing nickel concentration, 0-5g/L on measured copper showing relative error, Δ within 5% error.

The interference of cobalt on nickel was < 2%, until the concentration of cobalt is almost equivalent to the nickel concentration and then the error is ~ 7%, as shown in Fig 4.10 below. This is evidence that as the concentration of cobalt approaches the concentration of nickel, the spectral interference of cobalt on nickel is the greatest. There is a positive bias, showing that the presence of cobalt in solution enhances the determination of nickel. (appendix, Table 5)

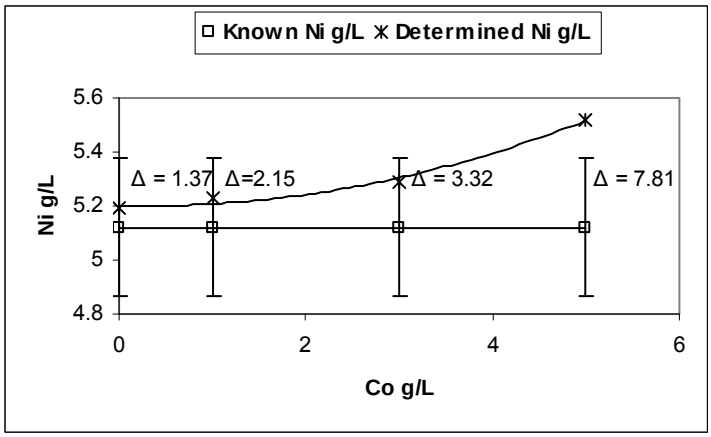

Fig 4.10 Graph depicting the effect of increasing cobalt concentration, 0-5g/L on measured nickel, showing relative error, Δ within 5% error.

However, the potential interference of copper on nickel is ~ 4%, as the copper concentration approaches the nickel concentration. The presence of copper suppresses the determination of nickel.(see Fig 4.11 below)

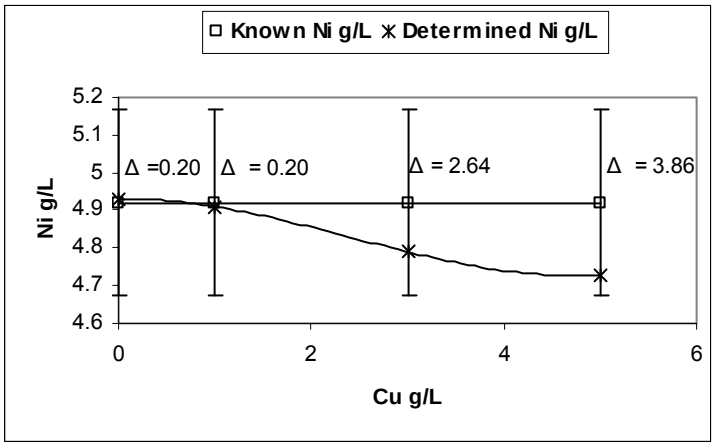

Fig 4.11 Graph depicting the effect of increasing copper concentration, 0-5g/L on measured nickel, showing relative error, Δ within 5% error.

The interference of copper and cobalt is greatest when their concentrations are equivalent. In refinery streams, however, it will be unlikely that copper and cobalt concentrations are similar. (appendix, Table 6)

The differences of nickel and copper on cobalt was <2% as shown in Fig 4.12 below. This error is not significant and falls within the 5% error margin.

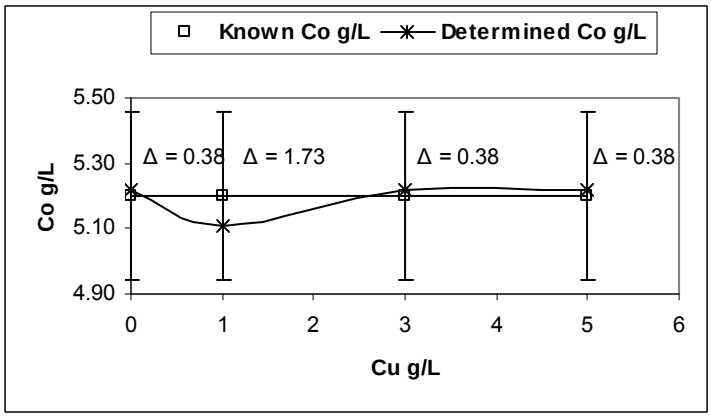

Fig 4.12 Graph depicting the effect of increasing copper concentration, 0-5g/L on measured cobalt, showing relative error, Δ within 5% error.

Similarly the interference of nickel on cobalt is <2% and this is insignificant. (see Fig 4.13) Therefore the interference from nickel and copper on cobalt is negligible. see appendix, Table 7, 8).

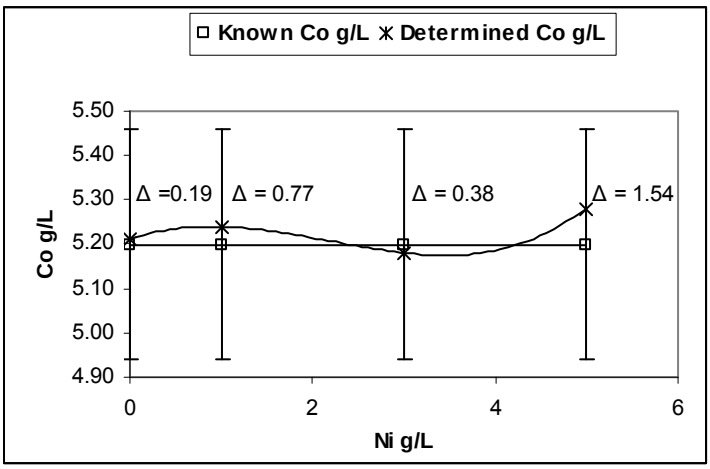

Fig 4.13 Graph depicting the effect of increasing nickel concentration, 0-5g/L on measured cobalt, showing relative error, Δ within 5% error.

The interference of cobalt and nickel on copper is <5% and the interference of copper on nickel <5%. In the case of the interference of cobalt on nickel, the interference <5% up to 4g/L cobalt, however, at almost equivalent concentration of nickel, the relative error increases to ~7%. It is important to remember that in real plant streams, it is impossible to find cobalt and nickel in the equivalent quantities. Therefore, the interference of copper and cobalt on nickel can be ignored, since the relevant concentrations exist on the plant. The interference of copper and nickel on cobalt is <2%.

All the above differences are <5% and still within the 10% plant criterion. As a result, it can be concluded that interferences that exist in the binary system is not significant. However,

it will assist in understanding three components in a mixture based on the errors that already exist from the binary mixture.

Copper, nickel and cobalt can be analysed simultaneously in a binary mixture within 5% accuracy. The errors that exist in the analysis may be attributed to systematic and random errors. Therefore, plant refinery streams that consist of any of the above two species, may be analysed simultaneously within the same error margin.

4.5 Analysis of ternary mixtures

The fact that two component mixtures may be successfully analysed to well within a 5% error, stimulated an investigation of three-system mixtures, i.e. mixtures that consist of copper, nickel and cobalt.

Standard mixtures containing Cu^{2+}(aq), Ni^{2+}(aq) and Co^{2+}(aq) in 25 different combinations, based on factorial design were made up in the diluent. (see Table 4.3)

The standard mixtures was a simulation of the BMR input streams. The spectra of these mixtures were then recorded and absorbance data at the wavelengths of interest, were used to calculate the concentration of the $[Cu(H_2O)_6]^{2+}$, $[Ni(H_2O)_6]^{2+}$ and $[Co(H_2O)_6]^{2+}$ in solution using Solver in Excel(see Calculations in Appendix), solving a simultaneous equation. Replicate measurements were taken for all the experiments within 0.05 standard deviation.

The concentration determined for each of the species from the experiment was compared against the known concentrations prepared in the standard mixtures. (see appendix, table 9). If there is no bias between the determined metal ion concentration and the known concentration of the metal ion, the plot of the determined vs the known concentration of the metal ion should give a slope of 1 and intercept at 0.

Table 4.3 Model simulating the refinery input streams for $[Cu(H_2O)_6]^{2+}$, $[Co(H_2O)_6]^{2+}$, $[Ni(H_2O)_6]^{2+}$ species.

Standards	$[Ni(H_2O)_6]^{2+}$ g/L	$[Co(H_2O)_6]^{2+}$g/L	$[Cu(H_2O)_6]^{2+}$ g/L
1	2.00	6.02	4.03
2	2.00	8.00	6.00
3	2.00	10.02	8.00
4	2.00	4.00	2.02
5	2.00	2.00	10.00
6	4.00	8.00	6.00
7	4.00	10.02	8.00
8	4.00	2.00	10.00
9	4.00	4.00	2.02
10	4.00	6.02	4.03
11	6.00	10.02	8.00
12	6.00	2.00	10.00
13	6.00	4.00	2.02
14	6.00	6.02	4.03
15	6.00	8.00	6.00
16	8.00	2.00	10.00
17	8.00	4.00	2.02
18	8.00	6.02	4.03
19	8.00	8.00	6.00
20	8.00	10.02	8.00
21	10.00	4.00	2.02
22	10.00	6.02	4.03
23	10.00	8.00	6.00
24	10.00	10.02	8.00
25	10.00	2.00	10.00

The known concentration was plotted against the determined concentrations, and this shows the expected linear trend. Ni^{2+} (aq) determinations had a linear regression correlation coefficient R^2 = 0.997, std. error =0.17, m= 1.04 and c= 0.25. Similarly $[Cu(H_2O)_6]^{2+}$determinations had R^2=0.999, std error = 0.05 , m= 1.03 and c= 0.01 and finally $[Co(H_2O)_6]^{2+}$determinations had R^2 = 0.998, std error= 0.16, m=1.00 and c=0.17.(see Fig 4.14, Fig 4.15 and Fig 4.16).

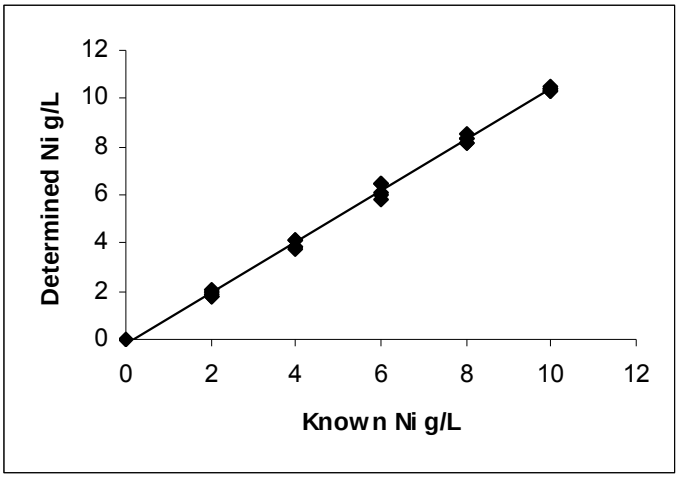

Fig 4.14 Graph describing the plot between the known concentration of Ni^{2+}(aq) in the ternary mixtures and the determined concentration. y = 1.0577 x - 0.202, λ_{max}= 394nm, R^2 = 0.997

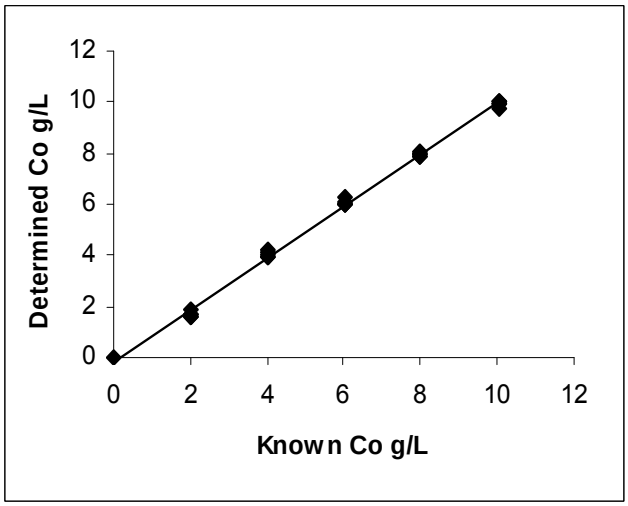

Fig 4.15 Graph describing the plot between the known concentration of Co^{2+}(aq) in the mixtures and the determined concentration. y = 1.0146 x – 0.1438, λ_{max}= 512nm R^2 = 0.998.

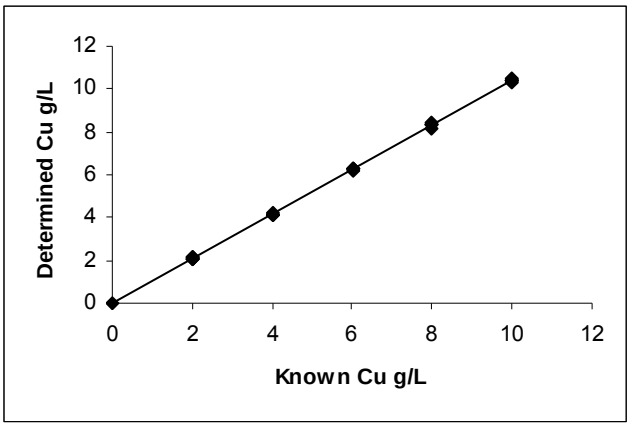

Fig 4.16 ***Graph describing the plot between the known concentration of $[Cu(H_2O)_6]^{2+}$ in the ternary mixtures and the determined concentration., y= 1.0425 x - 0.0189, λ_{max}= 804nm, R^2 = 0.999.***

However, the differences for the correlation between the known and the determined must be justified to identify interferences between elements in a three system. (see Appendix, Table 10).

From Fig 4.17 it can be seen that the nickel determination, the error is larger (>5%) at lower concentrations of nickel in the mixture, i.e. 2-6g/L nickel, however, as the concentration of nickel increases from 8-10g/L, the error is lower (<5%). At mixture nos. 3,5,13, and 14, the error is considerably higher than other mixtures. Mixture no.3, 5 have low nickel and high cobalt and high copper respectively. Mixture no. 13 and 14 has a similar concentration of copper (~4g/L) and cobalt (~2g/L). Based on binary mixture studies above, copper and cobalt will have some contribution to the error on the nickel determination. Also, the absorption of cobalt neighbours the nickel absorption region (see Fig 4.4). However, the determination of the nickel species is still within the 10% plant criterion of acceptability. (see Fig 4.17)

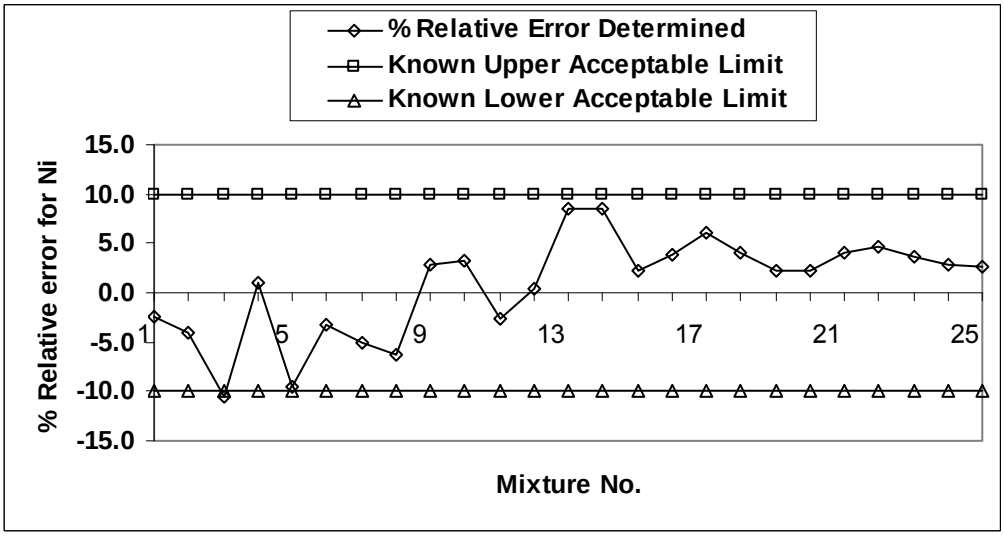

Fig 4.17 ***Comparison of % relative error for determined nickel and known nickel, g/L in the 25 mixtures within 10% accuracy.***

Mixture no. 18 and 21 represent the nickel product and nickel feed streams closely and even here, the error is within 5%. Also, in mixture no. 24, where the species present are in relatively high concentrations, the error is still within the specified accuracy.

Therefore, nickel can be analysed in a mixture containing three species within the plant criterion of acceptability. As a result, in a real stream, where there are three species present, nickel can be determined in that stream within 5% accuracy.

In the cobalt determination, the error is generally much lower than that of nickel, except in mixture no. 5,8,12 and 25. In these mixtures, there is a relatively large amount of copper, i.e. 10g/L relative to cobalt and the nickel present. Copper may interfere with cobalt, when in combination with another species such as nickel. It seems that copper in mixture no. 5,8,12 and 25 shows a negative bias on the cobalt determination. (see Fig 4.18 and 4.4)

However, in the refinery, this is unlikely to be the case where the copper is present in the above concentrations, such as specific mixtures mentioned. Mixture no. 1 represents the cobalt sample closely and the error on this mixture is <1%. The general error is low for determination of cobalt and is within the specified accuracy. Therefore cobalt can be analysed in a mixture containing three species and in the refinery streams, similar to the mixtures.(see Fig 4.18 below).

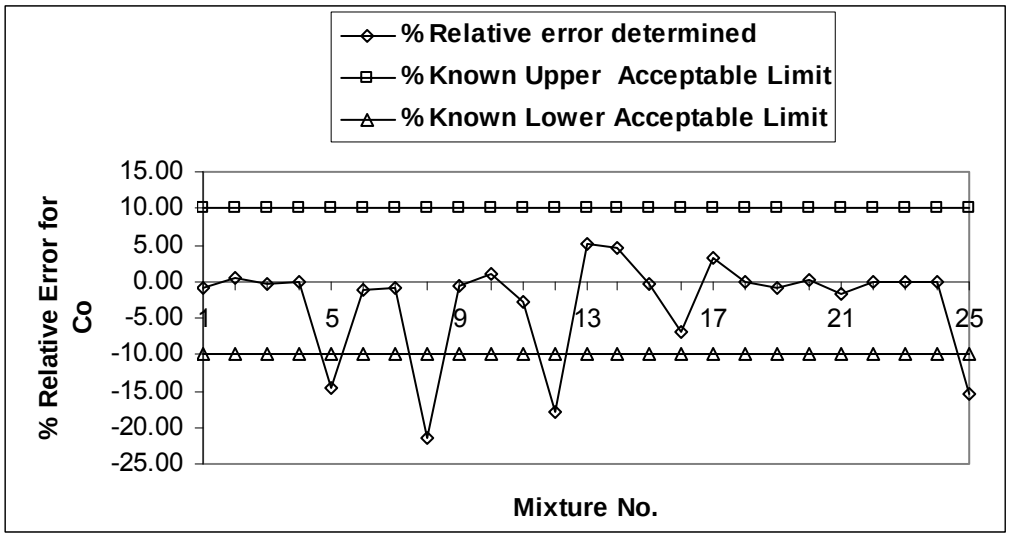

Fig 4.18 Comparison of % relative error for determined cobalt and known cobalt, g/L in the 25 mixtures within 10% accuracy.

All the results fall within the specified accuracy, and as a result, this method can be used for the determination of cobalt.

In the copper determination, there seems to be a high bias in the mixtures. Only mixture no. 7 and 13, have errors greater than 5%. There is no common denominator between the two mixtures. The large cobalt concentration in mixture no. 7 does not correlate with the low cobalt concentration in mixture no. 13. Aside from this, the errors still fall within the specified accuracy.

Mixture no. 10 represents the "copper feed" and "copper spent" samples closely. In this mixture, the error for copper is <3%. Therefore copper in a mixture containing the three species within 5% and also can be determined in the refinery stream samples containing those species. (see Fig 4.19).

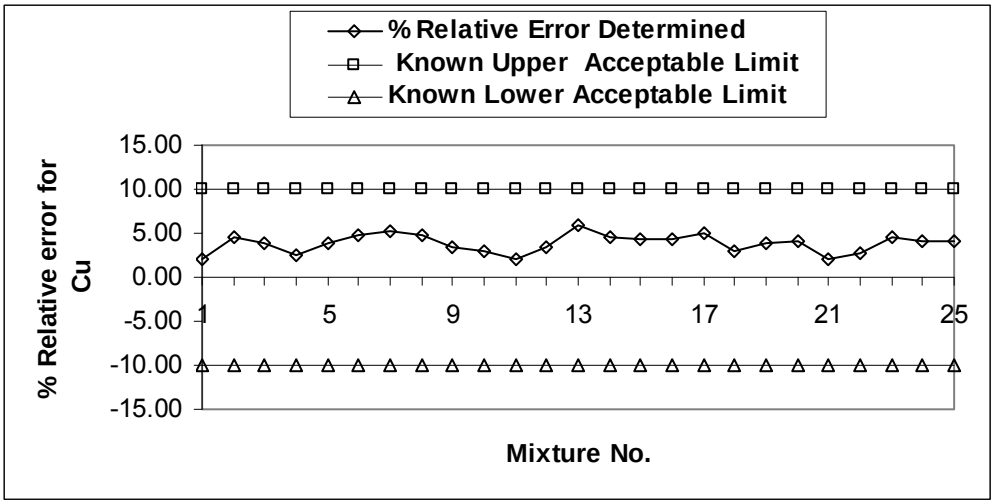

Fig 4.19 Comparison of % relative error for determined copper and known copper, g/L in the 25 mixtures within 10% criterion of acceptability.

The determination of copper in the mixture using this method of analysis is possible, within the specified accuracy. However, the precision and accuracy of the simultaneous method must be determined. Ten separate solutions of a mixture containing 8g/L nickel, 6g/L cobalt and 6g/L copper was prepared and the concentration of the $[Cu(H_2O)_6]^{2+}$, $[Ni(H_2O)_6]^{2+}$ and $[Co(H_2O)_6]^{2+}$ was determined. The standard deviation of each concentration was calculated and it was found that nickel, cobalt and copper has a precision of 8.15 ± 0.16, 5.87± 0.14 and 6.11 ± 0.05 respectively. (see Appendix, Table 11).

The comparison between the predicted concentrations and the known concentrations of the copper, nickel and cobalt in the 25 standard mixtures was used to determine the accuracy of the analysis. The species $[Ni(H_2O)_6]^{2+}$, $[Co(H_2O)_6]^{2+}$and $[Cu(H_2O)_6]^{2+}$ has an

accuracy of 4.25, 4.04 and 3.82 %. These fall within the 10% accuracy requirement of the BMR for process control and this means that in real samples, one expects this level of accuracy.

4.6 Effect of $Fe(aq)^{2+}$ on the determination of $[Ni(H_2O)_6]^{2+}$, $[Co(H_2O)_6]^{2+}$and $[Cu(H_2O)_6]^{2+}$

As mentioned above, $Fe(aq)^{2+}$ is present in the BMR in < 1g/L range. The effect of $Fe(aq)^{2+}$ on the determination of copper, nickel and cobalt was investigated. Standard mixtures containing $[Cu(H_2O)_6]^{2+}$, $[Co(H_2O)_6]^{2+}$ and $[Ni(H_2O)_6]^{2+}$ species in the same 25 combinations as well as 0.08g/L $Fe(aq)^{2+}$ was made up with diluent. The spectra of these mixtures were recorded and the absorbance data used to calculate the concentration of the species. (see Appendix, Table 13).

In the same manner, as three component analysis before, the known concentrations were compared with the determined concentrations from the experiment in the presence of $Fe(aq)^{2+}$. The known and determined concentration of the three-system mixture showed good correlation as before. The determined concentrations were compared to the determined concentrations in the absence of iron and this showed good comparison. (see Appendix, Table 13).

Similarly as above, the known concentration was plotted against the determined and $[Ni(H_2O)_6]^{2+}$ had a correlation coefficient of 0.997, std error of 0.15, gradient of 1.01 and intercept, 0.17. Similarly, $Cu^{2+}(aq)$ had correlation coefficient of 0.999, std error, 0.04, gradient of 1.02 and intercept of 0.03 and $[Co(H_2O)_6]^{2+}$ had a correlation coefficient of 0.998, std error of 0.14, gradient of 1.02 and intercept of 0.19. (see Fig 4.20,21,22).

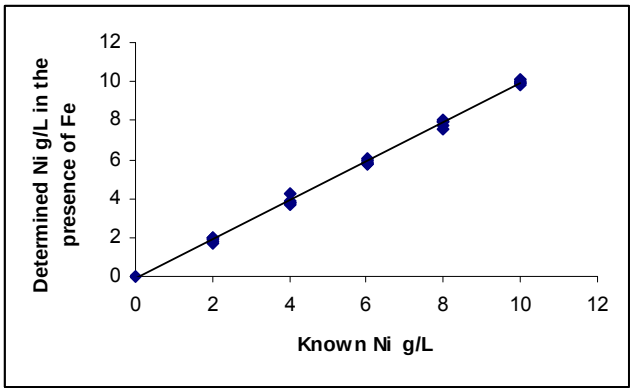

Fig 4.20 ***Graph describing the correlation between the known concentration of $[Ni(H_2O)_6]^{2+}$ in the mixtures and the determined concentration in the presence of $Fe(aq)^{2+}$. y = 1.0031x – 0.1295, λ_{max} = 394nm, R^2 = 0.997.***

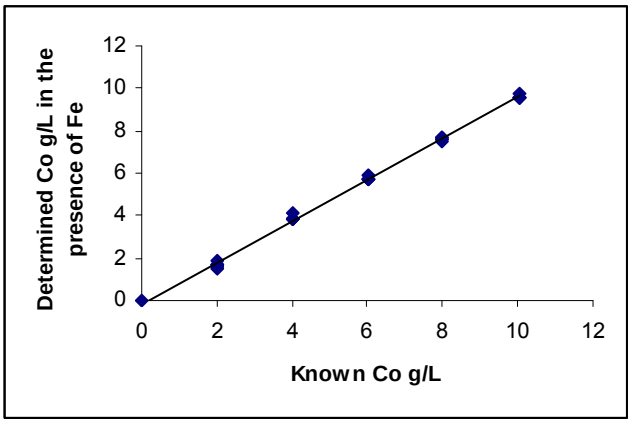

Fig 4.21 ***Graph describing the correlation between the known concentration of $[Co(H_2O)_6]^{2+}$ in the mixtures and the determined concentration in the presence of Fe^{2+}. y = 0.9742x – 0.1436, λ_{max} = 512nm, R^2 = 0.998***

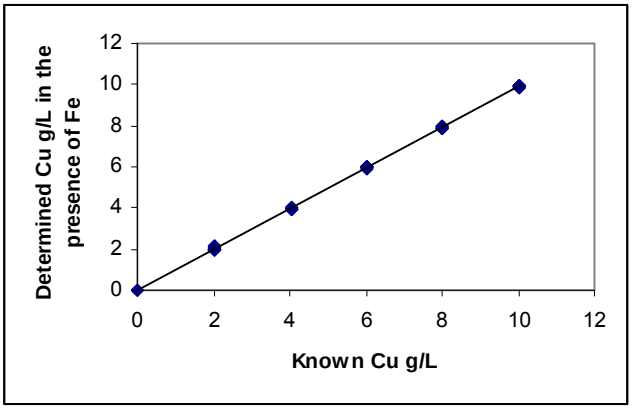

Fig 4.22 ***Graph describing the correlation between the known concentration of $[Cu(H_2O)_6]^{2+}$ in the mixtures and the determined concentration in the presence of Fe^{2+}. y = 0.9897x – 0.0124, λ_{max} = 804nm, R^2 = 0.999.***

In general, the relative error on the nickel determination is higher (~1%) in the presence of $Fe(aq)^{2+}$ than without $Fe(aq)^{2+}$. Similarly, this is observed in the cobalt determination (~3%). On the contrary in the copper determination, the relative error is lower in the presence of $Fe(aq)^{2+}$, than without $Fe(aq)^{2+}$.(~2%)

Since the copper absorption maximum is 804nm for $[Cu(H_2O)_6]^{2+}$, and iron absorption maximum is 240nm for $Fe(aq)^{2+}$, Cu^{2+} is the furthest away from $Fe(aq)^{2+}$ in the spectrum, the least interference is observed for this species. The neighbouring species, i.e. $[Co(H_2O)_6]^{2+}$ λ_{max} = 512nm and $[Ni(H_2O)_6^{2+}$ λ_{max} = 394nm, to $Fe(aq)^{2+}$ is most interfered. (see Fig 4.23, 4.24, 4.25).

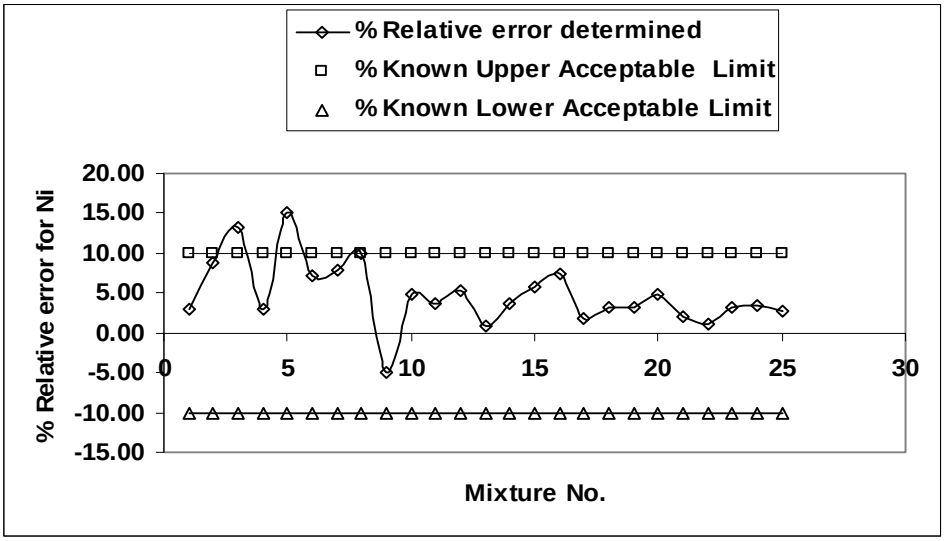

Fig 4.23 Comparison of the known $[Ni(H_2O)_6]^{2+}$ and determined $[Ni(H_2O)_6]^{2+}$, g/L in the presence of 0.08g/L $Fe(aq)^{2+}$ within 10% accuracy.

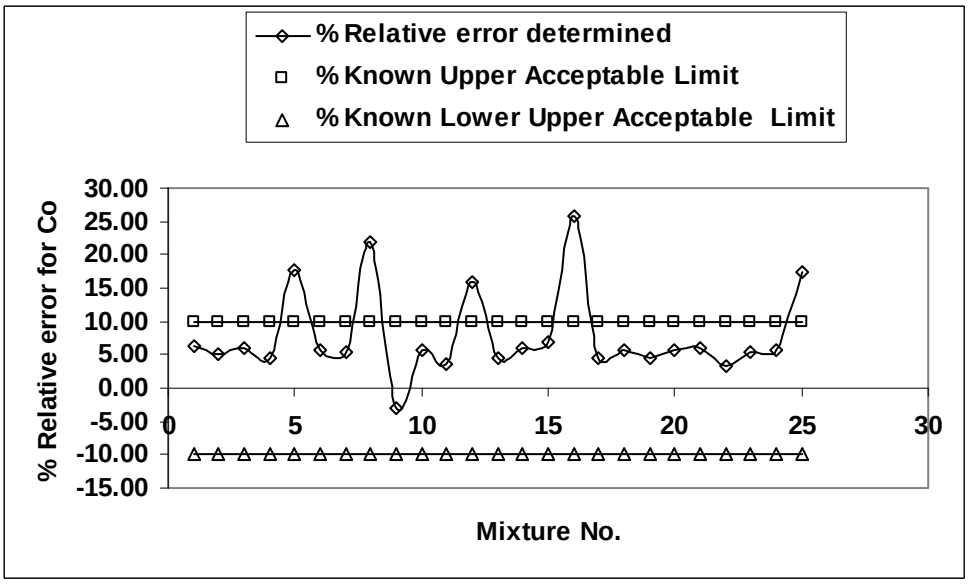

Fig 4.24 Comparison of the known $[Co(H_2O)_6]^{2+}$ and determined $[Co(H_2O)_6]^{2+}$, g/L in the presence of 0.08g/L $Fe(aq)^{2+}$ within 10% accuracy.

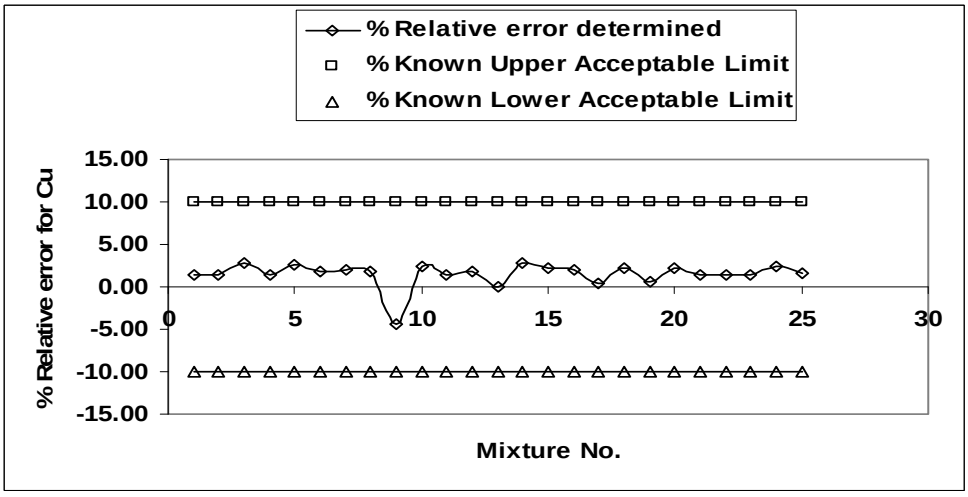

Fig 4.25 Comparison of the relative error for the known $[Cu(H_2O)_6]^{2+}$ and determined $[Cu(H_2O)_6]^{2+}$, g/L in the presence of 0.08g/L $Fe(aq)^{2+}$ within 10% accuracy.

Mixture no. 3,5,8,12,16,25 shows the most deviation from the upper and lower limit of acceptability. In some cases, there is high concentration of cobalt in these mixtures, in other combinations, high concentration of nickel. It seems that the interference from cobalt or nickel, is enhanced in the presence of iron.

The general trend reveals a high bias on the determination of copper, nickel and cobalt in the presence of iron. However, the errors fall within the plant criterion of acceptability and the interference of $Fe(aq)^{2+}$ is not significant for in the multicomponent analysis of the copper, nickel and cobalt species. Hence, $Fe(aq)^{2+}$ need not be included in the equation for quantification of copper, nickel and cobalt. Also, as mentioned earlier, obtaining a reproducible molar absorptivity is experimentally not possible for $Fe(aq)^{2+}$ and as a result the concentration of $Fe(aq)^{2+}$ cannot be determined. The simultaneous equations will only include copper, nickel and cobalt contribution in the determination of concentration.

4.7 Effect of the sulphuric acid concentration: on the determination $[Cu(H_2O)_6]^{2+}$, $[Ni(H_2O)_6]^{2+}$ and $[Co(H_2O)_6]^{2+}$

On the plant, the concentration of sulphuric acid in the streams vary, depending on the stage in the process in the region of 20-100g/L. The effect of this change was investigated. A mixture containing approximately 8g/L nickel, 6g/L cobalt and 4g/L copper was made up in varying concentrations of sulphuric acid, 2-10g/L. The concentration of $[Cu(H_2O)_6]^{2+}$, $[Ni(H_2O)_6]^{2+}$ and $[Co(H_2O)_6]^{2+}$ species was calculated and compared to the known values.

The difference on the nickel determination was ~ 2%. (see Fig 4.26). The percentage difference falls within the specified limits and therefore effect of acid concentration on nickel determination is not significant.

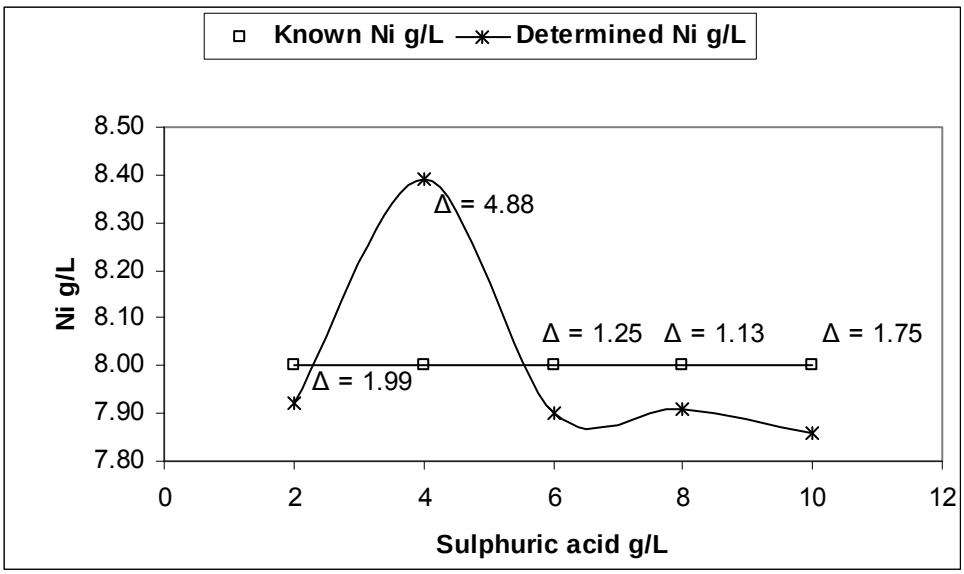

Fig 4.26 Effect of H_2SO_4 concentration on the nickel determination in the mixture of copper, nickel and cobalt.

In the cobalt determination, in the presence of increased acid, has a constant bias ~7%. It is possible that sulphate or phosphate complexes are formed at high acid concentrations. These species are known and can cause a shift in the standard absorption spectra, e.g. measuring $[Co(H_2O)_6]^{2+}$at 512nm, when there may be another species present, and as a result obtain a lower value for cobalt than there really is at 512nm.(see Fig 4.27)

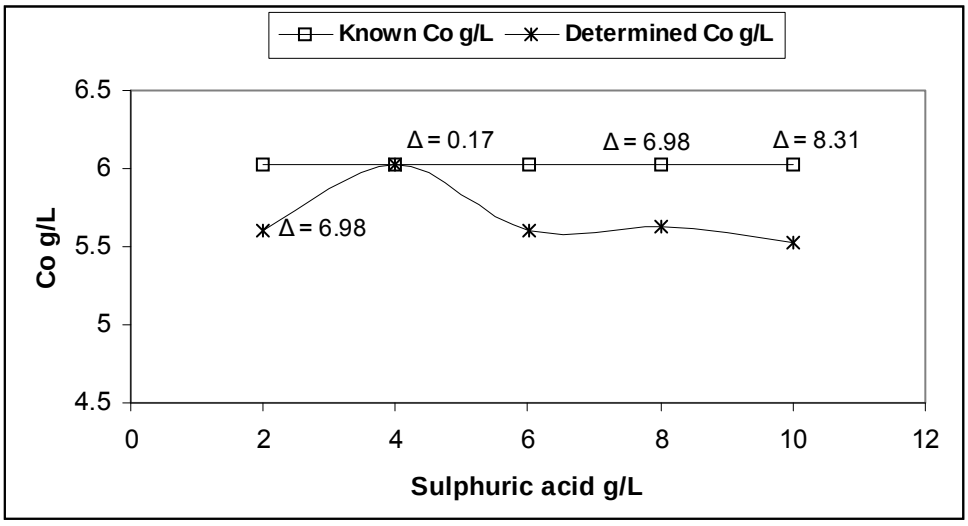

Fig 4.27 Effect of H_2SO_4 concentration on the cobalt determination in the ternary mixture of copper, nickel and cobalt.

In the determination of copper, the percentage difference is within 3% and the effect of acid on copper determination is not significant. (see Fig 4.28).

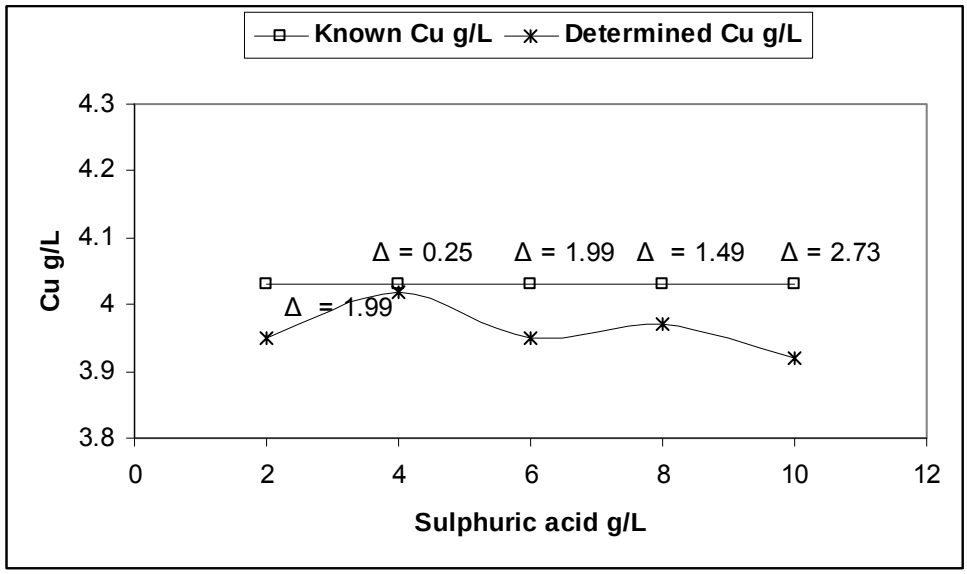

Fig 4.28 Effect of H_2SO_4 concentration on the copper determination in the mixture of copper, nickel and cobalt.

Therefore, copper, nickel and cobalt can be analysed within the specified accuracy, should the sulphuric acid concentration vary from 2-10g/L.

4.8 Effect of temperature on the analysis of the ternary species

Like acid, the temperature of the refinery streams vary based on the stage in the process. In view of potential on-line analysis where the sample is diluted insitu, absorbance measured and concentration determined, it is necessary to understand the effect of temperature on the analysis. The standard mixtures, mentioned before have been analysed at 25^0C.

The effect of temperature was investigated first on pure element solutions (see Fig 4.29) and then on a three-system mixture in the temperature range of 25-58^0C. Standard solutions of 6g/L cobalt, 8g/L nickel and 6g/L copper was prepared in the diluent. These standard solutions were then heated on a waterbath to 60^0C and spectra recorded as the temperature dropped at 5^0C intervals. A thermometer was used to monitor the temperature change.

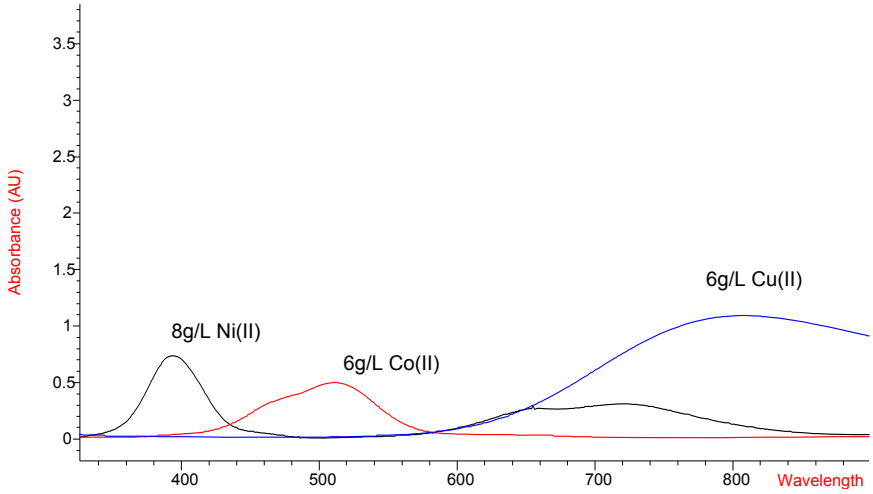

Fig 4.29 ***Spectra of 8g/L $[Ni(H_2O)]_6^{2+}$; 6g/L $[Co(H_2O)]_6^{2+}$ and 6g/L $[Cu(H_2O)_6]^{2+}$ species in 1M sulphuric and 0.7M orthophosphoric acid at 25^oC.***

In the case of nickel, there is an increase in error in the standard solution from 0.27-2.05% and in the mixture there is an increase in error from 0.43-1.28% (refer to Appendix, Table 14 and 15). The effect of temperature on nickel determination is negligible and it can be ignored for the temperature range of 25-60^{0}C.(see Fig 4.30, 4.31).

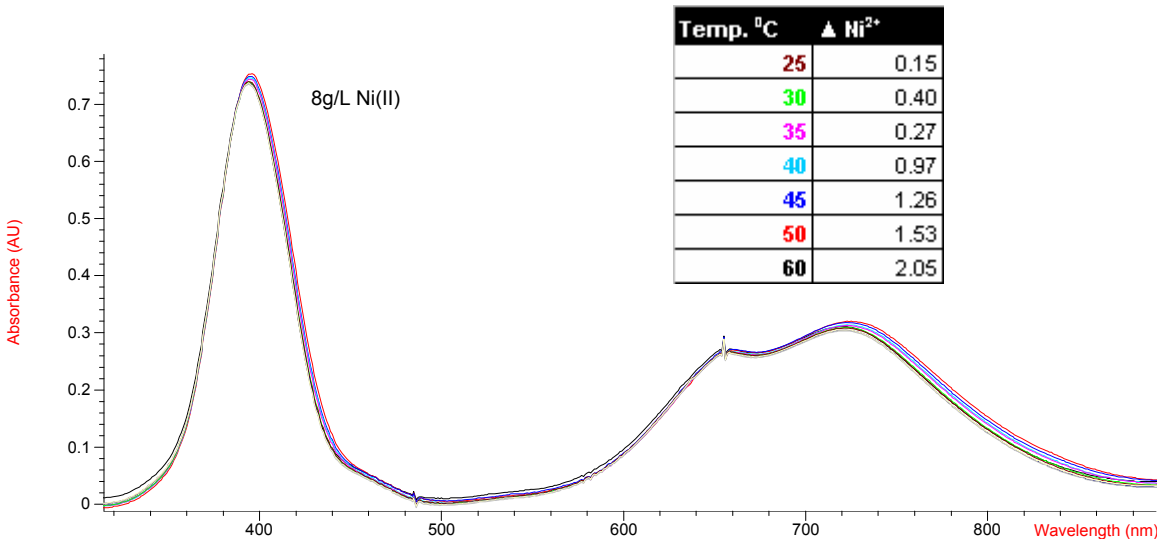

Fig 4.30 ***Absorption spectrum for 8g/L $[Ni(H_2O)]_6^{2+}$ in 1M sulphuric and 0.7M orthophosphoric acid at temperature range 25-60^{0}C, showing change in relative error, Δ % as the temperature is increased. (Δ % = [known conc.] –[determined conc.]/[known conc.] *100)***

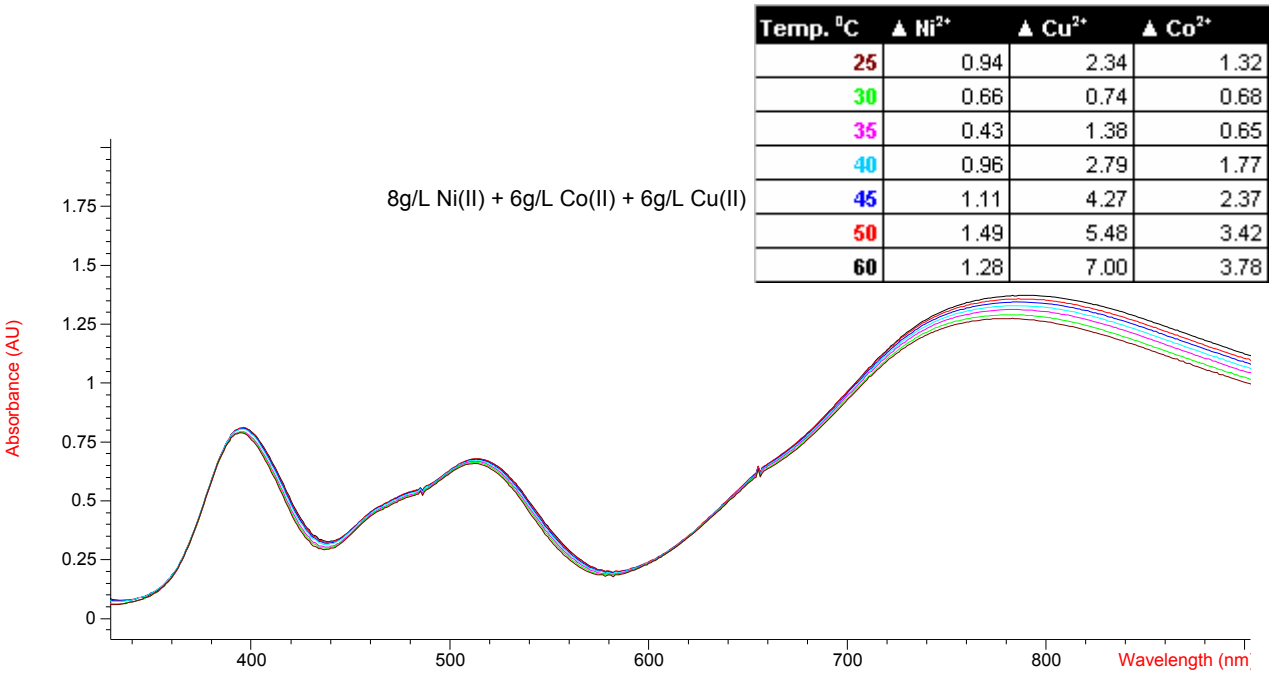

Temp. ^{0}C	▲ Ni^{2+}	▲ Cu^{2+}	▲ Co^{2+}
25	0.94	2.34	1.32
30	0.66	0.74	0.68
35	0.43	1.38	0.65
40	0.96	2.79	1.77
45	1.11	4.27	2.37
50	1.49	5.48	3.42
60	1.28	7.00	3.78

Fig 4.31 ***Absorption spectrum for 8g/L $[Ni(H_2O)]_6^{2+}$, 6g/L $[Co(H_2O)]_6^{2+}$ and 6g/L $[Cu(H_2O)_6]^{2+}$ mixture in 1M sulphuric and 0.7M orthophosphoric acid at temperature range 25-60^{0}C showing change in relative error, Δ % as the temperature is increased.***

In the case of copper, there is a significant increase in the absorbance as the temperature increases in the standard and similarly in the tertiary mixture. Hence, an increase in the calculated concentration of copper. (see Fig 4.32 and 4.31)

In view of the fact that, nickel absorbs in the region (λ= 804nm) that copper absorbs, it is possible that the cumulative effect that temperature has on copper and nickel is increased. Therefore, the determination of copper concentration is affected more significantly than nickel.

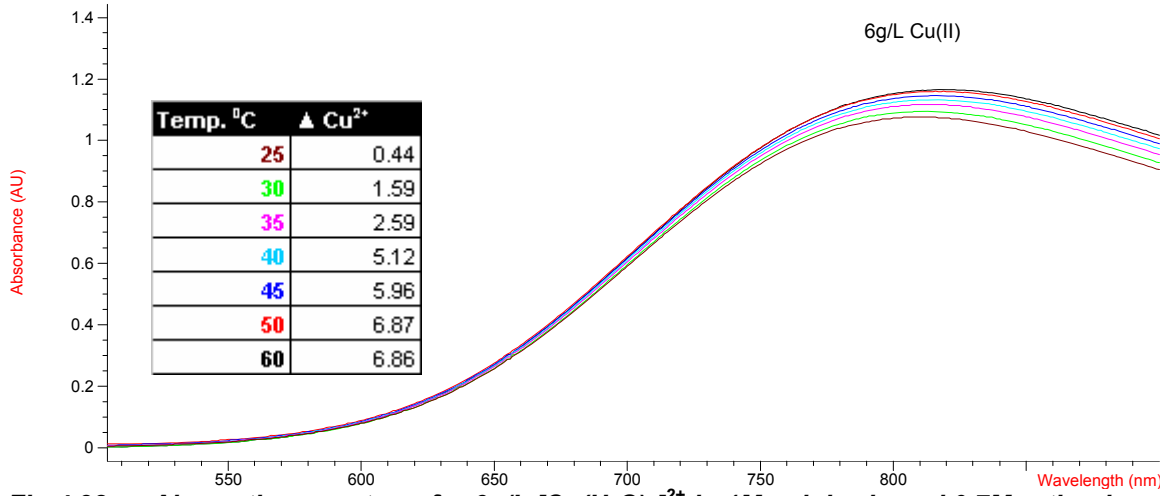

Temp. ^{0}C	▲ Cu^{2+}
25	0.44
30	1.59
35	2.59
40	5.12
45	5.96
50	6.87
60	6.86

Fig 4.32 ***Absorption spectrum for 6g/L $[Cu(H_2O)_6]^{2+}$ in 1M sulphuric and 0.7M orthophosphoric acid at temperature range 25-60^{0}C showing change in relative error, Δ % as the temperature is increased.***

In the case of cobalt, similarly an increase in absorbance is observed in the standard and in the mixture. (see Fig 4.33 and 4.31 and table 17 in Appendix.). However, the relative error observed is much lower than that of copper. (see Fig 4.33 and 4.31 and table 17 in appendix.)

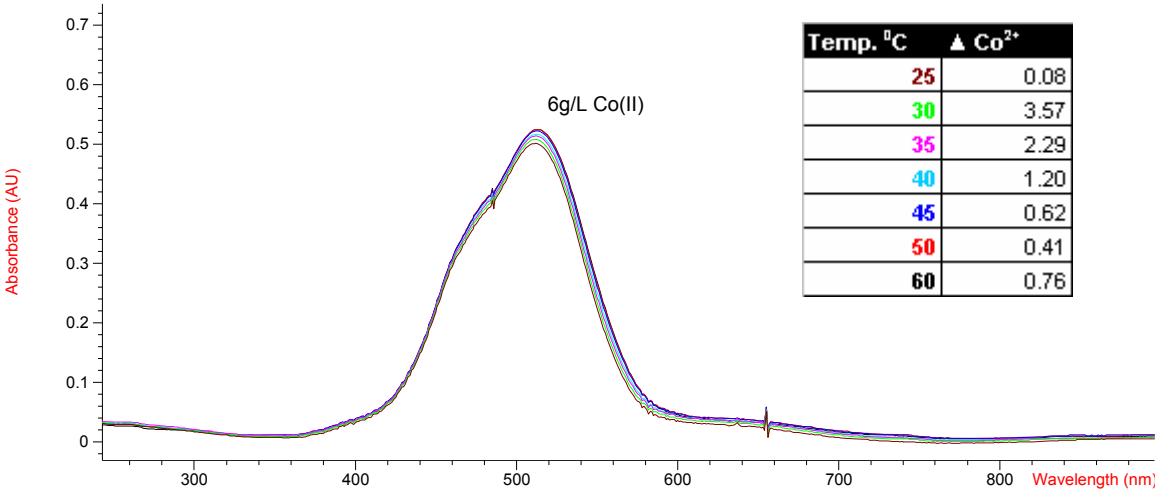

Temp. ^{0}C	▲ Co^{2+}
25	0.08
30	3.57
35	2.29
40	1.20
45	0.62
50	0.41
60	0.76

Fig 4.33 Absorption spectrum for 6g/L $[Co(H_2O)]_6^{2+}$ in 1M sulphuric and 0.7M orthophosphoric acid at temperature range 25-60^{0}C showing change in relative error, % Δ as the temperature is increased.

The relative error on copper increases between 0.74-7% as the temperature increases, however, at 25^{0}C, there is an error of approximately 2%.(see Appendix, Table 16). The error on cobalt can go up to 4% as the temperature increases. It appears that cobalt and nickel are less significantly affected than copper at high temperature. This increase in absorbance may be due to a shift in equilibrium and the formation of species at 804nm ($\lambda_{maxCu(aq)}^{2+}$) which are not known. This shift in equilibria causes an increase in absorbance and it seems that more than one species is present at that wavelength, not only $[Cu(H_2O)_6]^{2+}$. The temperature bias must be considered when developing an on-line system.

In an on-line system, the sample from the refinery stream at high temperature (30-50^{0}C) will be diluted with the diluent, i.e. 0.7M sulphuric and 1M orthophosphoric acid which is at 25^{0}C. This dilution will cool the sample stream to a lower temperature. At a lower temperature, the error on analysis is lower as shown above. Depending on what the temperature eventually is, better accuracy is expected, due to the low error. This means that effect for temperature may not be corrected if the error on that temperature falls within the required accuracy.

The effect of temperature can be accounted for to achieve optimum results, although analysis of copper, nickel and cobalt can be determined within the required accuracy with varying temperature.

4.9 Validation of the method on BMR plant solutions

Within the achievable accuracy, precision, temperature, sulphuric acid concentration and pH effects, the spectrophotometric method was tested using authentic plant stream samples from the refinery. The standard mixtures were used as a calibration matrix for the determination of $[Cu(H_2O)_6]^{2+}$, $[Co(H_2O)_6]^{2+}$ and $[Ni(H_2O)_6]^{2+}$ species in refinery streams.

The refinery streams, i.e. “nickel feed”, “nickel product”, “copper feed”, ”copper spent” and “cobalt sample”, mentioned earlier in the chapter, were analysed. A 2mL aliquot of these streams were pipetted into 25ml volumetric flasks and made up to mark using the diluent. The spectra were recorded and the concentration of the $[Cu(H_2O)_6]^{2+}$, $[Co(H_2O)_6]^{2+}$ and $[Ni(H_2O)_6]^{2+}$ present in the samples determined from the calibration curve.

These refinery samples were analysed over a month using the new method. These samples were also analysed by the refinery laboratory using different analytical methods mentioned in Chapter 1, as well as by an independent laboratory using Inductively Coupled Plasma analysis, in order to compare the new method to the conventionally accepted refinery laboratory method.

These three comparisons would define the ruggedness of the method. The comparison of the new method of analysis and the independent laboratory compared even more closely. This was confidence that this new method is rugged and can be definitely used to analyse refinery samples.(see Fig 4.34,35,36,37 and 38 below).

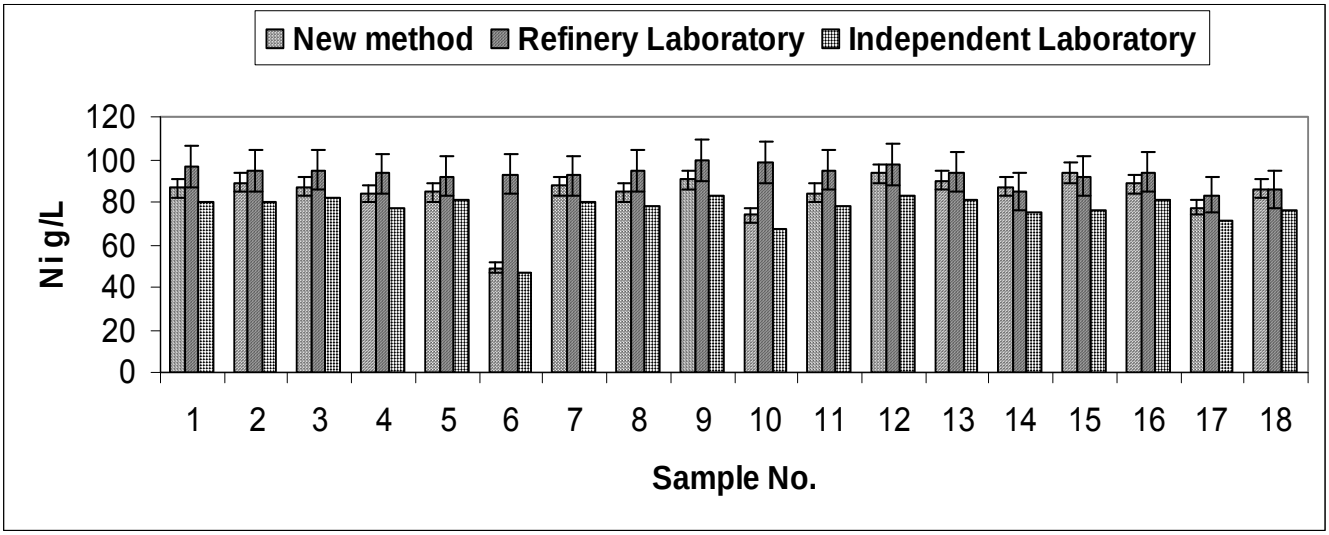

Fig 4.34 Comparison between three methods for nickel determination for "nickel product" in 0.7M H_3PO_4 and 1M H_2SO_4 mixture.

The analysis for sample no. 6 was interesting. The results obtained from the new method and the independent laboratory were close to the observed nickel concentration by the spectrophotometric method. However, the result obtained from the refinery laboratory was significantly higher, which could suggest a systematic error in the laboratory method. Yet, this is an outlier compared to the hypothesis for the other 17 samples analysed.

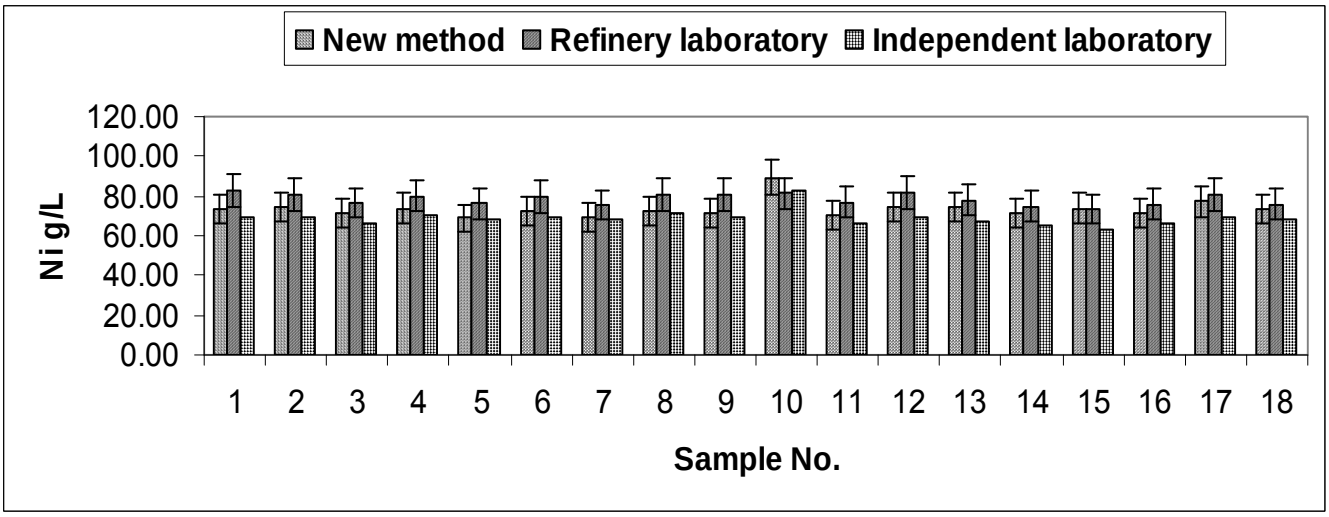

Fig 4.35 Comparison between three methods for nickel determination in "nickel feed" in 0.7M H_3PO_4 and 1M H_2SO_4 mixture.

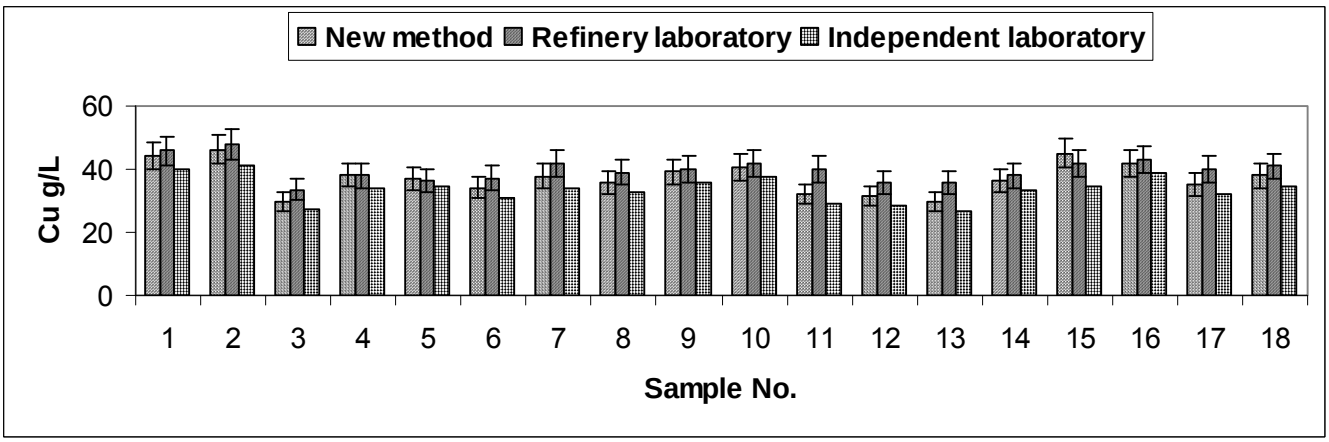

Fig 4.36 Comparison of three methods for copper determined for "copper feed" in refinery streams in 0.7M H_3PO_4 and 1M H_2SO_4 mixture.

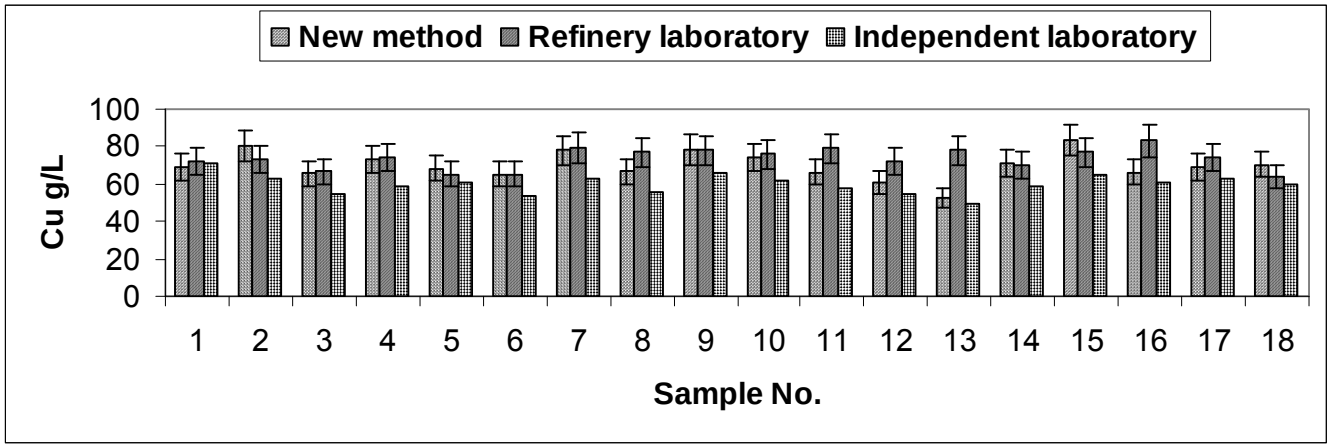

Fig 4.37 Comparison of three methods for copper determined for "copper spent" in refinery streams in 0.7M H_3PO_4 and 1M H_2SO_4 mixture.

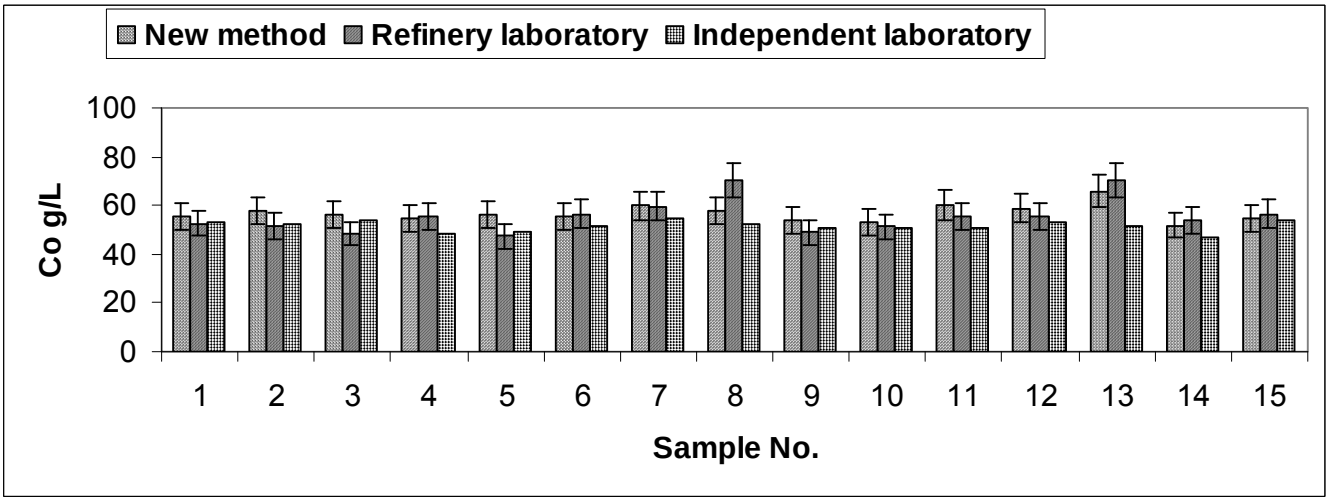

Fig 4.38 Comparison of three methods for cobalt determined in refinery streams in 0.7M H_3PO_4 and 1M H_2SO_4 mixture.

The mean concentration and standard deviation for each metal ion was calculated for each method i.e. the refinery method, new method and independent method. (see Table 4.4)

Table 4.4 The mean and standard deviation of the samples analysed.

Sample	$x_{ref} \pm s$	$x_{new} \pm s$	$x_{ind} \pm s$
$[Cu^{2+}(aq)]$ g/L Cu Feed	73.55 ± 5.49	69.91 ± 7.46	59.84 ± 5.13
$[Cu^{2+}(aq)]$ g/L Cu Spent	39.88 ± 3.63	37.33 ± 4.96	33.72 ± 4.12
$[Co^{2+}(aq)]$ g/L Co Sample	55.58 ± 6.80	56.78 ± 3.50	51.55 ± 2.25
$[Ni^{2+}(aq)]$ g/L Ni Feed	78.48 ± 2.87	73.43 ± 4.43	68.74 ± 4.02
$[Ni^{2+}(aq)]$ g/L Ni Product	93.12 ± 4.47	86.33 ± 4.97	78.21 ± 4.13

The confidence limits were then determined at 95% confidence for each of the methods. Comparing the limits for the three different analyses, there are many overlap regions between the methods. (see Table 4.5)

Table 4.5 The confidence limits(CL) obtained for the refinery method, new method and the independent method with 95 % confidence.

Sample	CL_{ref}	CL_{new}	CL_{ind}
$[Cu^{2+}(aq)]$ g/L Cu Feed	70.83 - 76.27	66.22 - 73.6	57.30 - 62.38
$[Cu^{2+}(aq)]$ g/L Cu Spent	38.09 - 41.67	34.88 - 39.78	31.68 - 35.76
$[Co^{2+}(aq)]$ g/L Co Sample	59.32 - 51.84	54.86 - 58.70	50.31 - 52.79
$[Ni^{2+}(aq)]$ g/L Ni Feed	77.84 - 79.12	71.34 - 75.72	66.75 - 70.73
$[Ni^{2+}(aq)]$ g/L Ni Product	95.34 - 90.90	83.9 - 88.76	76.10 - 80.32

Paired *t*-test was carried out to determine if the difference between the refinery method and the new method was significant. The *t*-test showed that the difference with 95 % confidence is not significant. The new method may be submitted for current refinery method.

All the analyses for copper, nickel and cobalt fall within the required accuracy of the plant of 10% criterion of acceptability. For each of the cases, at least two of three results compare fairly closely. In the refinery laboratory, there is more variation, due to the fact, that there are several operators on shift, which may influence inconsistent data. However, in the other two methods, only one operator analysed the samples in each case. Generally overall, the new method compares fairly with the other two methods of analysis, but validation of this method is essential.

Method validation is critical for any new method to determine its credibility. The standard criteria are the following. [6]

- Linearity
- Range

- Accuracy
- Precision
- Sensitivity
- Selectivity
- Temperature
- Ruggedness

The above parameters have been fulfilled and fully discussed above. This proves that the method is ready for use and is credible.

4.10 Recommendations and Conclusion

UV-visible spectrophotometry is a simple analytical tool that can be used for the qualitative and quantitative analysis of $Cu(aq)^{2+}$, $Co(aq)^{2+}$, $Ni(aq)^{2+}$ in 0.7M H_3PO_4/ IM H_2SO_4 mixture. This analytical technique allows the simultaneous determination of these species in a synthetic mixture for the wide linear dynamic range of 2-10g/L for each of the species.

These species can be analysed successfully within 5% accuracy. However, $Fe(aq)^{2+}$ may not be analysed by this method. This method is applicable to synthetic mixtures containing <1g/L $Fe(aq)^{2+}$, however, this is a limitation of the method.

The determination of $Cu(aq)^{2+}$, $Co(aq)^{2+}$, $Ni(aq)^{2+}$ in a synthetic mixture is achieved by simple spreadsheet calculations, fundamentally solving a simultaneous equation, using absorbance data at $\lambda_{394,512 \text{ and } 804nm}$ specifically for each of the individual species.

This simultaneous method can be applied to refinery plant streams, i.e. “copper feed”, “copper spent”, “nickel feed”, “nickel product” and “cobalt sample” for the determination of $Cu(aq)^{2+}$, $Co(aq)^{2+}$, $Ni(aq)^{2+}$ in solution. Since refinery streams are in the concentration range of 20-100g/L, the method requires dilution of the samples to the linear range determined for the synthetic mixture, i.e. 2-10g/L of $Cu(aq)^{2+}$, $Co(aq)^{2+}$, $Ni(aq)^{2+}$in the diluent. However, samples cannot be measured directly and require dilution.

The attributes of this method, where sample is diluted, measured and determinations of three species can be obtained immediately with reasonable accuracy poses an attractive alternative, for on-line application.

Currently, the sample is collected by a sampler, filtered, undergoes the necessary treatment and then analysed by three different methods for three different determinations to achieve the three results which is processed to the plant and the necessary changes made for process control. This is time-consuming, inefficient and also the safety of the sampler is a concern. The samples in the refinery are in sulphuric acid medium ranging from 20-100g/L.

On the other hand, application of the new method to on-line analysis, where the sample is channeled directly from a sampling system, diluted and measured immediately using the

simultaneous method, the results are available instantaneously and the plant can make changes real-time. This new method is faster and more efficient. Also, it eliminates the risk attached to the sampler being in contact with the acidic samples.

In off-line analysis, the sample is allowed to cool before the analysis. In on-line analysis, the entire system can be temperature controlled and thus, correct for biases attributed to temperature effects. Also, an accurate volume of sample will be dispensed by the system and diluted.

Spectrophotometric on-line analysis

UV-visible spectrophotometry offers the following advantages that make it suitable for on-line analysis:

The simplified sample preparation procedure involves a small dilution of the sample and hence reduces the large dilution error. Measurement time for analysis is short (<1minute) and calculation of concentrations from the instrument signal.

The UV-visible spectrometer is generally very stable and it is only necessary to check the calibration of the instrument every three months depending on the frequency of use. This instrument is low maintenance and cost effective. Optimisation on a daily basis is not necessary, unlike the Atomic absorption spectrometer that requires optimization of the lamp for each elemental analysis.

The method of analysis requires the use of one diluent which is the 0.7M H_3PO_4/1M H_2SO_4 mixture and does not make use of several reagents as in the case of the current titrimetric methods of analysis. There are fewer steps in the method to achieve one result and this reduces the overall error of the analysis largely.

The UV lamp has a lifetime of 1000 hours. This, however, is a limitation if the instrument is used on a 24-hour basis, the lamp would have to be replaced frequently.

Also, this method could be investigated and implemented without interrupting the existing operations.

Further work

The implementation of the new method on an on-line system would entail a feasibility study of the Rustenburg Base Metal Refinery process area where the method can be optimally maximized.

The pressure of the process streams of interest will need to be studied, as well as design of a good sampling system for sample introduction into the UV-visible spectrometer. The five streams studied are indicative of five different regions in the Base Metal Refinery. Ideally, as many refinery streams as possible in close proximity to each other will be channelled into an on-line UV-visible spectrometers.

Software, that is suitable for the application and that also facilitates interface between the instrument and the process control room will need to be written. In view, greater accuracy, efficient process control and increased safety, the on-line implementation of the new method is highly recommended.

The attempt to simultaneously analyse copper, nickel and cobalt in synthetic mixtures and in refinery streams was successful.

References

1. Z.Hofirek and D.G.E. Kerfoot, *Hydrometallurgy*, 1992, **29**, 357-381.
2. Skoog, West and Holler, *Fundamentals of Analytical Chemistry*, 7th edn, 560.
3. A.M.Garcia Rodriguez, A. Garcia de Torres, J.M. Cano Pavon and C. Bosch Ojeda, *Talanta*, 1998,**47**, 463-470.
4. James N.Miller, *Analyst*, 1991,**116,** 3-14.
5. Angus M. Brown, *A step-by-step guide to non-linear regression analysis of experimental data using a Microsoft Excel spreadsheet, Computer methods and programs in Biomedicine,* 2001, **65**,191-200.
6. John K.Taylor, *Analytical Chemistry*, 1983, **55**,600-608.

Appendix

Table 1 Absorbance measurements and known concentrations for copper, nickel and cobalt in 0.7M H_3PO_4 and 1M H_2SO_4 mixture used to determine the molar absorptivities for each of the elements.

Standard	Absorbance	Cu^{2+} g/L	Standard	Absorbance	Ni^{2+} g/L	Standard	Absorbance	Co^{2+} g/L
Std 1	0.401	2.02	**Std 1**	0.192	2.05	**Std 1**	0.169	2.03
Std 2	0.764	4.05	**Std 2**	0.371	4.09	**Std 2**	0.345	4.05
Std 3	1.161	6.07	**Std 3**	0.570	6.14	**Std 3**	0.513	6.08
Std 4	1.531	8.09	**Std 4**	0.763	8.09	**Std 4**	0.679	8.11
Std 5	1.900	10.11	**Std 5**	0.932	10.23	**Std 5**	0.843	10.13

Table 2 Absorptivities of the $[Ni(H_2O)_6]^{2+}$, $[Co(H_2O)_6]^{2+}$ and $[Cu(H_2O)_6]^{2+}$ species at $\lambda_{389-398}$, $\lambda_{508-517}$ and $\lambda_{800-809nm.}$ in 0.7M H_3PO_4 and 1M H_2SO_4 mixture used to determine the wavelength of least interference and greatest sensitivity.

Species	389	390	391	392	393	394	395	396	397	398
Ni^{2+}	0.0903	0.0911	0.0918	0.0921	0.0923	0.0922	0.0919	0.0916	0.0913	0.0894
Cu^{2+}	0.0047	0.0047	0.0047	0.0047	0.0047	0.0047	0.0047	0.0047	0.0047	0.0234
Co^{2+}	0.0053	0.0051	0.0049	0.0048	0.0046	0.0044	0.0043	0.0041	0.0040	0.0038

Species	508	509	510	511	512	513	514	515	516	517
Ni^{2+}	0.0026	0.0026	0.0026	0.0026	0.0024	0.0025	0.0023	0.0023	0.0024	0.0115
Cu^{2+}	0.0049	0.0049	0.0049	0.0048	0.0047	0.0048	0.0047	0.0046	0.0047	0.0046
Co^{2+}	0.0827	0.0832	0.0836	0.0839	0.0842	0.0843	0.0844	0.0843	0.0842	0.0840

Species	800	801	802	803	804	805	806	807	808	809
Ni^{2+}	0.0153	0.0156	0.0158	0.0160	0.0163	0.0166	0.0168	0.0171	0.0174	0.0176
Cu^{2+}	0.1911	0.1911	0.1911	0.1910	0.1910	0.1910	0.1909	0.1908	0.1907	0.1906
Co^{2+}	0.0020	0.0020	0.0020	0.0020	0.0020	0.0020	0.0019	0.0020	0.0019	0.0019

Table 3 Comparison between change in copper concentration as the cobalt concentration increases to determine the potential interference of cobalt on copper.

Co g/L	Known Cu g/L	Detemined Cu g/L	Difference	% Difference
0	4.69	4.70	0.01	0.24
1	4.69	4.71	0.02	0.49
3	4.69	4.76	0.07	1.41
5	4.69	4.72	0.03	0.54

Table 4 Comparison between change in copper concentration as the nickel concentration increases to determine the potential interference of nickel on copper.

Ni g/L	Known Cu g/L	Determined Cu g/L	Difference	% Difference
0	4.69	4.60	-0.09	1.92
1	4.69	4.60	-0.09	1.90
3	4.69	4.63	-0.06	1.36
5	4.69	4.59	-0.10	2.06

Table 5 Comparison between the change in nickel concentration as the cobalt concentration increases to determine the potential interference of cobalt on nickel.

Co g/L	Known Ni g/L	Determined Ni g/L	Difference	% Difference
0	5.12	5.19	0.07	1.37
1	5.12	5.23	0.11	2.15
3	5.12	5.29	0.17	3.32
5	5.12	5.52	0.40	7.81

Table 6 Comparison between the change in nickel concentration as the copper concentration increases to determine the potential interference of copper on nickel.

Cu g/L	Known Ni g/L	Determined Ni g/L	Difference	% Difference
0	4.92	4.93	0.01	0.20
1	4.92	4.91	-0.01	0.20
3	4.92	4.79	-0.13	2.64
5	4.92	4.73	-0.19	3.86

Table 7 Comparison between the change in cobalt concentration as the copper concentration increases to determine the potential interference of copper on cobalt.

Cu g/L	Known Co g/L	Detemined Co g/L	Difference	% Difference
0	5.20	5.22	0.02	0.38
1	5.20	5.11	-0.09	1.73
3	5.20	5.22	0.02	0.38
5	5.20	5.22	0.02	0.38

Table 8 Comparison between the change in cobalt concentration as the nickel concentration increases to determine the potential interference of nickel on cobalt.

Ni g/L	Known Co g/L	Detemined Co g/L	Difference	% Difference
0	5.20	5.21	0.01	0.19
1	5.20	5.24	0.04	0.77
3	5.20	5.18	-0.02	0.38
5	5.20	5.28	0.08	1.54

Table 9 Comparison between known concentrations in the mixtures against the determined concentrations for copper, nickel and cobalt in 0.7M $H_3PO_4$and 1M H_2SO_4 mixture.

	Known g/L			Determined g/L		
Standards	**Ni^{2+}**	**Co^{2+}**	**Cu^{2+}**	**Ni^{2+}**	**Co^{2+}**	**Cu^{2+}**
1	2.00	6.02	4.03	1.95	5.97	4.11
2	2.00	8.00	6.00	1.92	8.03	6.27
3	2.00	10.02	8.00	1.79	9.98	8.30
4	2.00	4.00	2.02	2.02	4.00	2.07
5	2.00	2.00	10.00	1.81	1.71	10.39
6	4.00	8.00	6.00	3.87	7.91	6.28
7	4.00	10.02	8.00	3.8	9.94	8.42
8	4.00	2.00	10.00	3.75	1.57	10.48
9	4.00	4.00	2.02	4.11	3.97	2.09
10	4.00	6.02	4.03	4.13	6.09	4.15
11	6.00	10.02	8.00	5.84	9.75	8.16
12	6.00	2.00	10.00	6.02	1.64	10.34
13	6.00	4.00	2.02	6.51	4.20	2.14
14	6.00	6.02	4.03	6.51	6.30	4.21
15	6.00	8.00	6.00	6.13	7.98	6.26
16	8.00	2.00	10.00	8.31	1.86	10.44
17	8.00	4.00	2.02	8.49	4.13	2.12
18	8.00	6.02	4.03	8.32	6.02	4.15
19	8.00	8.00	6.00	8.18	7.92	6.23
20	8.00	10.02	8.00	8.18	10.04	8.32
21	10.00	4.00	2.02	10.4	3.93	2.06
22	10.00	6.02	4.03	10.46	6.02	4.14
23	10.00	8.00	6.00	10.36	8.00	6.27
24	10.00	10.02	8.00	10.28	10.00	8.32
25	10.00	2.00	10.00	10.27	1.69	10.42

Table 10 Percentage difference between the determined values and known values for the 25 mixtures, showing the simultaneous analysis within 10% accuracy.

	% Difference		
Standards	**Ni^{2+}**	**Co^{2+}**	**Cu^{2+}**
1	2.50	0.83	1.99
2	4.00	0.37	4.50
3	10.50	0.40	3.75
4	1.00	0.00	2.48
5	9.50	14.50	3.90
6	3.25	1.13	4.67
7	5.00	0.80	5.25
8	6.25	21.50	4.80
9	2.75	0.75	3.47
10	3.25	1.16	2.98
11	2.67	2.69	2.00
12	0.33	18.00	3.40
13	8.50	5.00	5.94
14	8.50	4.65	4.47
15	2.17	0.25	4.33
16	3.88	7.00	4.40
17	6.13	3.25	4.95
18	4.00	0.00	2.98
19	2.25	1.00	3.83
20	2.25	0.20	4.00
21	4.00	1.75	1.98
22	4.60	0.00	2.73
23	3.60	0.00	4.50
24	2.80	0.20	4.00
25	2.70	15.50	4.20

Table 11 Comparison of known values and predicted values to determine accuracy and precision of standard mixtures.

	Known g/L			Predicted g/L		
Standards	Ni^{2+}	Co^{2+}	Cu^{2+}	Ni^{2+}	Co^{2+}	Cu^{2+}
1	8.00	6.02	6.00	8.19	5.93	6.09
2	8.00	6.02	6.00	8.08	5.81	6.06
3	8.00	6.02	6.00	8.04	5.79	6.07
4	8.00	6.02	6.00	8.00	5.73	6.06
5	8.00	6.02	6.00	8.48	6.16	6.19
6	8.00	6.02	6.00	8.06	5.77	6.10
7	8.00	6.02	6.00	8.12	5.82	6.08
8	8.00	6.02	6.00	8.02	5.75	6.11
9	8.00	6.02	6.00	8.14	5.89	6.18
10	8.00	6.02	6.00	8.39	6.03	6.13

Table 12 Comparison between known values in mixture against the determined values in the presence of Fe^{2+}

		Known g/L			Determined g/L		
Standards	Fe^{2+}	Ni^{2+}	Co^{2+}	Cu^{2+}	Ni^{2+}	Co^{2+}	Cu^{2+}
1	0.08	2.00	2.00	2.02	1.98	1.89	1.99
2	0.08	2.00	8.00	6.00	1.86	7.68	5.99
3	0.08	2.00	10.02	8.00	1.77	9.52	7.86
4	0.08	2.00	4.00	2.02	1.98	3.87	1.99
5	0.08	2.00	2.00	10.00	1.73	1.66	9.85
6	0.08	4.00	8.00	6.00	3.79	7.62	5.96
7	0.08	4.00	10.02	8.00	3.76	9.57	7.93
8	0.08	4.00	2.00	10.00	3.67	1.58	9.94
9	0.08	4.00	4.00	2.02	4.28	4.17	2.11
10	0.08	4.00	6.02	4.03	3.88	5.72	3.95
11	0.08	6.00	10.02	8.00	5.91	9.75	7.97
12	0.08	6.00	2.00	10.00	5.8	1.7	9.93
13	0.08	6.00	4.00	2.00	6.07	3.87	2.02
14	0.08	6.00	6.02	4.03	5.9	5.69	3.94
15	0.08	6.00	8.00	6.00	5.77	7.52	5.94
16	0.08	8.00	2.00	10.00	7.56	1.5	9.91
17	0.08	8.00	4.00	2.02	8.02	3.87	2.01
18	0.08	8.00	6.02	4.03	7.91	5.72	3.96
19	0.08	8.00	8.00	6.00	7.91	7.71	6.03
20	0.08	8.00	10.02	8.00	7.78	9.55	7.92
21	0.08	10.00	4.00	2.00	10	3.81	1.99
22	0.08	10.00	6.02	4.03	10.1	5.86	3.99
23	0.08	10.00	8.00	6.00	9.88	7.64	5.98
24	0.08	10.00	10.02	8.00	9.86	9.54	7.9
25	0.08	10.00	2.00	10.02	9.93	1.67	9.95

Table 13 Comparison of differences in analysis between the three-system mixtures with Fe^{2+} and three-system mixtures without Fe^{2+}.

	% Difference with Fe^{2+}			% Difference without Fe^{2+}			% Difference between the 2 analyses		
Standards	Ni^{2+}	Co^{2+}	Cu^{2+}	Ni^{2+}	Co^{2+}	Cu^{2+}	Ni^{2+}	Co^{2+}	Cu^{2+}
1	1.00	5.50	1.49	2.50	0.83	1.99	-1.50	4.67	-0.50
2	7.00	4.00	0.17	4.00	0.37	4.50	3.00	3.63	-4.33
3	11.50	4.99	1.75	10.50	0.40	3.75	1.00	4.59	-2.00
4	1.00	3.25	1.49	1.00	0.00	2.48	0.00	3.25	-0.99
5	13.50	17.00	1.50	9.50	14.50	3.90	4.00	2.50	-2.40
6	5.25	4.75	0.67	3.25	1.13	4.67	2.00	3.63	-4.00
7	6.00	4.49	0.88	5.00	0.80	5.25	1.00	3.69	-4.38
8	8.25	21.00	0.60	6.25	21.50	4.80	2.00	-0.50	-4.20
9	7.00	4.25	4.46	2.75	0.75	3.47	4.25	3.50	0.99
10	3.00	4.98	1.99	3.25	1.16	2.98	-0.25	3.82	-0.99
11	1.50	2.69	0.38	2.67	2.69	2.00	-1.17	0.00	-1.63
12	3.33	15.00	0.70	0.33	18.00	3.40	3.00	-3.00	-2.70
13	1.17	3.25	1.00	8.50	5.00	5.94	-7.33	-1.75	-4.94
14	1.67	5.48	2.23	8.50	4.65	4.47	-6.83	0.83	-2.23
15	3.83	6.00	1.00	2.17	0.25	4.33	1.67	5.75	-3.33
16	5.50	25.00	0.90	3.88	7.00	4.40	1.63	18.00	-3.50
17	0.25	3.25	0.50	6.13	3.25	4.95	-5.88	0.00	-4.46
18	1.13	4.98	1.74	4.00	0.00	2.98	-2.88	4.98	-1.24
19	1.13	3.63	0.50	2.25	1.00	3.83	-1.13	2.63	-3.33
20	2.75	4.69	1.00	2.25	0.20	4.00	0.50	4.49	-3.00
21	0.00	4.75	0.50	4.00	1.75	1.98	-4.00	3.00	-1.48
22	1.00	2.66	0.99	4.60	0.00	2.73	-3.60	2.66	-1.74
23	1.20	4.50	0.33	3.60	0.00	4.50	-2.40	4.50	-4.17
24	1.40	4.79	1.25	2.80	0.20	4.00	-1.40	4.59	-2.75
25	0.70	16.50	0.70	2.70	15.50	4.20	-2.00	1.00	-3.50

Table 14 Effect of pH and acid concentration on determination of concentration of Cu^{2+}, Ni^{2+} and Co^{2+} species in solution.

		Known g/L			Determined g/L			% Difference		
H_2SO_4 g/L	pH	Ni^{2+}	Co^{2+}	Cu^{2+}	Ni^{2+}	Co^{2+}	Cu^{2+}	Ni^{2+}	Co^{2+}	Cu^{2+}
2	1.58	8.00	6.02	4.03	7.92	5.60	3.95	1.00	6.98	1.99
4	1.32	8.00	6.02	4.03	8.39	6.03	4.02	4.88	0.17	0.25
6	1.16	8.00	6.02	4.03	7.90	5.60	3.95	1.25	6.98	1.99
8	1.04	8.00	6.02	4.03	7.91	5.63	3.97	1.13	6.48	1.49
10	0.96	8.00	6.02	4.03	7.86	5.52	3.92	1.75	8.31	2.73

Table 15 Effect of temperature on nickel determination in the nickel standard and in the ternary mixture.

Temp. ^0C	Known Ni^{2+} g/L	Determined Ni^{2+} g/L	% Difference in Std. Ni^{2+} g/L	% Difference in Mixture Ni^{2+} g/L
25	8.00	7.99	0.15	0.94
30	8.00	8.03	0.4	0.66
35	8.00	8.02	0.27	0.43
40	8.00	8.08	0.97	0.96
45	8.00	8.10	1.26	1.11
50	8.00	8.12	1.53	1.49
60	8.00	8.16	2.05	1.28

Table 16 Effect of temperature on copper determination in copper standard and in the ternary mixture.

Temp. ^{0}C	Known Cu^{2+} g/L	Determined Cu^{2+} g/L	% Difference in Std. Cu^{2+} g/L	% Difference in Mixture Cu^{2+} g/L
25	5.95	5.92	0.44	2.34
30	5.95	6.04	1.59	0.74
35	5.95	6.10	2.59	1.38
40	5.95	6.25	5.12	2.79
45	5.95	6.30	5.96	4.27
50	5.95	6.36	6.87	5.48
60	5.95	6.36	6.86	7.00

Table 17 Effect of temperature on cobalt determination in cobalt standard and in the ternary mixture.

Temp.^{0}C	Known Co^{2+} g/L	Determined Co^{2+} g/L	% Difference in Std. Co^{+} g/L	% Difference in Mixture Co^{2+} g/L
25	6.00	5.92	0.08	1.32
30	6.00	5.96	3.57	0.68
35	6.00	6.04	2.29	0.65
40	6.00	6.11	1.20	1.77
45	6.00	6.14	0.62	2.37
50	6.00	6.21	0.41	3.42
60	6.00	6.23	0.76	3.78

Table 18 Comparison between three methods of analysis for nickel determination in nickel product sample in the refinery.

Day No.	UV Ni^{2+}	Refinery Lab. Ni^{2+}	Independent Lab. Ni^{2+}
1	86.57	96.60	80.1
2	89.20	94.50	80.2
3	86.97	95.09	82.1
4	83.79	93.30	77.2
5	84.46	91.90	80.5
6	49.04	92.70	46.9
7	87.78	92.50	79.8
8	84.66	94.80	78.5
9	90.28	99.50	82.6
10	73.82	98.30	67.3
11	84.26	95.00	78.4
12	93.26	98.00	82.5
13	89.98	94.00	81.1
14	86.91	85.00	74.7
15	93.58	92.00	76.3
16	88.46	94.00	80.8
17	77.55	83.00	71.1
18	86.08	86.00	76.3

Table 19 Comparison between three methods of analysis for nickel determination in nickel feed sample in the refinery.

Day No.	UV Ni^{2+}	Refinery Lab. Ni^{2+}	Independent Lab. Ni^{2+}
1	73.65	82.80	69.1
2	74.64	80.70	69.0
3	71.08	76.60	65.8
4	73.84	79.98	69.9
5	68.82	76.30	68.5
6	72.40	79.80	69.2
7	69.43	75.40	68.2
8	72.67	80.70	71.3
9	71.41	81.00	68.9
10	89.17	81.30	82.9
11	70.40	77.00	66.3
12	74.34	82.00	69.0
13	74.53	78.00	67.1
14	71.58	75.00	65.6
15	73.95	73.00	63.2
16	71.08	76.00	66.0
17	77.31	81.00	69.0
18	73.22	76.00	68.1

Table 20 Comparison between the three methods of analysis for determination of copper in copper spent refinery sample.

Day No.	UV Cu^{2+}	Refinery Lab. Cu^{2+}	Independent Lab. Cu^{2+}
1	44.30	45.80	40.0
2	46.20	48.00	41.5
3	29.64	33.40	27.2
4	38.05	38.00	34.2
5	36.97	36.50	34.3
6	34.23	37.20	30.9
7	37.83	42.00	34.1
8	35.64	39.00	32.9
9	39.33	40.00	35.6
10	40.62	42.00	37.4
11	32.08	40.00	29.4
12	31.39	36.00	28.7
13	29.71	36.00	27.0
14	36.27	38.00	33.6
15	44.94	42.00	34.8
16	41.63	43.00	38.7
17	35.15	40.00	31.9
18	37.96	41.00	34.8

Table 21 Comparison between three methods for analysis of determination of copper in copper feed refinery sample.

Day No.	UV Cu^{2+}	Refinery Lab. Cu^{2+}	Independent Lab. Cu^{2+}
1	69.00	72.00	71.3
2	80.34	73.00	62.9
3	65.59	66.70	54.2
4	73.10	74.00	59.1
5	68.37	65.40	60.7
6	65.31	65.40	53.9
7	77.96	79.40	62.6
8	66.77	77.00	56.1
9	78.32	78.00	65.6
10	74.15	76.00	61.8
11	66.27	79.00	57.5
12	60.48	72.00	55.0
13	52.22	78.00	49.0
14	70.89	70.00	59.2
15	83.71	77.00	64.7
16	66.35	83.00	60.9
17	68.90	74.00	63.0
18	70.59	64.00	59.6

Table 22 Comparison between three methods of analysis for determination of cobalt in refinery cobalt sample.

Day No.	UV Co^{2+}	Refinery Lab. Co^{2+}	Independent Lab. Co^{2+}
1	55.58	52.66	53.5
2	57.74	51.6	52.2
3	56.40	48.44	54.2
4	54.47	55.60	48.1
5	56.12	47.30	49.2
6	55.25	56.60	51.9
7	59.84	59.60	54.7
8	57.79	70.10	52.5
9	53.76	48.90	50.5
10	53.00	51.21	50.5
11	60.26	55.40	50.7
12	58.97	55.70	53.0
13	65.88	70.00	51.5
14	51.94	54.10	46.9
15	54.73	56.50	53.7

Calculations

***Determination of the concentration of copper, nickel and cobalt from raw absorbance data and absorptivities for each of the different species at a specified wavelength*.**

Solver is a tool in Excel used with tangential estimate, forward derivative and Newton search.

This tool was selected under data analysis in Excel, the necessary inputs and output tables setup and a macro written to allow efficient calculation of concentration of the elements.